Math-for-industry
Education & Research Hub

ISSN 2188-1200

Inverse problems for practice, the present and the future

Editor: Takashi Takiguchi and Hiroshi Fujiwara

九州大学マス・フォア・インダストリ研究所

MI Lecture Note Vol.54 : Kyushu University

Inverse problems for practice, the present and the future

Editor: Takashi Takiguchi
Hiroshi Fujiwara

About MI Lecture Note Series

The Math-for-Industry (MI) Lecture Note Series is the successor to the COE Lecture Notes, which were published for the 21st COE Program "Development of Dynamic Mathematics with High Functionality," sponsored by Japan's Ministry of Education, Culture, Sports, Science and Technology (MEXT) from 2003 to 2007. The MI Lecture Note Series has published the notes of lectures organized under the following two programs: "Training Program for Ph.D. and New Master's Degree in Mathematics as Required by Industry," adopted as a Support Program for Improving Graduate School Education by MEXT from 2007 to 2009; and "Education-and-Research Hub for Mathematics-for-Industry," adopted as a Global COE Program by MEXT from 2008 to 2012.

In accordance with the establishment of the Institute of Mathematics for Industry (IMI) in April 2011 and the authorization of IMI's Joint Research Center for Advanced and Fundamental Mathematics-for-Industry as a MEXT Joint Usage / Research Center in April 2013, hereafter the MI Lecture Notes Series will publish lecture notes and proceedings by worldwide researchers of MI to contribute to the development of MI.

September 2013
Masato Wakayama
Director
Institute of Mathematics for Industry

Inverse problems for practice, the present and the future

MI Lecture Note Vol.54, Institute of Mathematics for Industry, Kyushu University
ISSN 2188-1200
Editor: Takashi Takiguchi and Hiroshi Fujiwara
Date of issue: 30 January 2014
Publisher:
Institute of Mathematics for Industry, Kyushu University
Graduate School of Mathematics, Kyushu University
Motooka 744, Nishi-ku, Fukuoka, 819-0395, JAPAN
Tel +81-(0)92-802-4402, Fax +81-(0)92-802-4405
URL http://www.imi.kyushu-u.ac.jp/

Printed by
Kijima Printing, Inc.
Shirogane 2-9-6, Chuo-ku, Fukuoka, 810-0012, Japan
TEL +81-(0)92-531-7102 FAX +81-(0)92-524-4411

Preface

These are the proceedings of the conference "Inverse problems for practice, the present and the future", held at IMI, Kyushu University, from September second to September fourth, 2013. It was held in order to promote the collaboration and mutual understanding between engineers, in both theory and practice, mathematicians and all those who may apply inverse problems for practice. Recently, there being many mathematical researches in inverse problems, it seems that few of them meet the real demands of practical application where the problems originated. The other aim of this conference was to study inverse problems in order to meet the real demands of practical application. During the conference, the following problems and invetigations on them were reported and lively dicussions were had on them.

- A control problem of the temperature in the production process of automobile components
- A new numerical approach to an inverse source problem for the wave equation
- An inverse problem to detect the degree of fixation for the frame structure in the buildings
- Inverse problems in risk managements
- Inverse problems on magnetic resonance imaging
- An inverse problem for the pipe flow model in karst aquifers
- An inverse problem of the heat equation in view of practical application

Every problem is based on the practice and its investigations are in process with the return of their results to practice in mind. We wish that we would have more opportunities to hold such conferences to discuss inverse problems from the viewpoint of both the theory and the practice.

At the end of the preface, we would express our gratefulness to Ms. Kyoko Sakaguchi, the secretary of this conference, for her faithful help and contribution for success of our conference.

December 15, 2013

Takashi Takiguchi
Hiroshi Fujiwara

Contents

Invese problems for practice, the present and the future

September 2-4, 2013

IMI, Ito Campus, Kyushu Univeristy
Lecture Room L-3, Faculty of Mathematics building
744 Motooka, Nishi-ku Fukuoka 819-0395, Japan

September 2nd, Monday

13:50 Opening

(Chair: T. Takiguchi)

14:00-15:00 Shohei Nagano and Makoto Kobayashi (CalsonicKansei)
Demands of technology component analysis in manufacturing technique development

15:30-16:30 Jin Cheng (Fudan University)
On the inverse problems for the coupled continuum pipe flow model for flows in karst aquifers

September 3rd, Tuesday

(Chair: T. Ohe)

11:00-12:00 Ryuji Endo (Polytechnic University of Japan)
System Identification on a Frame Structure Using Variable Parametric Projection Filter

(Chair: H. Fujiwara)

14:00-15:00 Masahiro Yamamoto (The University of Tokyo)
Mathematical analysis for inverse problems in risk managements

15:30-16:30 Shin-ich Urayama (Kyoto University)
Inverse problem on Magnetic Resonance Imaging (MRI)

September 4th, Wednesday

(Chair: T. Sakurai)

10:30-11:30 Takashi Ohe (Okayama University of Science)
A numerical method for an inverse source problem for a scalar wave equation without optimization procedures.

11:40-12:20 Takashi Takiguchi (National Defense Academy of Japan)
An inverse problem to detect an inclusion in a homogenous medium by the Dirichet to Dirichet data for the heat equation

12:20 Closing

This conference is supported by IMI, Kyushu University, JSPS Grant-in-Aid for Scientific Research (C) 22540214 and JSPS Grant-in-Aid for Young Scientists (B) 23740075.

Problems arisen in the joint research with KalsonicKansei

Takashi TAKIGUCHI*

Abstract

In this note, we report several problems arisen in the joint research with KalsonicKansei. We report how the problems were posed, especially, in view of practical application. We also report how they are being studied for the time being.

Keywords: inverse problems, collaboration with industry

1 Preface

It has been three years since KalsonicKansei and the author began discussion on the problems arisen in the production process of automobile components. Through these discussions, a number of problems were studied, among which, new research tasks were created and are under study.

Though, in the conference "Inverse problems for practice, the present and the future", held at IMI, Kyushu University, from September second to September fourth, 2013, Mr. Shohei Nagano and Mr. Makoto Kobayashi from CalsonicKansei gave a talk on the title "Demands of technology component analysis in manufacturing technique development", it is a pity to tell that they could not submit their report to these proceedings in the point of view of confidentiality in CalsonicKansei.

In this report, the author, instead of S. Nagano and K. Kobayashi, shortly reports their talk in the conference and introduces several inverse problems arisen in the joint research with KalsonicKansei to the extent that there is no conflict with the confidentiality in CalsonicKansei.

Throughout this paper, all contents being arranged in order that there is no conflict with the confidentiality in CalsonicKansei, some of them may be unclear and not easily understandable, for which the author is very sorry.

*Supported in part by JSPS Grant-in-Aid for Scientific Research (C) 22540214. Department of Mathematics, National Defense Academy of Japan, 1-10-20, Hashirimizu, Yokosuka, Kanagawa, 239-8686, JAPAN tel: +81-46-841-3810 (ext. 3249) fax: +81-46-844-5902 (shared) email: takashi@nda.ac.jp

2 Talk by S. Nagano and K. Kobayashi

In the conference "Inverse problems for practice, the present and the future", S. Nagano and K. Kobayashi posed problems arisen in the production process.

Problem 1. *The following problems were posed in the talk by S. Nagano and K. Kobayashi.*

(a) *How to optimize the production process.*

(b) *Problems to control a molding device.*

(c) *How to control the temperature of the welding material in the welding.*

We shortly introduce what Problem 1 is about. We cannot comment on the problem (a) much in detail since it may conflict with the confidentiality in CalsonicKansei, however, this problem is very new, challenging and complicated to find a suitable mathematical model. In the problem (b), they posed a problem to control a device to mold aluminium. Operation of the molding device is very sensitive to the environment, especially when the plate of aluminium to be molded is very thin. They posed a problem to find a method in order that the operation of the molding device works with no error from the beginning of the operation in a new factory. Solution to this problem can be of great help by cutting off the cost to send the learned engineers to the factory to adjust the molding device. In problem (c), they posed a problem to control the temperature of the welding material especially in MIG welding. For this problem, some research is under investigation. It being very hard to control the temperature of the welding material in MIG welding, it is possible in TIG welding since we can control the temperature of the heat source in this method. The author is studying how to modify this method for MIG welding.

3 Inverse Problems arisen in the joint research with KalsonicKansei

Let us introduce some inverse problems arisen in the joint research by KalsonicKansei and the author and some relating results. We also mention how they are being studied for the time being. There are many problems created in the discussion by KalsonicKansei and the author. Among them are optimization and control problems mentioned in the previous section. In this section, we introduce two inverse problems arisen in the joint research by KalsonicKansei and the author.

Problem 2. *Following problems are created through the discussion by KalsonicKansei and the author.*

(i) *Non-destructive testing for die casting of the aluminium.*

(ii) *How to control the temperature in the interior of the furnace in the brazing process of the aluminium.*

First, let us explain what the problem (i) is about. In the die casting of the aluminium, liquid aluminium is poured into a mold. After it gets cold, it is taken out of the mold. After the heat treatment and the final treatment, the die casting component of the aluminium is complete. The process of pouring the aluminium into a mold must be finished quickly, otherwise the aluminium would be solid, the mold of the aluminium contains blow holds inside it. If there is a blow hole near the boundary (or edge) of the mold of the aluminium, then, after the heat treatment, it will swell up and the mold would be defective. It is desirable to solve the following problem before the heat and final treatment of the die casting product.

Problem 3. *Let $D,\ \Omega \subset \mathbb{R}^n$ be open sets satisfying $D \subset \Omega$. Decide whether*

$$d(\partial\Omega, \partial D) := \inf_{x\in\partial\Omega,\ y\in\partial D} |x - y| \tag{1}$$

is small or not, without accessing the interior of Ω.

This problem has a close relation with the typical inverse problem to reconstruct inclusions in a homogeneous medium. For the time being, application of the same algorithm as the computerized tomography (CT) is being investigated for this kind of problem. Since the objects in these problems are much simpler than the interior structure of the human body, it is expected to reduce the X-ray data for the reconstruction of the object. This problem is closely related to the geometric tomography and there are many studies on it both in the viewpoint of theory and in the viewpoint of application. For example, confer [1, 7, 8] for the results in the viewpoint of theory and [2, 9, 10, 11] for the studies in the viewpoint of practical application. Unfortunately, the results mentioned above are not still satisfactory for practical application in view of the following points.

- In the case where we project parallel beams of the X-ray from two directions, we can classify the shape of the inclusions into the two classes, one is the uniquely determined ones by these data and the other is non-uniquely determined one ([7, 8, 9]). For the unique class, reconstruction formulas ([7, 9]) are given and we gave further studies, treatment of the errors, construction of a reconstruction algorithm and its implementation by computers and so on, satisfactory for practical application ([2, 9]). It is, however, proved that there are very few sets reconstructed by this method ([10]) and it is not known how to find the exact two directions for the reconstruction for the uniquely reconstructed sets, even if they exist.

- For general inclusions, the exact data of the beams of the X-ray for the reconstruction are not known. Needless to say their reconstruction methods, treatment of the errors, construction of an approximate reconstruction algorithm, its implementation by computers and so on.

- Since they adopt cone beams of the X-rays in many industrial CT devices, we have to study the above two problems for the cone beams of projections as well as for the parallel beams of projections.

There are other problems of the use of the X-ray tomography.

- The cost of the testing is not cheap if we apply the X-ray tomography.
- We cannot ignore the bad effect of the X-ray to the human body.

The problem of the cost seems to be fatal. If we apply the existing industrial CT to the problem (i), then the cost of the testing is more expensive than the price of the die casting product. In order to solve this problem, development of a new algorithm, as well as the idea of development a new CT machine for die casting products, is under investigation by the author.

There are other approaches. One idea is to detect an inclusion in a homogeneous medium applying the heat conduction. For this purpose, the author is studying some modifications of the theory by M. Ikehata and M. Kawashita [3, 4, 5, 6]. There also are other ideas to solve problem (i) under investigation, which shall be introduced when they are ready to be published.

Let us turn to the problem (ii). This is a mixed problem of an inverse and a control problems. For the time being, there is no method to know the distribution of the temperature inside the furnace completely. This is a typical inverse problem to reconstruct the solution of the heat equation by the observation of some boundary value. The author is afraid that this problem seems to be very simple and easy, but it is not so simple by the following points in view of practice.

- We cannot observe the boundary value on the whole boundary. What we can do is to observe the heat at finite points on the boundary. Technically, we put thermocouples inside the furnace and observe the temperature.
- On some subset of the boundary of the domain, where the heat equation holds, the insulation condition does not hold. Instead, there is complicated heat convection there.

There are more problems to make the situation more complicated. The study of the problem (ii) is under investigation by considering which condition is to be taken or to be thrown away to develop a suitable mathematical model of this problem. The process requires close collaboration between the theory and the practice. We first propose a model with some hypotheses and check its appropriateness by the experiment. After the model is decided to be appropriate, we can go for the next step. Step by step, we shall be approaching the solution to the final problem.

References

[1] Gardner R.J. : *X-rays of polygons,* Discrete Comput. Geom., **7** (1992), pp. 281-293.

[2] Huang L. and Takiguchi T. : *The reconstruction of uniquely determined plane sets from two projections,* J. Inv. Ill-Posed Problems, **6** (1998), pp. 217-242.

[3] Ikehata M. : *Reconstruction of the support function for inclusion from boundary measurements,* J. Inv. Ill-Posed Problems, **8** (2000), pp. 367-378.

[4] —— : *Extracting discontinuity in a heat conductive body. One-space dimensional case,* Appl. Anal., **86** (2007), pp. 963-1005.

[5] Ikehata M. and Kawashita M. : *The enclosure method for the heat equation,* Inverse Problems, **25** (2009), 075005.

[6] —— : *On the reconstruction of inclusions in a heat conductive body from dynamical boundary data over a finite time interval,* Inverse Problems, **26** (2010), 095004.

[7] Kuba A. and Volčič A. : *Characterization of measurable plane sets which are reconstructable from their two projections,* Inverse Problems, **4** (1988), pp. 513-527.

[8] Lorentz G.G. : *A problem of plane measure,* Amer. J. Math., **71** (1949), pp. 417-426.

[9] Takiguchi T. : *Reconstruction of measurable plane sets from their orthogonal projections,* Contemporary Mathematics, **348** (2004), pp. 199-208.

[10] —— : *Reconstruction of the measurable sets in the two dimensional plane by two projections,* Journal of Physics, Conference Series, **73** (2007), 012022.

[11] —— : *Non-uniqueness of the reconstruction for connected and simply connected sets in the plane by their fixed finite projections,* Acta Mathematica Scientia, **32B** (2012), pp. 1637-1646.

On the Inverse Problems for the Coupled Continuum Pipe Flow model for flows in karst aquifers

Jin Cheng (Fudan University, Shanghai)

Joint work with Nan Chen, Xinming Wu, Shuai Lu (Fudan University, Shanghai)
and Philipp Kügler (Hohenheim University, Germany)

Workshop on Applied Mathematics
September 2nd, 2013 Japan

Outline

Outline

Introduction

Geological description of the karst aquifers

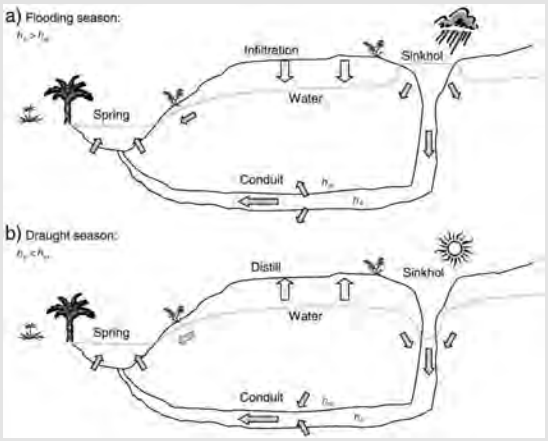

Figure: The geological description of the karst aquifers. h_m is the hydraulic head in the matrix and h_c is the hydraulic head in the conduit.

Simplified model

The classic discrete model

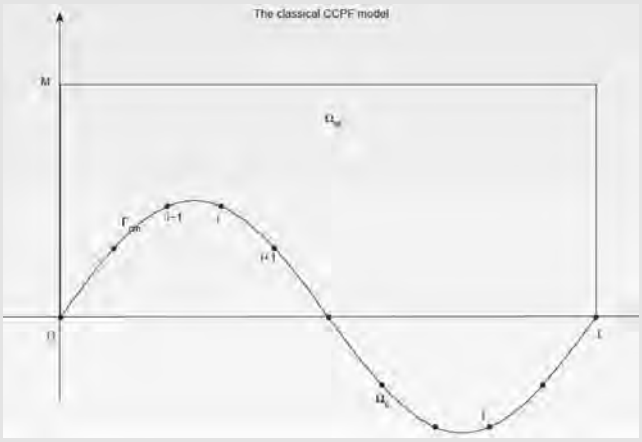

Figure: The discrete 2-D CCPF model of the karst aquifers.

The classic discrete model

Geology description

h_m, h_c the hydraulic head in the matrix and conduit;

f_m, f_c the recharge rate to the matrix and conduit;

$\mathbb{K}$ the hydraulic conductivity;

S the storativity of the water;

Q_{ij} the flow rate from node j to node i;

D the Poiseuille constant.

Hydraulic head $h_m = z + \frac{p_m}{\rho g}$

z relative depth;

p_m dynamic pressure;

ρ the density;

g gravitational acceleration.

The classic discrete model

MODFLOW-2005: US Geologyical Survey's Software

$$\begin{aligned}
\nabla\cdot(\mathbb{K}\nabla h_m)-\Gamma_{ex}+f_m &= S\frac{\partial h_m}{\partial t}, \quad \text{(conservation of mass);}\\
\sum_j Q_{ij}+q_{ex,i}+f_{c,i} &= 0, \quad \text{(Kirchhoff's law).}\\
\Gamma_{ex} &= \sum_i \delta(\mathbf{x}-\mathbf{x_i})q_{ex,i}V^{-1},\\
q_{ex,i} &= \alpha_{ex,i}(h_{m,i}-h_{c,i}),\\
Q_{ij} &= -D\frac{h_{c,i}-h_{c,j}}{L_{ij}}, \quad \text{(Poiseuille flow formula).}
\end{aligned}$$

The continuous model

2-D continuous steady model

$$\begin{aligned}
-\nabla\cdot(\mathbb{K}\nabla h_m) &= -\alpha(h_m-h_c)\delta_{\Omega_c}+f_m \qquad in \quad \Omega_m\\
-\frac{\partial}{\partial\tau}(D\frac{\partial h_c}{\partial\tau}) &= \alpha(h_m|_{\Omega_c}-h_c)+f_c, \qquad in \quad \Omega_c
\end{aligned}$$

3-D continuous steady model

$$\begin{aligned}
-\nabla\cdot(\mathbb{K}\nabla h_m) &= -\alpha(h_m\delta_\Gamma-h_c\delta_\Gamma)/|\Gamma_x|+f_m \quad in \quad \Omega_m\\
-\frac{\partial}{\partial\tau}(D\frac{\partial h_c}{\partial\tau}) &= \alpha(\frac{1}{|\Gamma_x|}\int_{\Gamma_x}h_m\mathrm{d}l_x-h_c)+f_c, \qquad in \quad \Omega_c
\end{aligned}$$

References: Hua (2009), Wang (2010), Cao,Gunzburger,Hua,Wang (2011)

Outline

Analysis of the forward model

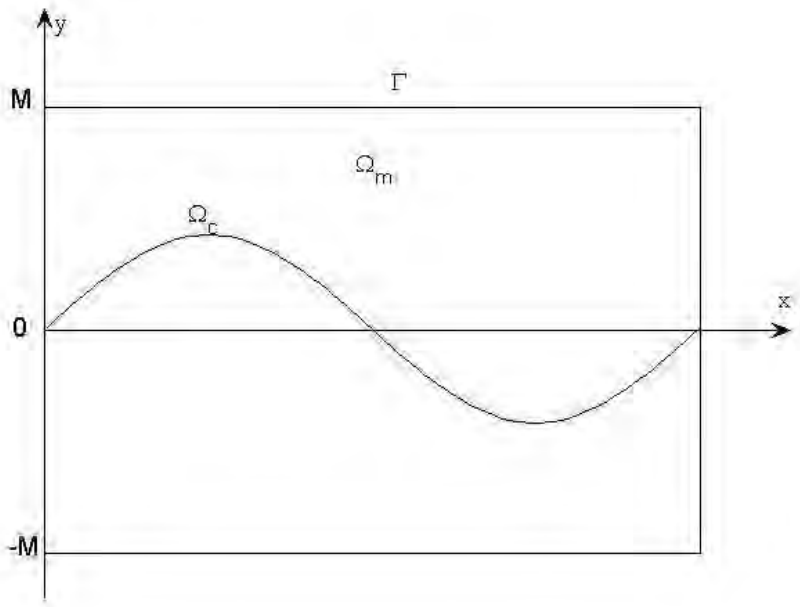

Analysis of the forward model

The forward model

$$\begin{cases} -\nabla\cdot(\mathbb{K}\nabla h_m) = -\alpha(h_m - h_c)\delta_{\Omega_c} + f_m & \text{in} \quad \Omega_m, \\ -\frac{\partial}{\partial\tau}(D\frac{\partial h_c}{\partial\tau}) = \alpha(h_m|_{\Omega_c} - h_c) + f_c, & \text{in} \quad \Omega_c \end{cases}$$

where δ_{Ω_c} is the Dirac delta function concentrated on Ω_c and $\alpha(s)$ is the exchange function such that $\alpha(s) \in L^\infty_+(\Omega_c)$ where s presents the arc length variable along the conduit Ω_c.

Bilinear form

Denoting $h_c' := \frac{\partial h_c}{\partial x}$, we define a bilinear form $a(\cdot,\cdot)$ of the system on $\mathbf{H}\times\mathbf{H}$ with $\mathbf{H} := H_0^1(\Omega_m)\times H_0^1(\Omega_c)$ as follows:

$$\begin{aligned} a(\mathbf{h},\mathbf{v}) := & \int_{\Omega_m} \mathbb{K}\nabla h_m(x,y)\cdot\nabla v_m(x,y)dxdy \\ & + \int_0^L \frac{Dh_c'(s(x))v_c'(s(x))}{\sqrt{1+[\psi'(x)]^2}}dx \\ & + \int_0^L \alpha(s(x))(h_m(x,\psi(x)) - h_c(s(x)))v_m(x,\psi(x))\sqrt{1+[\psi'(x)]^2}dx \\ & - \int_0^L \alpha(s(x))(h_m(x,\psi(x)) - h_c(s(x))v_c(s(x)))\sqrt{1+[\psi'(x)]^2}dx \end{aligned}$$

where $\mathbf{h} = (h_m, h_c) \in \mathbf{H}$ and the test functions $\mathbf{v} = (v_m, v_c) \in \mathbf{H}$. The weak solution yields

$$a(\mathbf{h},\mathbf{v}) = \langle f_m, v_m\rangle_{L^2(\Omega_m)} + \langle f_c, v_c\rangle_{L^2(\Omega_c)}$$

for all $\mathbf{v} \in \mathbf{H}$.

Existence of the forward model

Existence

Assume that $f_m \in H^{-1}(\Omega_m)$, $f_c \in H^{-1}(\Omega_c)$ and $\alpha \in L^\infty_+(\Omega_c)$. Then the weak solution $\mathbf{h}$ of uniquely exists and satisfies the estimation

$$\|\mathbf{h}\|_{\mathbf{H}} \leq C(\|f_m\|_{H^{-1}(\Omega_m)} + \|f_c\|_{H^{-1}(\Omega_c)})$$

where C is a constant independent of f_m and f_c.

Sketch of the proof [Hua(2009), Cao,Gunzburger,Hua,Wang (2011)]

Coercivity of the bilinear form

$$a(\mathbf{h},\mathbf{h}) \quad \geq \quad \int_{\Omega_m} \mathbb{K}\nabla h_m(x,y)\cdot\nabla h_m(x,y)dxdy + \int_{\Omega_c} D\left(\frac{dh_c(s)}{ds}\right)^2 ds.$$

The rest of the proof follows the Lax-Milgram theorem and the trace theorem.

Regularity of the forward model

Regularity

Assume that $f_m \in H^{-\frac{1}{2}}(\Omega_m)$, $f_c \in L^2(\Omega_c)$ and $\alpha(x) \in L^\infty_+(\Omega_c)$. Then the weak solution $\mathbf{h}$ satisfies $\mathbf{h} \in H^{\frac{3}{2}-\varepsilon}(\Omega_m)\times H^2(\Omega_c)$ for all $\varepsilon \in (0,\frac{1}{2})$ and

$$\|\mathbf{h}\|_{H^{\frac{3}{2}-\varepsilon}(\Omega_m)\times H^2(\Omega_c)} \leq C(\varepsilon)(\|f_m\|_{H^{-\frac{1}{2}}(\Omega_m)} + \|f_c\|_{L^2(\Omega_c)}).$$

Consequently, $h_m|_{\Omega_c} \in H^{1-\varepsilon}(\Omega_c)$.

Why the low regularity? [Hua(2009), Cao,Gunzburger,Hua,Wang (2011)]

By taking the test function v_c in the conduit identically to zero in the weak form, we obtain the following weak form for $\mathbf{h}$ such that

$$\int_{\Omega_m} \mathbb{K}\nabla h_m(x,y)\cdot\nabla v_m(x,y)dxdy = -\int_{\Omega_c} \alpha(s)(h_m|_{\Omega_c} - h_c(s))v_m|_{\Omega_c} ds + \int_{\Omega_m} f_m v_m dxdy, \quad \forall v_m \in H^1_0(\Omega_m).$$

Sketch of the proof II

Why the low regularity? Cont.

From the assumption that $f_m \in H^{-\frac{1}{2}}(\Omega_m)$, $h_c \in H^2(\Omega_c)$ and $\alpha(s) \in L^\infty_+(\Omega_c)$, we know that for all $v_m \in H^1_0(\Omega_m)$ there holds

$$\begin{aligned}\int_{\Omega_c} \alpha(s)(h_m|_{\Omega_c} - h_c(s))v_m|_{\Omega_c} ds &\le C(\|h_m\|_{L^2(\Omega_c)} + \|h_c\|_{L^2(\Omega_c)})\|v_m\|_{L^2(\Omega_c)} \\ &\le C(\varepsilon)(\|h_m\|_{H^1(\Omega_m)} + \|h_c\|_{L^2(\Omega_c)})\|v_m\|_{H^{\frac{1}{2}+\varepsilon}(\Omega_m)}.\end{aligned}$$

One can observe that $\int_{\Omega_c} \alpha(s)(h_m|_{\Omega_c} - h_c(s))v_m|_{\Omega_c} ds$ defines a bounded linear functional $\alpha(s)(h_m|_{\Omega_c} - h_c(s)) \in H^{-\frac{1}{2}-\varepsilon}(\Omega_m)$ on $H_0^{\frac{1}{2}+\varepsilon}(\Omega_m)$ and

$$\|\alpha(s(x))(h_m(x,\psi(x)) - h_c(s(x)))\|_{H^{-\frac{1}{2}-\varepsilon}(\Omega_m)} \le C(\varepsilon)(\|h_m\|_{H^1(\Omega_m)} + \|h_c\|_{L^2(\Omega_c)}).$$

One then concludes that the righthand side of the first equation $-\alpha(h_m - h_c)\delta_{\Omega_c} + f_m \in H^{-1/2-\varepsilon}(\Omega_m)$. By the elliptic regularity in domain with corners, we conclude that $h_m \in H^{3/2-\varepsilon}(\Omega_m)$. Consequently, by the trace theorem, $h_m|_{\Omega_c} \in H^{1-\varepsilon}(\Omega_c)$ since $\varepsilon \in (0, 1/2)$.

Local regularity

Darcy law

$$\mathbf{v} = -\mathbb{K}\nabla h_m$$

where $\mathbf{v}$ denotes the seepage velocity of fluid flows in the matrix.

Local regularity

Assume that $f_m \in L^2(\Omega_m)$, $f_c \in L^2(\Omega_c)$, $\alpha(x) \in L^\infty_+(\Omega_c)$ and each component in $\mathbb{K}$ belongs to $C^1(\bar{\Omega}_m)$. Suppose $\mathbf{h} \in \mathbf{H}$ be the weak solution with homogeneous Dirichlet boundary conditions. Then for each open set $V \subset \Omega_m$ with $V \cap \Omega_c = \emptyset$ we have the local regularity such that $h_m \in H^2(V)$.

Local regularity

Sketch of the proof

By taking the test function v_c in the conduit identically to zero in the weak form, we obtain the following weak form for $\mathbf{h}$ such that

$$\int_{\Omega_m} \mathbb{K}\nabla h_m(x,y)\cdot\nabla v_m(x,y)dxdy = -\int_{\Omega_c} \alpha(s)(h_m|_{\Omega_c} - h_c(s))v_m|_{\Omega_c} ds + \int_{\Omega_m} f_m v_m dxdy, \quad \forall v_m \in H_0^1(\Omega_m).$$

Take

$$v_m := -\mathscr{D}_k^{-l}(\eta^2 \mathscr{D}_k^l h_m)$$

where $\mathscr{D}_k^l h_m$ denotes the difference quotient. For $V \Subset W \Subset \Omega_m$ and $W \cap \Omega_c = \emptyset$, we have

$$\int_{\Omega_m} \mathbb{K}\nabla h_m(x,y)\cdot\nabla\left(-\mathscr{D}_k^{-l}(\eta^2\mathscr{D}_k^l h_m)\right)dxdy = \int_{\Omega_m} f_m\left(-\mathscr{D}_k^{-l}(\eta^2\mathscr{D}_k^l h_m)\right)dxdy.$$

Analysis of the forward model

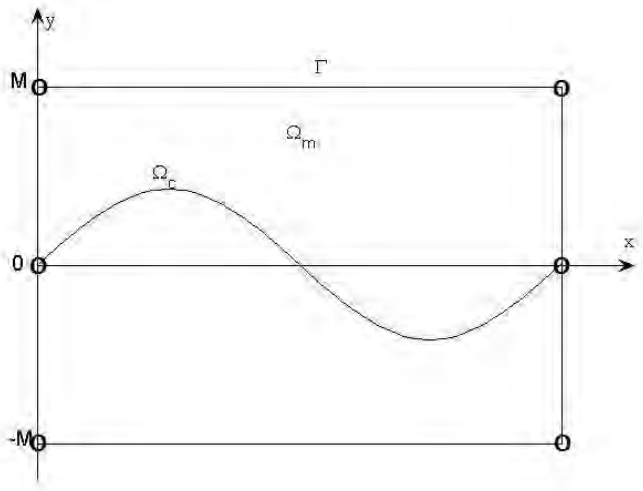

Figure: Singular points for the Neumann boundary conditions

Example 1 with Dirichlet boundary conditions

- $\Omega_m = (0,1)\times(-1/2,1/2)$, $\Omega_c = (0,1)\times\{0\}$;
- $\mathbb{K} = diag\{1,1\}$, $D = 1$, $\alpha = 1$;
- $h_m = \sin(2\pi x)(\max\{y,0\}+1)$ and $h_c = 2\sin(2\pi x)$.

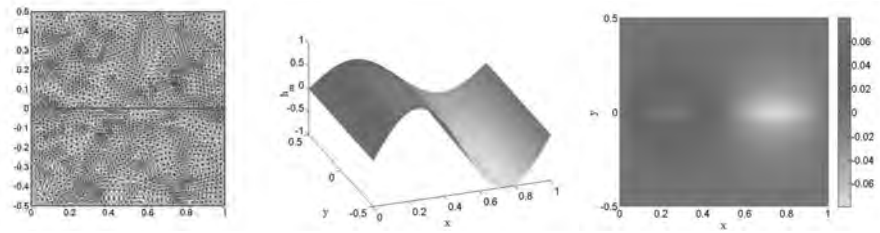

Figure: Left: the domain and mesh. Middle: the FEM solution of h_m. Right: the error between the FEM solution and the exact solution

Example 2 with Dirichlet boundary conditions

- $\Omega_m = (0,1)\times(-1/2,1/2)$, Ω_c are two half spheres;
- $\mathbb{K} = diag\{1,1\}$, $D = 1$, $\alpha = 1$;
- $h_m = \sin(2\pi x)(\max\{y,0\}+1)$ and $h_c = 2\sin(2\pi x)$.

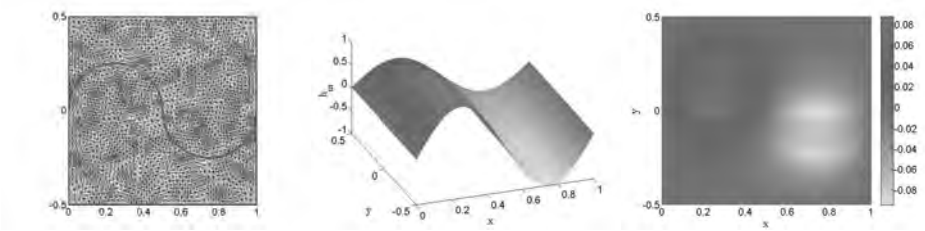

Figure: Left: the domain and mesh. Middle: the FEM solution of h_m. Right: the error between the FEM solution and the exact solution

Outline

Inverse Problems

J. B. Keller. Inverse problems. *Am. Math. Mon.*, 83:107–118, 1976

"We call two problems *inverses* of one another if the formulation of each involves all or part of the solution of the other. Often, for historical reasons, one of the two problems has been studied extensively for some time, while the other is newer and not so well understood. In such cases, the former problem is called the *direct problem*, while the latter is called the *inverse problem*."

IP (Determining the exchange rate function $\alpha(x)$)

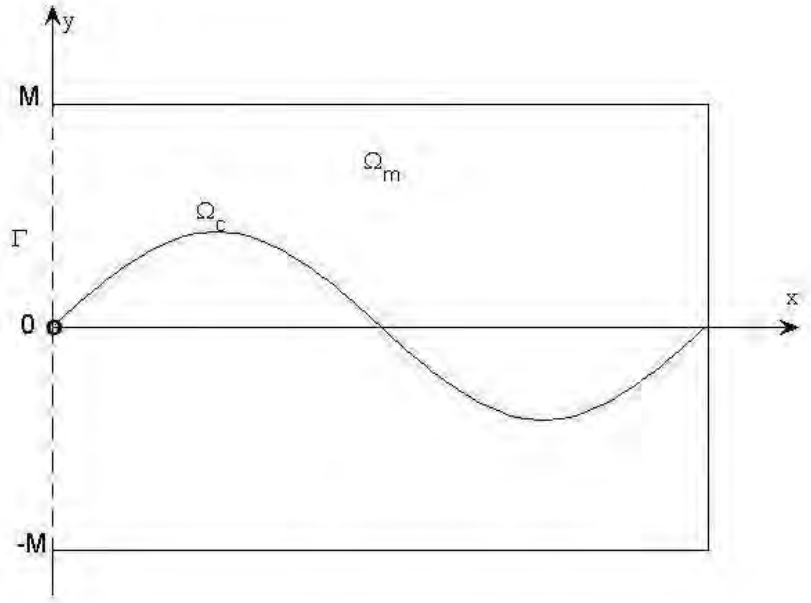

Cauchy data

Cauchy data

We assume, at part of the matrix boundary $\partial\Omega_m$, the following Cauchy boundary data

$$h_m(0,y)|_\Gamma = p(y)|_\Gamma,$$
$$\frac{\partial h_m(x,y)}{\partial x}|_\Gamma = q(y)|_\Gamma,$$

where Γ is chosen as a part of the y-axis such that $\Gamma := \{0\} \times (-M,0) \cup (0,M)$.
The Cauchy data at the conduit boundary Ω_c are assumed to be known similarly i.e.

$$h_c(0) = b_1 \quad \text{and} \quad \frac{\partial h_c(s)}{\partial \tau}|_{s=0} = b_2.$$

Uniqueness theorem

Uniqueness theorem

Denote $k(x) = \alpha(s(x))(h_m(x,\psi(x)) - h_c(s(x)))$, if there exist two functions $k_1(x)$ and $k_2(x)$ for the CCPF model

$$\begin{cases} -\nabla\cdot(\mathbb{K}\nabla h_m) = -\alpha(h_m - h_c)\delta_{\Omega_c} + f_m & \text{in} \quad \Omega_m \\ -\frac{\partial}{\partial\tau}(D\frac{\partial h_c}{\partial\tau}) = \alpha(h_m|_{\Omega_c} - h_c) + f_c, & \text{in} \quad \Omega_c \end{cases}$$

having the same Cauchy data, there holds $k_1(x) = k_2(x)$ almost everywhere.

Sketch of the proof

Holmgren's theorem and the fact that

$$\hat{k}(x) = k_1(x) - k_2(x),$$
$$\int_{\Omega_c} \hat{k}\chi ds = 0, \quad \text{for all} \quad \chi \in C_0^\infty(\Omega_c).$$

The forward problems

$$\textbf{ForP}\begin{cases} -\nabla\cdot(K\nabla h_m) = -\alpha(x)(h_m - h_c)\delta_{\Omega_c} + f_m \ in\ \Omega_m = (0,1)\times(-1,1) \\ -\frac{\partial}{\partial x}(D\frac{\partial h_c}{\partial x}) = \alpha(x)(h_m|_{\Omega_c} - h_c) + f_c \ in\ \Omega_c = (0,1)\times 0 \end{cases}$$

and the boundary conditions

$$\textbf{ForP BouCond}: \quad h_m|_{\partial\Omega_m} = g_D, \quad h_c(0) = c_1, \quad h_c(1) = c_2.$$

The goal is to identify the parameter function $\alpha(x)$ from additional observations of the Neumann boundary data

$$K\frac{\partial h_m}{\partial n}|_{\Gamma_1} = n_1(y), \quad K\frac{\partial h_m}{\partial n}|_{\Gamma_2} = n_2(y), \quad D\frac{\partial h_c}{\partial n}|_{\Gamma_3} = c_3$$

from $\Gamma_1 = \{x = 0, y \in (-1,0)\}$, $\Gamma_2 = \{x = 0, y \in (0,1)\}$ and $\Gamma_3 = \{x = 0, y = 0\}$.

IP (Determining the exchange rate function $\alpha(x)$)

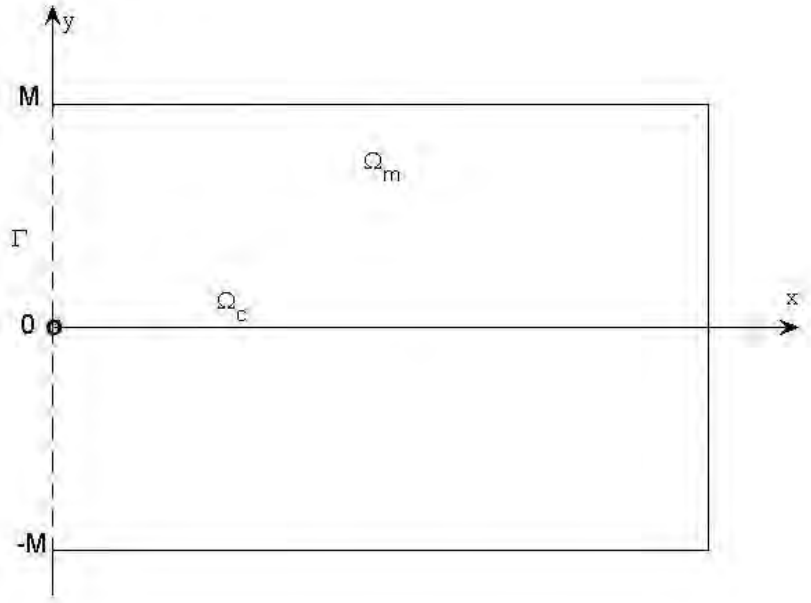

Parameter-to-output map

Nonlinear operator F

$$F : \alpha \to \left(K\frac{\partial h_m}{\partial n}|_{x=0,y\in(-1,0)}, K\frac{\partial h_m}{\partial n}|_{x=0,y\in(0,1)}, D\frac{\partial h_c}{\partial n}(0) \right).$$

Parameter to output: a compact operator

$$F(\alpha) = z$$

where $z = \left(K\frac{\partial h_m}{\partial n}|_{x=0,y\in(-1,0)}, K\frac{\partial h_m}{\partial n}|_{x=0,y\in(0,1)}, D\frac{\partial h_c}{\partial n}(0) \right)$.

Linearized problem

Linearized operator F'

Consider some test function $v(x)$, i.e. piecewise constants function for $\alpha(x)$ from the parameter function space. Then, the linearization of F at α is given by

$$F' = F'(\alpha) : v \to \left(K\frac{\partial u_m}{\partial n}|_{x=0,y\in(-1,0)}, K\frac{\partial u_m}{\partial n}|_{x=0,y\in(0,1)}, D\frac{\partial u_c}{\partial n}(0) \right).$$

$$\mathbf{LinP} \begin{cases} -\nabla\cdot(K\nabla u_m) = -\alpha(x)(u_m - u_c)\delta_{\Omega_c} - v(x)(h_m - h_c)\delta_{\Omega_c} \ in\ \Omega_m \\ -\frac{\partial}{\partial x}(D\frac{\partial u_c}{\partial x}) = \alpha(x)(u_m|_{\Omega_c} - u_c) + v(x)(h_m|_{\Omega_c} - h_c) \ in\ \Omega_c \end{cases}$$

with the linearized boundary conditions

$$\mathbf{LinP\,BouCond} \begin{cases} u_m|_{\partial\Omega_m} = 0, \\ u_c(0) = 0, \\ u_c(1) = 0. \end{cases}$$

Adjoint linearized problem

Adjoint linearized operator

Suppose we have an element $r = (r_1, r_2, r_3)$ belonging to the same space as our observation (which finally plays the role of **the iterative residual**). Then, the adjoint of $F'(\alpha)$ satisfies

$$\langle F'(\alpha)v, r\rangle_{\Gamma_1,\Gamma_2,\Gamma_3} = \langle v, F'(\alpha)^* r\rangle_{\Omega_c}.$$

Adjoint linearized problem

$$\mathbf{AdjP}\begin{cases} -\nabla\cdot(K\nabla\chi_m) = -\alpha(x)(\chi_m-\chi_c)\delta_{\Omega_c}\ in\ \Omega_m \\ -\frac{\partial}{\partial x}(D\frac{\partial\chi_c}{\partial x}) = \alpha(x)(\chi_m|_{\Omega_c}-\chi_c)\ in\ \Omega_c \end{cases}$$

with the boundary conditions

$$\mathbf{AdjP\,BouCond}\begin{cases} \chi_m|_{\Gamma_1} = r_1, \\ \chi_m|_{\Gamma_2} = r_2, \\ \chi_m|_{\Gamma_m\setminus(\Gamma_1\cup\Gamma_2)} = 0, \\ \chi_c(0) = r_3, \\ \chi_c(1) = 0 \end{cases}$$

with $\Gamma_1 = 0\times(-1,0)$, $\Gamma_2 = 0\times(0,1)$.

Iterative regularization schemes

Landweber iteration

Search for the fixed point

$$\alpha = \alpha + F'(\alpha)^*(z-F(\alpha)) \quad \text{or} \quad \min\|z-F(\alpha)\|^2$$

assuming that the operator F is Fréchet differentiable. The iteration form then is defined as follows

$$\alpha_{k+1} = \alpha_k + F'(\alpha_k)^*(z-F(\alpha_k)), \quad k = 1,2,\ldots.$$

Discrepancy principle (DP)

If the observation data contains noise, i.e. $z^\delta = z+\delta\xi$ where δ is the noise level and ξ is a random variable, the iteration will terminate at $k_* = k_*(\delta, z^\delta)$ step when the following criterion is satisfied

$$\|z^\delta - F(\alpha_{k_*+1})\| \le \tau\delta < \|z^\delta - F(\alpha_{k_*})\|$$

with $\tau \ge 1$.

Case study

The forward problem

$$\textbf{ForP}\begin{cases} -\Delta h_m = -\alpha(x)(h_m - h_c)\delta_{\Omega_c} + f_m \ in\ \Omega_m = (0,1)\times(-1,1) \\ -\frac{\partial^2 h_c}{\partial x^2} = \alpha(x)(h_m|_{\Omega_c} - h_c) + f_c \ in\ \Omega_c = (0,1)\times 0 \end{cases}$$

with exact exchange function $\alpha^\dagger(x) = 2+\sin(\pi x)$. Other functions are

$$\begin{aligned} h_c(x) &= 2\sin(\pi x) \quad \text{in} \quad x\in(0,1); \\ h_m(x,y) &= \sin(\pi x) \quad \text{in} \quad (x,y)\in(0,1)\times(-1,0); \\ h_m(x,y) &= (-(2+\sin(\pi x))y+1)\sin(\pi x) \quad \text{in} \quad (x,y)\in(0,1)\times(0,1). \end{aligned}$$

Initial guess

In all numerical tests, we choose the initial guess $\alpha_0 = 2$.

IRGNM algorithm

IRGNM iteration

The idea of the iteratively regularized Gauss-Newton method (IRGNM) is to find the next iteration solution α_{k+1} minimizing the following functional

$$\varphi(\alpha) := \|z - F(\alpha_k) - F'(\alpha_k)(\alpha-\alpha_k)\|^2 + \varepsilon_k\|\alpha-\alpha_0\|^2.$$

In an equivalent form (Euler equation), we obtain the iteratively regularized Gauss-Newton method

$$\alpha_{k+1} = \alpha_k + (F'(\alpha_k)^* F'(\alpha_k) + \varepsilon_k I)^{-1}(F'(\alpha_k)^*(z - F(\alpha_k)) + \varepsilon_k(\alpha_0 - \alpha_k))$$

where I is an identity matrix and ε_k is the regularization parameter.

Outline

Extended results: decoupling

Decoupled CCPF model

Assume the exchange coefficient function $\alpha(x) = \alpha$ with a constant $\alpha > 0$, $\Omega_m := (0,L) \times (-M,M)$ and $\Omega_c := (0,L) \times \{0\}$. The forward CCPF model with $\mathbb{K} = diag(1,1)$ and $D = 1$ yields

$$\begin{cases} -\triangle h_m = -\alpha(h_m - h_c)\delta_{\Omega_c} + f_m & \text{in} \quad \Omega_m, \\ -\frac{\partial}{\partial x}(\frac{\partial h_c}{\partial x}) = \alpha(h_m|_{\Omega_c} - h_c) + f_c, & \text{in} \quad \Omega_c. \end{cases}$$

Additionally, assume the Dirichlet boundary condition of Ω_m and Ω_c such that

$$\begin{aligned} h_c(0) &= h_m(0,y) = b_0, \\ h_c(L) &= h_m(L,y) = b_1, \\ h_m(x,-M) = b_0 + \frac{x}{L}(b_1 - b_0), &\quad h_m(x,M) = b_0 + \frac{x}{L}(b_1 - b_0), \end{aligned}$$

then there holds $h_m(x,y)|_{\Omega_c} = h_c(x)$ almost everywhere along the conduit Ω_c.

Extended results: conduit uniqueness

Uniqueness of the conduit

Under appropriate assumptions, if two conduits have the same Cauchy data for $h_{m,i}$ at the boundary $\Gamma := \{0\} \times (-M,0) \cup (0,M)$ such that

$$h_{m,i}(0,y)|_\Gamma = p(y)|_\Gamma,$$
$$\frac{\partial h_{m,i}(x,y)}{\partial x}|_\Gamma = q(y)|_\Gamma,$$

moreover, assume that $h_m|_{\Omega_c}(x) \neq h_c(x)$ almost everywhere, there holds $\Omega_{c,1} = \Omega_{c,2}$. Additionally, if the Cauchy data for $h_c(s)$ at $s = 0$ is known, namely,

$$h_c(0) = b_1 \quad \text{and} \quad \frac{\partial h_c(s)}{\partial \tau}|_{s=0} = b_2,$$

simultaneously we obtain $\alpha_1(s) = \alpha_2(s)$ almost everywhere along the conduit.

Summary

1. Introduction of the CCPF model;
2. Forward problems:
   Well-posedness and simulation of the model;
3. Inverse problems:
   Uniqueness and reconstruction of the exchange rate function.

References

F. Hua (2009)

Modeling, analysis and simulation of Stokes-Darcy system with Beavers-Joseph interface condition

Ph.D. dissertation, Florida State University, 2009.

X. Wang (2010)

On the coupled continuum pipe flow model (CCPF) for flows in karst aquifer

Discret. and Contin. Dyn. Sys. - Ser B 13: 489–501, 2010

Y. Cao, M. Gunzburger, F. Hua and X. Wang (2011)

Analysis and finite element approximation of a coupled, continuum pipe-flow/darcy model for flow in porous media with embedded conduits

Num. Meth. PDE 27: 1242–1252, 2011

S. Lu, N. Chen, B. Hu and J. Cheng (2012)

On the inverse problems for the coupled continuum pipe flow model for flows in karst aquifers

Inverse Problems 28, 065003(16pp), 2012.

Thank you for your attention.

Jin Cheng

School of Mathematical Sciences, Fudan University

Email: jcheng@fudan.edu.cn

/

System Identification on a Frame Structure Using Variable Parametric Projection Filter

Ryuji ENDO
Prof. of Dept. of Architecture,
Polytechnic University of Japan

1. はじめに

我が国の建築構造物のライフサイクルは欧米のそれに比べて極めて短いことが指摘されている。その理由の一つに地震国であり，厳しい耐震基準が挙げられている。わが国が規定している耐震コードは，中程度の地震に対する耐震コードと大地震に対する耐震コードに大別できる。中地震に対する耐震コードでは，地震後の損傷は許容しておらず，あくまでも弾性範囲の挙動であることが義務付けられている。これに対して，大地震に対する耐震設計では塑性変形を許容しているが，人命の確保を義務付けている。現実には地震後の建築物の剛性は，弾性範囲の挙動であったとしても幾らかの剛性低下は見られるし，大地震後では，目視による損傷まで達していなくても塑性化が進行している可能性がある。一方，新築時には厳しい耐震設計に基づいている建築物も，年数を重ねるごとに経年劣化の進行とともに，建物を構成する各部材の剛性が低下し，やがて部材レベルの剛性低下はシステムレベルの剛性低下に発展していくことになる。

建築物の耐震性は，強度と剛性の観点から評価されなければならない。強度の評価は，弾性範囲であれば部材に生じている応力が許容応力以下であることが必要とされ，塑性設計においては保有水平耐力が必要保有水平耐力以上であることが耐震設計の条件とされている。剛性の評価に関しては変形量として捉えられている。例えば，水平剛性が低下すると，水平方向の変形が大きくなり層崩壊を誘発する原因として考えられる。そこで，一般に建築物の耐震性もしくは健全性の評価に当たっては，水平剛性を非破壊的に求めることが提案されている。これらの方法は構造ヘルスモニタリングと呼ばれており，数理的手法では逆問題解析として定式化される。

こうした逆問題解析に基づく構造ヘルスモニタリングは，海洋中に建設された石油掘削プラットフォームの海中部分の構造体に関する健全性のチェック手法として提案された経緯がある。Paura F. Vioro ら [1]は，海洋プラットフォームの構造ヘルスモニタリングの方法における損傷検出方法として，Modal assurance criterion (MAC), Coordinate modal assurance criterion (COMAC), Modal scale factor (MSF), Modal shape relative difference method (RD)および Change in modal vector perpendicular to predominant modal direction　の 5 種類の手法を比較している。これらの方法は構造物の振動特性を利用するものであり，何らかの原因で損傷が生じ剛性が低下することに起因して，対象とする構造物の固有振動数および固有モードの変化からシステムの状態を検出する手法である。このように，モーダルパラメータの変化を用いてシステムの状態を推定するシステム同定は，先の 5 種類の方法の他に多くの研究者によって多くの方法が提案されている。濱本ら [2]は，アクティブ同定手法と名付けた構造ヘルスモニタリング手法を提案しているし，

三田ら[3]は,主に電気的・機械的制御システムを駆使することで損傷確率評価を報告している。竹脇ら[4]は高層建築物の剛性の同定に関して，せん断変形と曲げ変形を分離する方法を提案している。また，西谷ら[5]は，実大振動台実験データを用いて，部材レベルの損傷評価を提案している。さらに，古川ら[6]は構造物に用いられる鋼板に着目し，損傷に伴う鋼板の振動特性について検討した結果を報告している。

ここまで述べてきた比較的新しい手法の提案に対して，伝統的な逆解析手法としてカルマンフィルタを用いた方法がある。一般的なカルマンフィルタによる方法[7]は，時間とともに変化する信号の動特性，雑音の統計的性質，そして初期値に関する先見情報を与える線形確率ダイナミックシステムに関して，未来を予測する Prediction 問題，現在を推定する Filtering 問題そして過去を推定する Smoothing 問題において観測ベクトルを用いて状態ベクトルを推定する問題として発展してきた。これに対して，村上[8]はフィルタリングの過程で時間的遷移構造を持たないことを仮定することにより，フィルタ方程式を繰り返し計算アルゴリズムとして用い，有限要素法による離散化と組み合わせることにより，基礎構造物の状態を推定するためのカルマンフィルタ有限要素法を提案している。登坂[9]は離散化方法を有限要素法に替えて境界要素法を用いることにより，弾性板内に点在するき裂を想定した孔の位置と大きさを推定する方法を提案している。筆者[10]は，これらの方法を踏襲し，すなわちカルマンフィルタを繰り返し計算アルゴリズムとして用い，固有振動数を観測データとして中低層の建物の層剛性を同定する方法を提案した。

近年，こうした同定問題は大規模な変数を有する問題に適用することを念頭に，データ同化[11]によりパラメータを推定し，カルマンフィルタの有用性を引き出したアンサンブルカルマンフィルタ[12]が提案されている。これに対して筆者ら[13]は，Kalman フィルタに用いられている Wiener フィルタに変えてパラメトリック射影フィルタを用いることを提案した。パラメトリック射影フィルタには Tikhonov の正則化パラメータに対応する項が含まれていることに特徴を有している。数学的にはともかく，構造ヘルスモニタリングとしての工学問題では，正則化パラメータを計算的に決定することが望まれる。本報では，筆者らにより開発された各フィルタリングステップでパラメトリック射影フィルタの正則化パラメータを計算的に決定する，可変的パラメトリック射影フィルタを用いた逆問題解析に関し，固有振動数を観測データとして 5 層フレームモデルの層剛性を同定する問題において，振動モードを用いて決定する正則化パラメータの特性に基づく，可変的パラメトリック射影フィルタの特性について検討することを目的としている。

なお，本報では我が国において耐震性を検討する要因となる地震の頻発している現状を示し，さらに大地震に対する設計の方針を示すことから本研究の必要性を強調することにする。

2. 我が国における地震の発生状況と大地震における塑性変形

我が国は，地球を覆っている北米プレート，太平洋プレート，フィリピン海プレート及びユーラシアプレートがお互いに重なっているところに位置している。プレートテクトニクス理論に従えば，プレート境界ではプレートが移動し，プレート境界もしくはプレート内部において，蓄積されたひずみエネルギーがやがて地震となって解放される現象である。従って，日本の周辺では地震が多発することが理解できよう。Fig.1 に気象庁のホームページから引用したデータを用いた日本周辺と地球全体の過去の地震記録を示す。

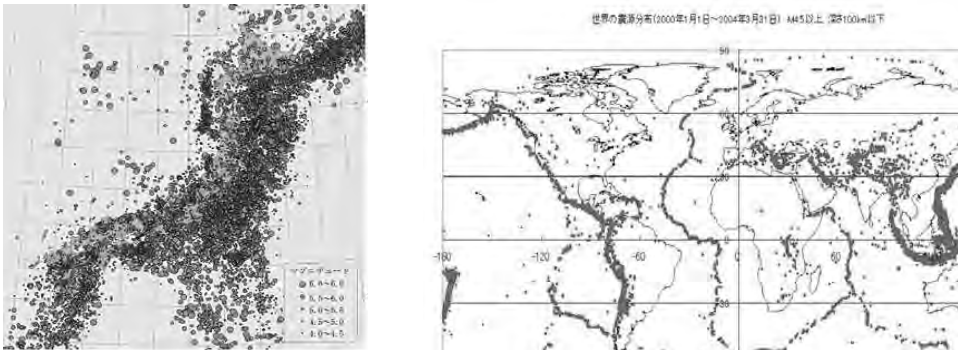

Fig.1　Japan and world maps of earthquake distribution.

Fig.1 に示す左の日本周辺では日本地図が判別できないくらい過去の地震記録で塗りつぶされており，また右の世界における地震記録では右端に位置する日本は特に濃く塗りつぶされていることがわかる。地震の大きさは，震源におけるエネルギーの大きさを表すマグニチュードと，建築物が存在するサイトにおける地震の大きさを表す目途となる震度階であらわされる。マグニチュードが大きくても，震源から遠く離れていれば構造物に地震の影響は生じない。さて，先に述べたように，耐震設計では地震を 2 種類に大別するが，中程度までの地震とは震度 5 程度までと考えられ，震度 5 強以上の地震は大地震といえよう。大地震における塑性変形のイメージを Fig.2 に示しておく。

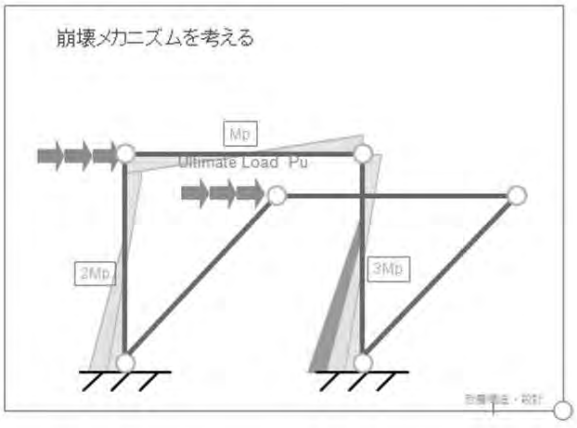

Fig.2 Collapse mechanism of frame structure.

Fig.2 における実線はフレーム構造に地震力を水平力として作用させた場合，塑性ヒンジを形成した状態が示されている。大地震が作用した構造物は塑性変形が許容されているが，実際には靭性を確保するため，曲げモーメントの大きいところで塑性ヒンジを形成させることになる。建築構造物に地震力が作用すると，その地震が比較的小さい地震でも水平剛性は低下しているし，大地震では塑性ヒンジによって剛性が低下するため固有周期

が変化する。本研究は，このように損傷によって剛性低下した状態を固有周期の変化から非破壊的に推定しようとするものである。

3. 逆問題解析の構成

地震や経年劣化によって剛性低下した建築構造物の状態を，固有周期を観測量として非破壊的に同定する逆問題解析を構成する。逆解析手法にはフィルタ理論を援用したフィルタリングアルゴリズムを採用し，復元作用素として筆者らが開発した可変的パラメトリック射影フィルタを用いた場合と，さらに比較の意味で Wiener フィルタを用いる場合についても述べることにする。

3.1 数理モデル

逆問題を離散的立場から扱うものとし，推定（同定）すべき未知量は有限次元ベクトルとすると，その逆問題の数理モデルは次のように与えることができる。

・観測方程式（システム方程式）

$$\boldsymbol{y} = \boldsymbol{M}\boldsymbol{z} + \boldsymbol{v} \tag{1}$$

・推定方程式（復元方程式）

$$\tilde{\boldsymbol{z}} = \boldsymbol{B}(\boldsymbol{y}) \tag{2}$$

ここで，ベクトル $\boldsymbol{z}$ は推定または同定すべき原ベクトル，$\boldsymbol{y}$ は観測ベクトル，$\tilde{\boldsymbol{z}}$ は $\boldsymbol{z}$ に対する推定ベクトル，$\boldsymbol{v}$ は観測に伴い混入する雑音ベクトル，行列 $\boldsymbol{M}$ は観測行列，$\boldsymbol{B}$ は推定行列（復元行列）とする。なお，上式中のベクトルは雑音ベクトル $\boldsymbol{v}$ の存在により，いずれも確率変数（ベクトル）として取り扱わねばならない。

この数理モデルにより，逆問題は，観測行列 $\boldsymbol{M}$ を与えてノイズ $\boldsymbol{v}$ の統計的性質と，与えられた観測ベクトル $\boldsymbol{y}$ のもとで，次の評価基準を満たす $\boldsymbol{z}$ の最良な推定ベクトル $\tilde{\boldsymbol{z}}$ を定めることになる。

$$\boldsymbol{J} = \boldsymbol{J}(\boldsymbol{z}, \tilde{\boldsymbol{z}}) \rightarrow Min \tag{3}$$

したがって，この最小化問題の解 $\boldsymbol{z}$ を与えるような推定行列 $\boldsymbol{B}$ を具体的に構成しなければならない。

3.2 フィルタ理論

推定行列 $\boldsymbol{B}$ を線形不偏推定条件のもとで構成することにすると $\boldsymbol{z}$ の期待値 $\bar{\boldsymbol{z}}$ を用いて推定ベクトルは次のように与えられる。

$$\tilde{\boldsymbol{z}} = \bar{\boldsymbol{z}} + \boldsymbol{B}\{\boldsymbol{y} - \boldsymbol{M}(\bar{\boldsymbol{z}})\} \tag{4}$$

したがって，推定行列 $\boldsymbol{B}$ が具体的に与られれば，観測ベクトル $\boldsymbol{y}$ を用いて上式（4）から推定ベクトル $\tilde{\boldsymbol{z}}$ が決定できる。

この推定行列として，評価基準(3)の具体的な表現に対応して Wiener フィルタ，射影フィルタ，パラメトリック射影フィルタ等が存在している。これらのフィルタの中でも本報

で対象とするフィルタはパラメトリック射影フィルタである。このフィルタは次の評価基準に対して構成される。

評価基準：

$$\boldsymbol{J(B)} := tr\{(\boldsymbol{BM} - \boldsymbol{P})(\boldsymbol{BM} - \boldsymbol{P})^{T}\} + \gamma\, \boldsymbol{E}_{v}\left[\|\boldsymbol{Bv}\|^{2}\right] \tag{5}$$

パラメトリック射影フィルタ：

$$\boldsymbol{B} = \boldsymbol{M}^{T}\left(\boldsymbol{M}\,\boldsymbol{M}^{T} + \gamma \boldsymbol{Q}\right)^{-1} \tag{6}$$

ただし，$\gamma > 0$ はいわゆる s/n としての意味を有するパラメータであり，$\boldsymbol{P}$ は射影行列とし，T は行列の転置操作を示し，tr は行列のトレース操作とし，雑音共分散行列を以下のように定義する。

$$\boldsymbol{Q} := E[\ \boldsymbol{vv}^{T}\ ] \tag{7}$$

ここに，E は期待値を意味する。

ここで，Wiener フィルタおよび射影フィルタと比較しながらパラメトリック射影フィルタの特徴を概説しておく。まず，Wiener フィルタは未知状態ベクトル $\tilde{\mathbf{z}}$ に関する平均操作を行っているため，出現確率の高い量ほど精度よく推定されるような評価関数を満足しており，個々の状態ベクトル $\mathbf{z}$ と推定量 $\tilde{\mathbf{z}}$ のノルム $\|\ \mathbf{z}-\tilde{\mathbf{z}}\ \|$ を最良近似する保証は存在しない。Fig.3 に Wiener フィルタの復元写像と評価基準および Wiener フィルタの具体的な表現を示す。

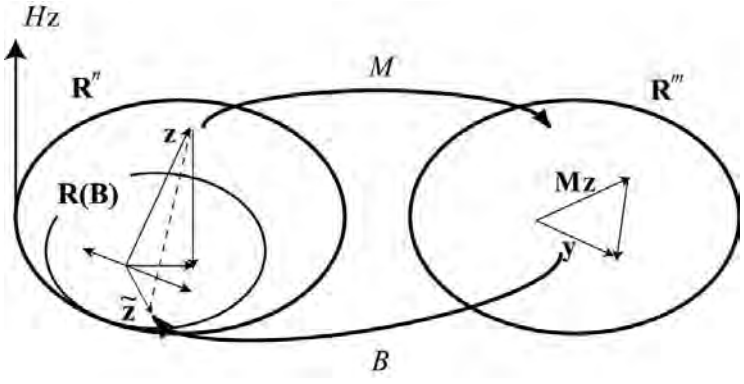

Fig.3　Restoration mapping of Wiener filter.

評価基準(Wiener フィルタ)：

$$EzEv\|z-\tilde{z}\|^{2} \rightarrow Min \tag{8}$$

Wiener フィルタ：

$$\boldsymbol{B} = \boldsymbol{RM}^{T}(\boldsymbol{MRM}^{T} + \boldsymbol{Q})^{-1} \tag{9}$$

これに対して射影フィルタは基本的に状態ベクトル $\boldsymbol{z}$ の射影 $\boldsymbol{Pz}$ が推定量 $\tilde{\boldsymbol{z}}$ と一致するように構成されている。通常，推定量 $\tilde{\boldsymbol{z}}$ は観測誤差の影響により，$\boldsymbol{z}$ の最良近似 $\boldsymbol{Pz}$ の周りに散らばることになる。射影フィルタは観測誤差ベクトルのみに関して平均操作を考慮した評価関数を満足する解として与えられるため，フィルタリング計算の安定性において大変厳しいフィルタといえる。Fig.4 に射影フィルタの復元写像と評価基準および射影フィルタの具体的な表現を示す。

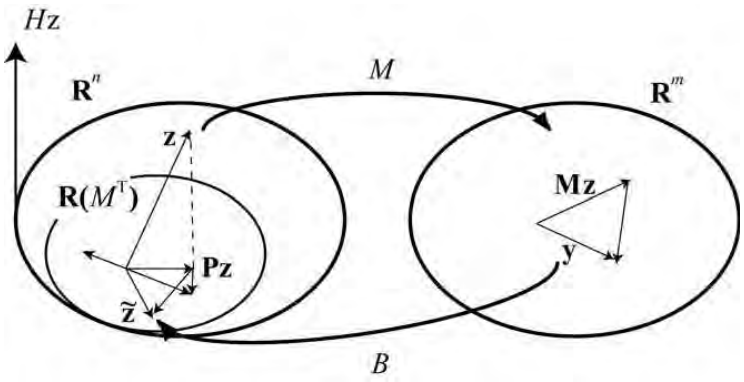

Fig. 4　Restoration mapping of Projection filter.

評価基準（射影フィルタ）：

$$E\boldsymbol{v}\left\|\tilde{\boldsymbol{Z}}-\boldsymbol{Pz}\right\|^2 = E\boldsymbol{v}\left\|\boldsymbol{Bv}\right\|^2 \rightarrow Min \tag{10}$$

射影フィルタ：

$$\boldsymbol{B}=(\boldsymbol{M}^T\boldsymbol{Q}^{-1}\boldsymbol{M})^{-1}\boldsymbol{M}^T\boldsymbol{Q}^{-1} \tag{11}$$

一方，パラメトリック射影フィルタの評価基準(5)は射影フィルタの制約条件を緩和すると同時に，これに伴うノイズを抑制する度合いのバランスをパラメータ γ によって調整していることになる。

ところで，よく知られているように，逆解析は一般に非適切性を伴うことになる。様々な逆解析に多用され，拡張 Kalman フィルタを構成することで知られている Wiener フィルタには推定誤差共分散が含まれており，フィルタリングステップに応じてこれを更新することで，フィルタリングの安定化を図る，いわゆる正則化の役割を担っていると考えられる。これに対して，射影フィルタは射影を介して直接目標値に対応する状態量と状態推定量を比較することになり，フィルタリング計算の安定化を図るための正則化項はまったく含まれていない。パラメトリック射影フィルタはこの点が改善されており，Tikhonov の正則化項に関連し，スカラー量で与えられるパラメータ γ が含まれていることによりフィルタリング計算が安定しているものと考えられる。換言すれば，パラメトリック射影フィルタを採用することは，パラメータ γ を正則化パラメータとして捉えることにより，安定化の一手法としてノイズの統計的な先見情報として共分散行列 $\boldsymbol{Q}$ を用いた正則化を図

る効果が期待される。Fig.5 にパラメトリック射影フィルタの復元写像を示す。

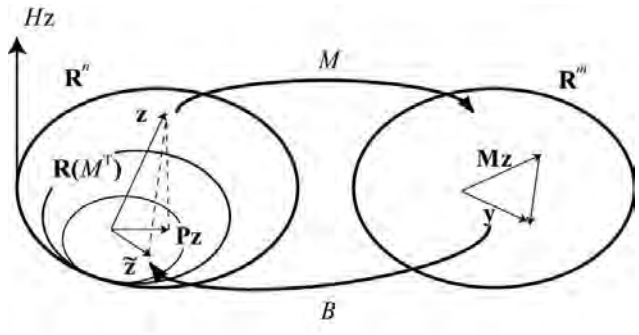

Fig.5　Restoration mapping of Parametric Projection filter.

3.3 可変的パラメトリック射影フィルタリングアルゴリズム

パラメトリック射影フィルタ(6)には，パラメータ γ が含まれているので，このフィルタを用いて推定を行うには γ の具体的な数値が必要となる。この数値の決定に関して，本報では以下に示すような可変的決定手法を導入することによって，任意の初期値からフィルタリングの計算過程を通して自律的に適切な数値を取ることのできる可変的パラメトリック射影フィルタリングアルゴリズムを構成する。

線形不偏推定式(4)に基づくフィルタリングアルゴリズムにおけるフィルタ方程式とフィルタゲインは次のように与えられる。ただし，これ以降，フィルタ方程式や復元作用素はフィルタリング過程において時間的遷移構造を持たないことを仮定し，添え字 t は時間ステップではなく繰り返しステップとして扱う。

フィルタ方程式：

$$\tilde{\boldsymbol{z}}_{t-1/t} = \tilde{\boldsymbol{z}}_{t/t} = \tilde{\boldsymbol{z}}_{t/t-1} + \boldsymbol{B}_t(\boldsymbol{y}_t - \boldsymbol{M}_t\tilde{\boldsymbol{z}}_{t/t-1}) \tag{12}$$

フィルタゲイン：

$$\boldsymbol{B}_t = \boldsymbol{M}_t^T(\boldsymbol{M}_t\boldsymbol{M}_t^T + \gamma\boldsymbol{Q}_t)^{-1} \tag{13}$$

ただし，推定ベクトル初期値を次のように与えるものとする。

$$\tilde{\mathbf{z}}_{0/-1} = \bar{\mathbf{z}}_0 \tag{14}$$

ここで，初期ステップにおいて，推定ベクトル $\tilde{\boldsymbol{z}}'_{0/-1}$ は観測ベクトル $\boldsymbol{y}_0$ のみによって決定しているので，それらの間に比例関係が成り立つものと仮定すると次のように書くことができる。

$$\tilde{\boldsymbol{z}}'_{0/-1} \fallingdotseq \boldsymbol{A}_0\boldsymbol{y}_0 (= \boldsymbol{A}_0\boldsymbol{M}_0(\tilde{\boldsymbol{z}}'_{0/-1})) \tag{15}$$

ただし, 行列 $\boldsymbol{A}_0$ は対角行列とする。一方, 初期ステップのフィルタ方程式は近似的に式(12)より次のように書くことができる。

$$\tilde{\boldsymbol{z}}'_{0/-1} \fallingdotseq \boldsymbol{B}_0 \boldsymbol{y}_0 \tag{16}$$

これらの式を等置することによって次式を得る。

$$\boldsymbol{A}_0 \boldsymbol{y}_0 = \boldsymbol{B}_0 \boldsymbol{y}_0 = \left(\boldsymbol{M}_0^T \boldsymbol{Q}_0^{-1} \boldsymbol{M}_0 + \gamma \boldsymbol{I}\right)^{-1} \boldsymbol{M}_0^T \boldsymbol{Q}_0^{-1} \boldsymbol{y}_0 \tag{17}$$

パラメトリック射影フィルタの表現(6)より，パラメータの初期値に関する次の関係式を得る。

$$\gamma_0 \tilde{\boldsymbol{z}}'_{0/-1} = \boldsymbol{b}_0 \tag{18}$$

ただし,

$$\boldsymbol{b}_0 = \boldsymbol{M}_0^T \boldsymbol{Q}_0^{-1} (\boldsymbol{I} - \boldsymbol{M}_0 \boldsymbol{A}_0) \boldsymbol{y}_0 \tag{19}$$

以上より，γ_0 は $\tilde{\boldsymbol{z}}'_{0/-1}$ と $\boldsymbol{b}_0$ との内積と $\tilde{\boldsymbol{z}}'_{0/-1}$ のノルムとを用いて次式で与えられる。

$$\gamma'_0 = \frac{\tilde{\boldsymbol{z}}_{0/-1} \cdot \boldsymbol{b}_0}{\left\| \tilde{\boldsymbol{z}}'_{0/-1} \right\|^2} \tag{20}$$

このように求められた γ'_0 を含んだパラメトリック射影フィルタを構成し，フィルタ方程式より $\tilde{\boldsymbol{z}}'_{0/-1}$ を求める。これらの計算をγの値が収束するまで繰り返し，その収束値をフィルタリング 1 回目の値とする。同様にして各フィルタリングのステップにおいて収束値の γ を決定することになる。

4. 構造損傷同定問題への適用

4.1 拡張フィルタリングアルゴリズム

固有振動数を観測データとして5層フレームモデルの各層の水平剛性を同定するために前章で述べたkalmanフィルタと筆者らが開発した可変的パラメトリック射影フィルタに基づくアルゴリズムを採用する。フィルタリング過程で状態量は時間的遷移構造を持たないことを仮定すると，遷移行列は単位行列 I で書くことができ，状態方程式は次式で書くことができる。

$$\hat{\boldsymbol{Z}}_{t+1} = \boldsymbol{I} \hat{\boldsymbol{Z}}_t \tag{21}$$

従って，添字 t は時間領域を表すものでなく，計算ステップの回数を意味し，改めて $\hat{\boldsymbol{Z}}$ は状態量の推定値を意味する。状態量である剛性と固有振動数との関係は非線形であるので観測方程式は次のように表すことにする。

$$\begin{aligned} \boldsymbol{y}_t &= m_t(\boldsymbol{z}_t) + \boldsymbol{\nu}_t \\ &\fallingdotseq \boldsymbol{M}_t \boldsymbol{Z}_t + \boldsymbol{\nu}_t \end{aligned} \tag{22}$$

ここに $\mathbf{y}_t$ は観測ベクトルであり，$m_t(\boldsymbol{z}_t)$ は非線形ベクトル関数である。$\boldsymbol{M}_t$ は非線形ベク

トル関数を Taylor 展開し高次項を無視した次式の感度行列である。

$$\boldsymbol{M}_t = \left(\frac{\partial m_t(\boldsymbol{Z}_t)}{\partial \boldsymbol{Z}_t} \right)_{\boldsymbol{Z}_t = \hat{\boldsymbol{Z}}_{t/t-1}} \tag{23}$$

繰り返し計算アルゴリズムを構成するフィルタ方程式は次式で表される。

$$\hat{\boldsymbol{Z}}_{t/t} = \hat{\boldsymbol{Z}}_{t/t-1} + \boldsymbol{B}\left(\boldsymbol{\omega} - m_t\left(\hat{\boldsymbol{Z}}_{t/t-1}\right)\right) \tag{24}$$

ここに，$\boldsymbol{\omega}$は観測ベクトルであり，各モードに対応する固有振動数である。また $\hat{\boldsymbol{Z}}_{t/t-1}$ は t-1 回目の情報に基づく t 回目の状態量である。$\boldsymbol{B}$はフィルタゲインであり，状態量$\boldsymbol{z}$の変化量をコントロールする役割を持っており，Wiener フィルタの評価基準を満足するフィルタゲインを用いると拡張カルマンフィルタのアルゴリズムとなり，射影フィルタ族としてのパラメトリック射影フィルタの評価基準を用いることもできる。本報では，次式に示すこれらの 2 種類のフィルタゲインを採用する。

Wiener フィルタ：

$$\boldsymbol{B}_w = \boldsymbol{R}\boldsymbol{M}_t^T(\boldsymbol{M}_t\boldsymbol{R}_t\boldsymbol{M}_t^T + \boldsymbol{Q})^{-1} \tag{25}$$

パラメトリック射影フィルタ：

$$\boldsymbol{B}_{ppf} = (\boldsymbol{M}_t^T\boldsymbol{Q}^{-1}\boldsymbol{M}_t + \gamma\boldsymbol{I})\boldsymbol{M}_t^T\boldsymbol{Q}^{-1} \tag{26}$$

ここに $\mathbf{R}_t$ は推定誤差共分散行列であり，Wienerフィルタおよびパラメトリック射影フィルタのそれらは次式で与えられる。

$$\hat{\boldsymbol{R}}_{t/t} = \hat{\boldsymbol{R}}_{t/t-1} - \boldsymbol{B}_w\boldsymbol{M}_t\hat{\boldsymbol{R}}_{t/t-1} \tag{27}$$

$$\hat{\boldsymbol{R}}_{t/t} = \hat{\boldsymbol{R}}_{t/t-1} + \boldsymbol{B}_{ppf}\left(\boldsymbol{M}_t\hat{\boldsymbol{R}}_{t/t-1}\boldsymbol{M}_t^T + \boldsymbol{Q}\right)\boldsymbol{B}_{ppf}^T - \boldsymbol{B}_{ppf}\boldsymbol{M}_t\boldsymbol{R}_{t/t-1} - \hat{\boldsymbol{R}}_{t/t-1}\boldsymbol{M}_t^T\boldsymbol{B}_{ppf}^T \tag{28}$$

$\boldsymbol{R}_t$ の計算では拡張カルマンフィルタは陽に計算され，状態量を収束させる性質として知られており，消極的な正則化と言えるかもしれない。しかし，パラメトリック射影フィルタには直接計算するための $\boldsymbol{R}_t$ は含まれていない。

また$\boldsymbol{Q}_t$は観測雑音共分散行列であり，観測量$\boldsymbol{\omega}$と計算値$m_t\left(\hat{Z}_{t/t-1}\right)$ とが一致するまで繰り返し計算することになる。ところでパラメトリック射影フィルタには正則化項γが含まれている。このγを各フィルタリングステップで計算的に決定するパラメトリック射影フィルタが可変的パラメトリック射影フィルタである。

フィルタ方程式 (24) は非線形であるため繰り返し計算アルゴリズムとする場合は，初期値 (29) が計算結果および計算安定性に影響するので初期値の設定は極めて重要である。

$$\hat{\boldsymbol{Z}}_{0/-1} = \overline{\boldsymbol{Z}}_0,\ \ \hat{\boldsymbol{R}}_{0/-1} = \boldsymbol{R}_0 \tag{29}$$

4.2 可変的アルゴリズムの正則化

正則化項を決定する式(20)の計算過程は近似的なフィルタ方程式を用いており，すなわちフィルタリング計算を正則化することなしに行っていることに等しく，ここでも非適切

性が生ずることになる。そこで本研究では，多変数で与えられる式(20)の計算において，対角行列$\mathbf{A_0}$の特定の成分に着目し，1変数として計算することにより正則化を図ることにする。これよりγを決定するための繰り返し計算はスカラー表記され，次式で表すことができる。

$$\gamma_{0/-1} = \mathrm{M}Q^{-1}(1 - a_{0n}\mathrm{M})\omega_{0/-1}\hat{Z}_{0/-1}^{-1} \qquad (30)$$

4.3 モード依存性

正則化項γの決定に当り，1変数とした式(30)を用いると，特定のモードの固有振動数$\omega_{0/-1}$に着目して計算する必要がある。本逆解析では1次～5次モードのいずれかを用いることができる。これまでの経験から1次～5次のモードの内，どのモードの固有値を用いることにより解の精度と安定性に影響することが分かっている。本研究では1次～5次モードの固有値を用いて正則化した解の精度と安定性についてモード依存性と呼び，検討を加えるものとする。

4.4 逆問題の対象としてフレームモデルと観測データ

本逆解析はFig.6に示す6種類の5層鋼製フレームモデルの水平剛性を実測された固有振動数を用いて同定する。詳細は後に譲るがTable 1及び2に観測データとしての固有振動数を示す。それぞれのモデルに対応して固有振動数が異なっていることがわかる。

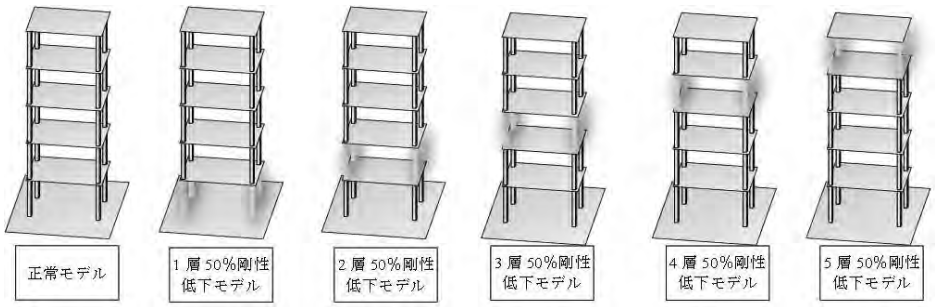

Fig.6　6 kinds of frame model used in experiments to measure observation data.

4.5 観測データの測定

観測データは固有振動数であることから，測定に当たっては実験モード解析を採用した。実験モード解析は固有振動数，固有モードおよび減衰比を求めるための実用的な実験解析手法であり，一般に加振実験から得られる周波数応答関数の測定と，モーダルパラメータの同定の２つのカテゴリーから成り立っている。加振実験では簡単な手法とされているインパクトハンマによる方法が用いられており，インパクトハンマに内蔵されているロードセルによる加振力と各層に設置された圧電型の加速度計からの応答によって周波数応答関数を求めモーダルパラメータを同定している。カーブフィットされた周波数応答関数のグラフをFig.8に示す。またTable 1に本研究で採用した非減衰せん断型質点系とした数理モデルによる解析値を示す。またTable 2に実験モード解析より得られた固有振動数の実測値を示す。

また，先に述べたフィルタリング過程における数理モデルとしての固有方程式は質点系としての次式を用いた。

$$\left|\boldsymbol{K}-\omega^2\boldsymbol{M}\right|=0 \qquad (31)$$

ここに $\boldsymbol{K}$ は水平剛性行列，$\boldsymbol{M}$ は質量行列，ω^2 は固有値を意味する。

実験モード解析のイメージをFig.7に示し，周波数応答関数をFig.8に示す。

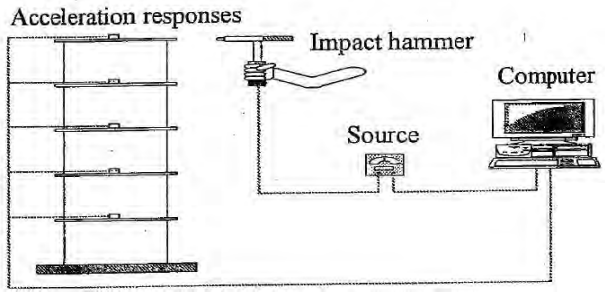

Fig.7　Experimental modal analysis system (EMA).

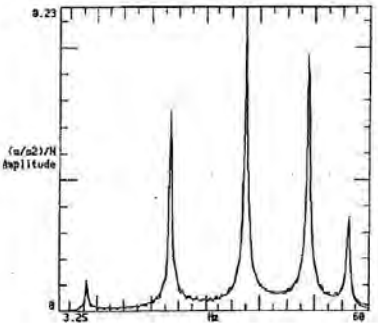

Fig.8　Frequency Response Function obtained by EMA.

式(31)により計算された固有振動数をTable 1に示し，実験モード解析より得られた固有振動数をtable 2に示す。両者はほぼ一致していることがわかる。この固有振動数より角速度を求め観測データとした。

Table 1 Natural frequencies calculated by Eq.(32).　　Unit (Hz)

Reduce	Original	1st Story	2nd Story	3rd Story	4th Story	5th Story
1st Mode	7.708	6.578	6.737	6.988	7.301	7.585
2nd Mode	22.501	20.232	22.192	21.355	19.349	19.969
3rd Mode	35.470	33.526	33.323	31.673	35.002	30.965
4th Mode	45.566	44.483	40.787	44.926	41.892	42.731
5th Mode	51.970	51.630	50.430	48.256	49.470	51.127

Table 2 Natural frequencies measured by EMA.　　Unit (Hz)

Reduce	Original	1st Story	2nd Story	3rd Story	4th Story	5th Story
1st Mode	7.970	6.760	6.902	7.185	7.516	7.781
2nd Mode	23.452	20.701	22.684	22.097	20.057	20.820
3rd Mode	37.532	35.130	34.963	33.177	36.687	32.534
4th Mode	48.859	47.080	42.997	47.567	44.179	45.114
5th Mode	56.159	55.195	53.586	51.679	52.751	54.470

5. 逆解析結果と検討

5.1 カルマンフィルタによる同定結果

Fig.9にカルマンフィルタ(KF)を用いて1層および3層が50%剛性低下したモデルの水平

剛性を同定した結果を示す。ところで，フィルタを繰り返し計算アルゴリズムとした場合，固有振動数と剛性の非線形の関係を有するフィルタ方程式を用いるため，解の収束性等に初期値の設定が大きく影響する。そこで，結果を表す図として，初期値の影響を考慮し，さらに明確な同定値を確認できるように工夫を施すことにした。この以降に示す結果を表す図はすべて，横軸は設定した初期値である。本問題で設定した初期値はすべてのモデルで，正常モデルの水平剛性を参考に1～272kg/cmとした。272kg/cmの値は正常モデルの水平剛性の2倍の値である。縦軸は同定すべき水平剛性である。得られた同定値が直線をなすようにプロットされている値が同定値を意味することになる。

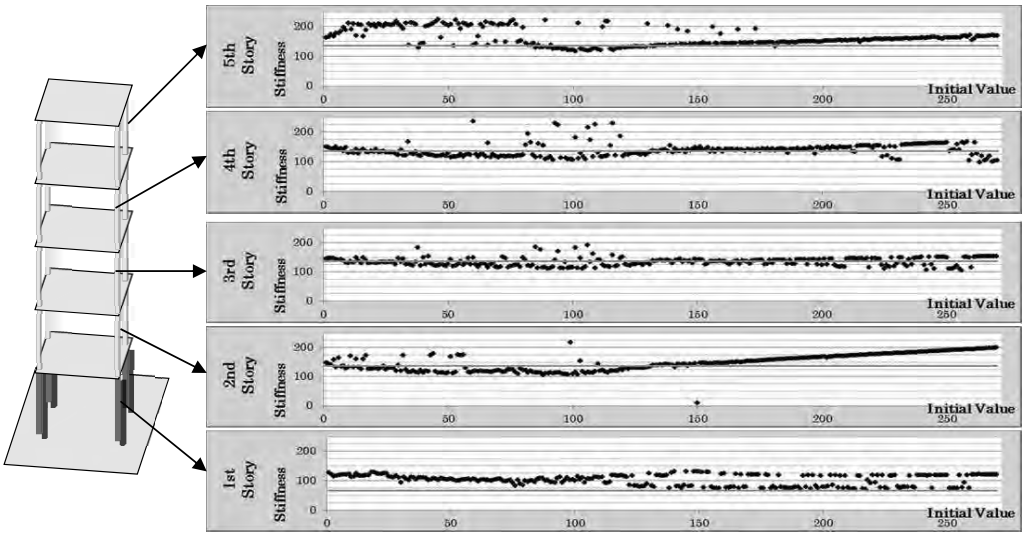

(a) Damaged at 1st story

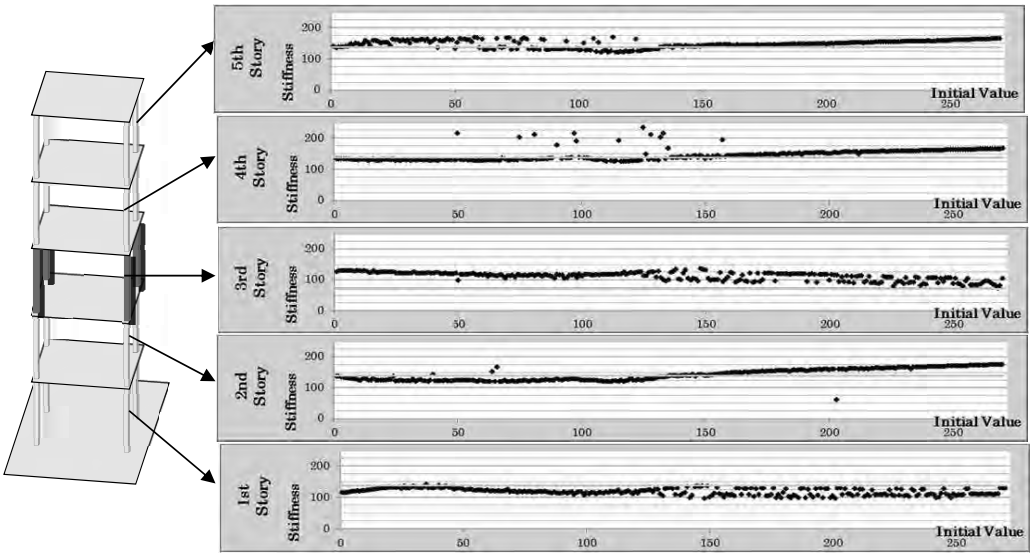

(b) Damaged at 3rd story

Fig.9 Results calculated by KF on damage grade with 50% at 1st and 3rd stories.

5.2 可変的パラメトリック射影フィルタによる同定結果

先にも述べたように，可変的パラメトリック射影フィルタによる逆解析(VPPF)では，正則化パラメータγを計算的に求める際にも正則化を施し，ベクトルの内積とノルムをスカラー化してγを決定している。ここでは，1次モードを用いて各フィルタリングステップでγを決定した場合と，2次モードを用いた場合について1層および3層が50%剛性低下したモデルの水平剛性を同定した結果をFig.10およびFig.11に示す

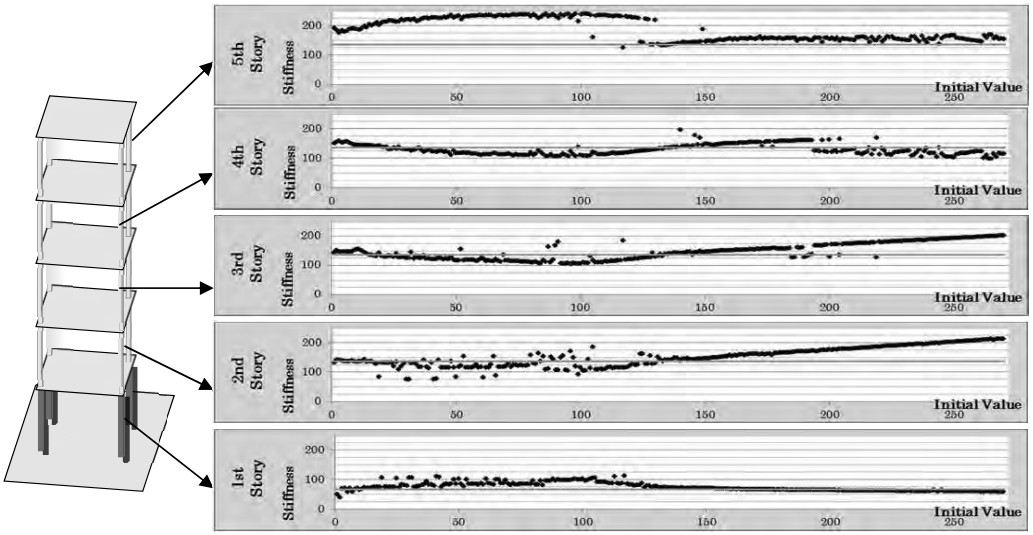

(a) Damaged at 1st story

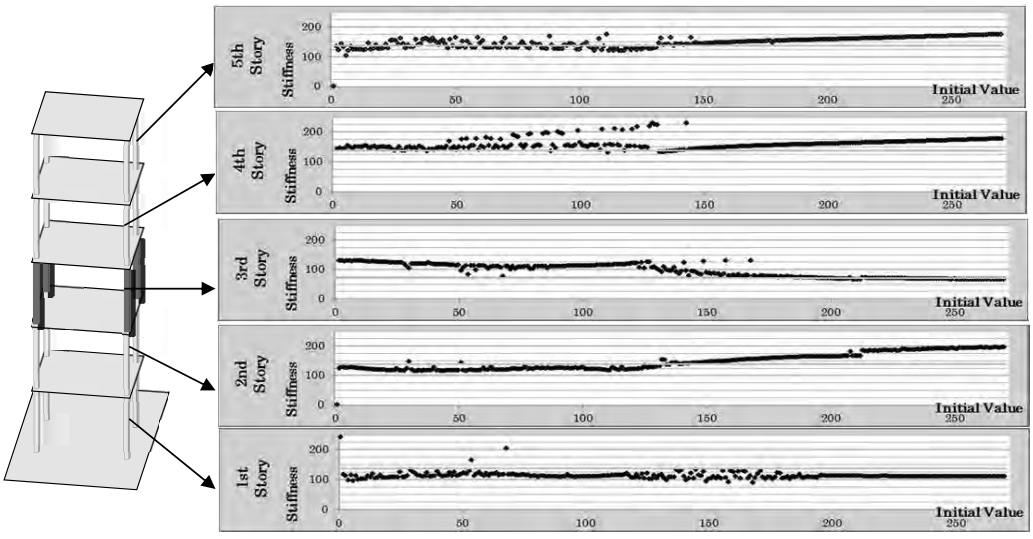

(b)Damaged at 3rd story

Fig.10 Results calculated by VPPF on damage grade with 50% at 1st and 3rd stories.
(Case where γ was calculated by using 1st mode)

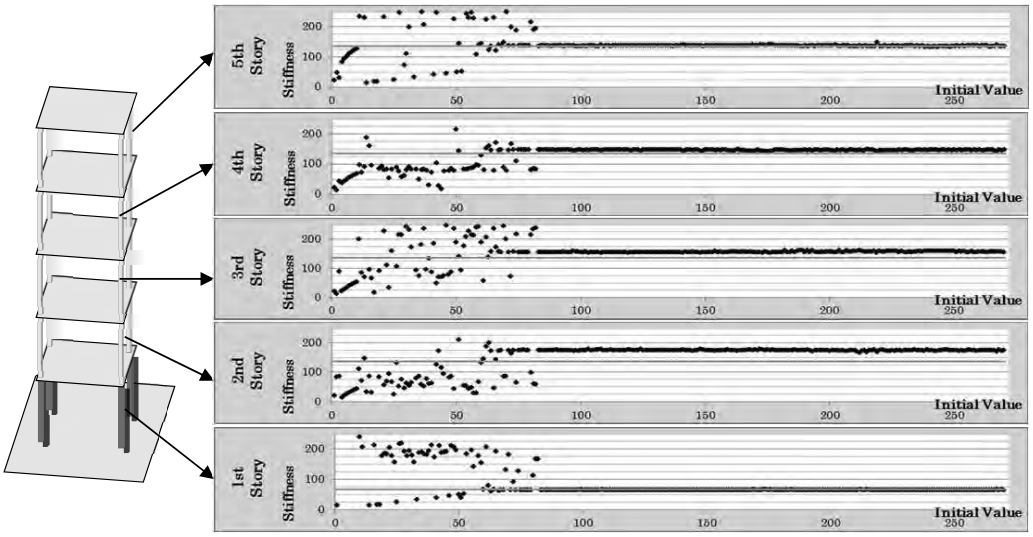

(a) Damaged at 1st story

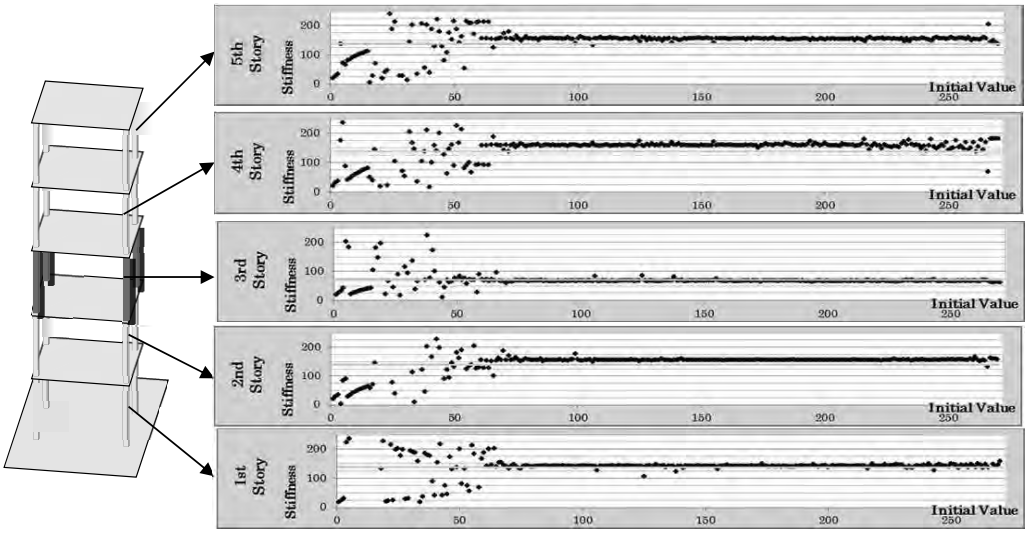

(b) Damaged at 3rd story

Fig.11 Results calculated by VPPF on damage grade with 50% at 1st and 3rd stories. (Case where γ was calculated by using 2st mode)

5.3　両フィルタによる結果の比較

kalmanフィルタを用いた場合，いずれの初期値を設定した場合にも同定結果にばらつきがみられ，収束はするものの明確な同定値が得られていない。先にも述べたように，kalmanフィルタは収束性を優先しており，解の精度に関しては初期値に依存した解が得られている。

可変的パラメトリック射影フィルタを用いた場合には，正則化パラメータγを決定する際に用いた振動モードに大きく依存している。すなわち，1次モードを用いてγを決定した

場合には，同定結果はほとんどkalmanフィルタを用いた場合と変わらず，改善が見られない。これに対して，2次モードを用いてγを決定した場合には，小さな初期値の場合には安定しないものの，設定する初期値が大きくなるにつれ同定結果は正解の位置に収束していくことがわかる。これらの結果から，モード依存性を考慮することにより，筆者らが開発した可変的パラメトリック射影フィルタが適応フィルタとして機能していると考えられる。

6. まとめ

本研究では中低層の既存建築物の水平剛性を同定する逆問題解析を構成し，逆解析手法として既存のkalmanフィルタと筆者らの開発した可変的パラメトリック射影フィルタに基づくフィルタリングアルゴリズムを用いて5層フレームモデルの水平剛性を同定する逆問題解析を行った。その結果，可変的パラメトリック射影フィルタの優位性を示すことができた。

参考文献

1) Paula F. Viero, Ney Roitman, Application of some damage identification method in offshore platforms, pp.107-126,Marine structure 12 1999
2) 濱本卓司，大浴佳治，三好敏晴，アクティブ同定手法を用いた多層建築物の損傷検出，pp.51-56，日本建築学会構造系論文集，539号，2001
3) 上林雅子，三田 彰，閉ループ制御を有する制振構造物のシステム同定，pp.77-83，日本建築学会構造系論文集，585号，2004
4) 南 良忠，城野みなみ，藤田皓平，竹脇 出，建物内部に未知の振動原を有する高層建物の曲げせん断型モデルとARXモデルを用いた剛性同定法，PP.1405-1412，日本建築学会構造系論文集，690号，2013
5) 畑田朋彦, 他, 層間変位計測に基づいた損傷評価法の実大建物振動台実験データを用いた検証, pp.703-711, 日本建築学会構造系論文集，Vol.78, 686号，2013
6) 古川愛子，小野達也，大塚久哲，高振動数で起振可能なアクチュエータの作成と損傷に伴う鋼板の振動特性の変化に関する実験的検討，pp.985-996，応用力学論文集，Vo.13,2010
7) 片山 徹，応用カルマンフィルタ，朝倉書店，1997
8) 村上章，長谷川高士，構造工学・地盤工学におけるKalmanフィルタの適用，pp.95-104，農業土木学会，Vol.158, 1992
9) Nobuyoshi Tosaka, Akihide Utani, Hideaki Takahashi, Unknown defect identification in elastic field by boundary element method with filtering procedure, pp.207-215, ELSEVIER, 1995
10) 遠藤龍司，登坂宣好，川上義嗣，塩田寿美子，パラメトリック射影フィルタに基づくアルゴリズムを用いた大型浮遊式海洋建築物の損傷同定解析，pp.237-244，日本建築学会構造系論文集， 539号，2013
11) 中村和幸，上野玄太，樋口知之，データ同化：その概念と計算アルゴリズム，pp.211-229，統計数理，第53巻第号，2002
12) R.Ghancm, G.Ferro, Health monitoring for strongly non-linear systems using the Ensemble Kalman Filter, pp.245-259, Struct. Countrol. Monit. Vol.13,2006
13) 遠藤龍司，登坂宣好，村山政昭，フレーム構造物のシステム同定に用いる可変的パラメトリック射影フィルタの特性，Vol.8, 計算数理工学論文集，2008

Mathematical Analysis for Inverse Problems in Risk Managements

Masahiro YAMAMOTO (The Univ. Tokyo)

2 September 2013

Kyushu University, IMI

Inverse Problems for Practice, the present and the future

Contents

- Introduction to inverse problems
- Inverse source problem of pollution
- Inverse problem for diffusion-refloating
  with Professor Yuko Hatano (Tsukuba Univ.)

1. Introduction to inverse problems

Inverse problem?

- Determine ”Cause” from ”Result”
- Determine ”Future” from ”Past”: forward problem
  Determine ”Past” from ”Future”: inverse problem
- useful for better prediction,
  identification of physical parameters
- Theoretical subjects: uniqueness, stability

- Numerical subject:
  Robust numerical methods against data errors

Example: archaeologoical IP

$\partial_t u(x,t) = \partial_x^2 u,\ 0 < x < 1,\ t > 0,$

$u(0,t) = u(1,t) = 0.$

IP: $u(x,T) \Longrightarrow u(\cdot, t_0)$

Here $0 \le t_0 < T$: once upon a time

Uniqueness: OK

Stability: NO in general

$u_n(x,t) := e^{-n^2\pi^2 t} \sin n\pi x,$

$u_n(\cdot, T) \to 0$ but $u_n(\cdot, 0) \not\to 0.$

Conditional stability:

Restored stability under a priori bound

- Hölder stability: For $t_0 > 0$, $\exists C, \theta \in (0, l)$ s.t. $\|u(\cdot, t_0)\|_{L^2(0,1)} \le C\|u(\cdot, T)\|^{\theta}_{L^2(0,1)}$
- Logarithmic stability:

$$\|u(\cdot, 0)\|_{L^2(0,1)} \le C\left(\log \frac{1}{\|u(\cdot,T)\|_{L^2(0,1)}}\right)^{-\theta}$$

where $\|\partial_x^2 u(\cdot, 0)\|_{L^2(0,1)} \le M$: a priori bound.

Lipschitz stability >> Logarithmic stability

But

Lipschitz stability: $10^{80} \times$ Data

Logarithmic stability: $10^{-80}(\log \frac{1}{\text{Data}})^{-1}$

Which is better? Better stability for inverse problem → good

Bad stability → not be disappointed!

Conditional stability $\Longrightarrow$

- How to choose admissible set of unknowns
- Balance between accuracy of available data and conditional stability:
  For bad stability, it is meaningless to find highly accurate data
- Giving guideline in choosing optimal mesh size, regularizing parameters, etc.

Available data for inverse problem are limited
$\Longrightarrow$ We cannot expect high accuracy in numerics for inverse problems
$\Longrightarrow$ We should not rely only on one method, but we should use suitable a priori knowledge or empirical knowledge

2. Inverse source problem of pollution

$\partial_t u(x,t) = \Delta u + \mu(t) f(x)$, $x \in \Omega$, $0 < t < T$,
B.C. $\partial_\nu u + \sigma(x) u = 0$ on $\partial\Omega$, $\sigma \geq 0$
$u(\cdot, 0) = 0$

$$D := \overline{\{x \in \Omega | f(x) \neq 0\}} \subset\subset \Omega$$

Inverse source problem of pollution

$f(x)$: given, $x_0 \in \Omega$: monitoring point

- $u(x_0, \cdot) \Longrightarrow \mu(t)$
- $u(\cdot, T) \Longrightarrow \mu(t)$

$\mu(t)$: given

- $u|_{\partial\Omega\times(0,T)} \Longrightarrow f(x)$
- $u(\cdot, T) \Longrightarrow f(x)$

ソース決定逆問題

古い(古典的な）形式の逆問題+ 環境問題、リスクマネージメント

$\Longrightarrow$ 新たな問題意識

「新しい酒を古い革袋に入れる」$\Longrightarrow$

あらたな研究の動機付け

IP 1: determine $\mu(t)$

I. Data: $u(x_0, t)$

$G(x, t)$: Green function for Δ with B.C.

$$u(x,t) = \int_0^t \int_\Omega G(x-y, t-s)\mu(s)f(y)dyds$$

$$w(x,t) := \int_\Omega G(x-y,t)f(y)dy$$

$$\Longrightarrow u(x_0,t) = \int_0^t w(x_0, t-s)\mu(s)ds,\ 0 < t < T$$

Uniqueness for general μ by data over $(0, T)$?

1. Stability for $\mu \geq 0$

Key lemma (reverse Hölder inequality)

Let $p \geq 1$, $0 \leq \lambda, \mu$ in $(0, T)$

Then:

$$\|\mu\|_{L^p(0,T)}\|\lambda\|_{L^p(0,\delta)} \leq M^{\frac{2p-2}{p}}\|\mu * \lambda\|^{\frac{1}{p}}_{L^1(0,T+\delta)}$$

(Saitoh-Vu-Yamamoto: 2002)

Theorem 1

$x_0 \in \Omega$: arbitrary,

$f \geq 0, \not\equiv 0, \in C^\infty[0,\infty)$

Assume $\mu \geq 0$. Then for any $\delta > 0$,

$$\|\mu\|_{L^p(0,T)} \leq C_\delta \|u(x_0,\cdot)\|^{\frac{1}{p}}_{L^1(0,T+\delta)}$$

Remark: OK for $f(x_0) = 0 \leftarrow$ monitor away from source

Proof: Set $\lambda(t) = w(x_0, t)$ in key lemma.

2. Stability by monitor inside of source

Let $f(x_0) \neq 0$.

$$u(x_0,t) = \int_0^t w(x_0, t-s)\mu(s)ds, \quad 0 < t < T.$$

$$f(x_0) \neq 0 \longrightarrow w(x_0,t) > 0,\ 0 \leq t \leq T.$$

$$\partial_t u(x_0, t) = w(x_0, 0)\mu(t) + \int_0^t \partial_t w(x_0, t-s)\mu(s)ds,$$

where $w(x_0, 0) = f(x_0) \neq 0$.
$\Longrightarrow$ Volterra equation of second kind

Theorem 2 Let $\Delta f \in L^\infty(\Omega)$. Then
$\|\mu\|_{L^2(0,T)} \leq C\|u(x_0, \cdot)\|_{H^1(0,T)}$.

3. Stability by monitor outside of source in a special case: Let $f(x_0) = 0$

Theorem 3 Let $n \leq 3$
$\Omega = \mathbb{R}^n$, $\mathcal{U} = \{\mu \in C[0, T] | \|\mu\|_{C[0,T]} \leq M$,
μ changes signs at most N-times $\}$.

Let $f \geq 0, \not\equiv 0$, $f \in L^2(\mathbb{R}^n)$ and
let $p > \frac{4}{4-n}$.
Then $\forall \delta > 0$, $\exists C > 0$ such that
$\|\mu\|_{L^p(0,T)} \leq C\|u(x_0, \cdot)\|^{1/p^N}_{L^1(0,T+\delta)}$ for all $\mu \in \mathcal{U}$.

Remark. For $n \geq 4$, we assume $f \in C^\infty(\mathbb{R}^n)$ and $p > 1$.

B. Data $u(\cdot, T)$

Let supp $f \subset\subset \Omega$, $f \geq 0$, $\not\equiv 0$,
μ analytic in $(0, \infty)$

Theorem 4 (uniqueness within analytic μ)

Let $u(\cdot, T) = 0$ in $\overline{\Omega \setminus \text{supp } f} \Longrightarrow$
$\mu \equiv 0$

Proof. $\partial_t u = \Delta u$ in $D := \Omega \setminus \operatorname{supp} f$,
$u(\cdot, T) = 0$ in D
μ: t-analytic $\Longrightarrow$ $u(\cdot, t)$: analytic in $t > 0$
$u(\cdot, T) = 0$ in $D \Longrightarrow \partial_t u(\cdot, T) = 0$ in $D \Longrightarrow \cdots$
$\Longrightarrow \partial_t^m u(\cdot, T) = 0$ in D for all m
By analyticity of u in t, we have
$u \equiv 0$ in $D \times (0, \infty)$

$u(x_0, t) = 0$, $\exists x_0 \in D$ for $0 < t < \infty \Longrightarrow$
$\int_0^t w(x_0, t-s)\mu(s)ds = 0$, $t > 0$
Laplace transform $\Longrightarrow \mu \equiv 0$

IP2. Determine $f(x)$
A. Data: $u|_{\partial\Omega \times (0,T)}$

Key:
$\partial_t u = \Delta u + \mu(t) f(x)$, $u(\cdot, 0) = 0$ + B.C.
$\partial_t z = \Delta z$, $z(\cdot, 0) = f$ + B.C.
$\Longrightarrow u(x, t) = \int_0^t \mu(t-s) z(x, s) ds$

Theorem 5

Let $\mu(0) \neq 0$, $\Gamma \subset \partial\Omega$: any subboundary

Then $u = 0$ on $\Gamma \times (0, T) \Longrightarrow f = 0$

Bad stability (logarithmic rate)

B. Data: $u(\cdot, T)$

Theorem 6

Let $\mu \geq 0, \not\equiv 0$.

Then $u(\cdot, T) = 0$ in $\Omega \Longrightarrow f = 0$

Notation

$$\|f\|_{L^2(\Omega)} = \left(\int_\Omega |f(x)|^2 dx\right)^{1/2}$$

$$(f, g) = \int_\Omega f(x)g(x)dx.$$

Proof: λ_n: eigenvalue of $-\Delta$ with B.C. including multiplicities

φ_n: eigenfunction for λ_n, $\|\varphi_n\|_{L^2(\Omega)} = 1$. Then

$u(x,t) = \sum_{n=1}^{\infty} \int_0^t e^{-\lambda_n(t-s)}(f, \varphi_n)\varphi_n(x)\mu(s)ds$

$u(\cdot, T) = 0 \Longrightarrow$

$\sum_{n=1}^{\infty} e^{-\lambda_n T}\left(\int_0^T e^{\lambda_n s}\mu(s)ds\right)(f, \varphi_n)\varphi_n(x)$

$= 0,\ x \in \Omega.$

$\mu \geq 0, \not\equiv 0 \Longrightarrow \int_0^T e^{\lambda_n s}\mu(s)ds \neq 0$

$\Longrightarrow (f, \varphi_n) = 0$ for all $n \Longrightarrow f = 0$

General $\mu(x, t)$: Let $\mu(\cdot, T) > 0$ on $\overline{\Omega}$.

Then IP $\Longrightarrow$

$f = \frac{-\Delta u(\cdot,T)}{\mu(\cdot,T)} + Kf$

Here $K : L^2(\Omega) \to L^2(\Omega)$ is compact

$\Longrightarrow$ Fredholm equation of second kind

- uniqueness implies the well-posedness
- generic well-posedness in some parameters
  ($\Leftarrow$ Analytic Fredholm perturbation theorem)

3. Inverse problem for diffusion-refloating

- cesium-137
- Asian Dust (Yellow sand)
- pollen

Field-data around Chernobyl and Fukushima

It is difficult to make long-term simulation of diffusion of cesium:
Consider wind and re-floating in each mesh (a few km X km)

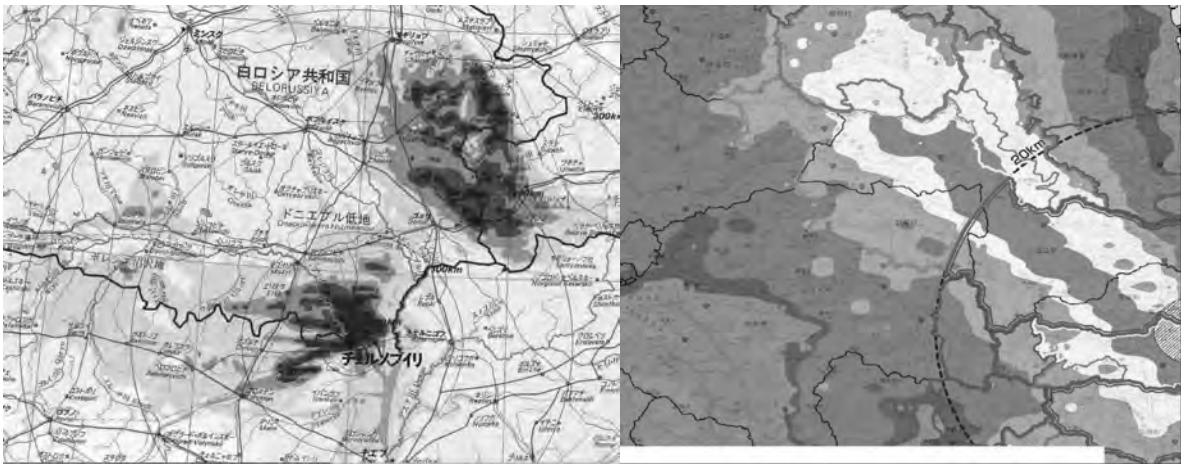

cesium-237: ~ 30 years (half-life period)
$\Longrightarrow$ serious effect to the health

Previous model for diffusion of density $C_1(x, t)$ of cesium-137

$$\partial_t C_1(x,t) = a\partial_x C_1 - \lambda_{dec} C_1$$

Here a: wind, λ_{dec}: decay constant
$\Longrightarrow$ not good matching

We must consider re-floating

Model for diffusion-reloating

$C_1(x, t)$; density of cesium in the air
$C_2(x, t)$: density of cesium on the ground
$\lambda_{down}(t)$: deposit rate of cesium in air to ground
$\lambda_{up}(t)$: re-floating rate of cesium on ground to air

$$\partial_t C_1(x, t) = a\partial_x C_1 - \lambda_{dec} C_1 - \lambda_{down} C_1 + \lambda_{up} C_2$$
$$\partial_t C_2(x, t) = -\lambda_{dec} C_2 + \lambda_{down} C_1 - \lambda_{up} C_2$$

$\lambda_{up}(t)$: important for estimating interior exposure to radiation (i.e., from mouth into body)

risk of interior exposure >> risk of exterior exposure

Inverse problem
Determine $\lambda_{up}(t)$ (and $\lambda_{down}(t)$).

Empirical formula

$$\lambda_{up}(t) \sim t^{-4/3}$$

Application: determine when explosion occurred

Inverse problem

$$\partial_t u_k = a\partial_x u_k - (\lambda_k(t) + b_1)u_k + \mu_k(t)v_k,$$
$$\partial_t v_k = \lambda_k(t)u_k - (\mu_k(t) + b_0)v_k,$$
$$0 < x < L,\ 0 < t < T,\ k = 1, 2,$$

$u_k(x, 0), v_k(x, 0)$: given

Take difference

$$u = u_1 - u_2, v = v_1 - v_2,$$
$$f = \lambda_1 - \lambda_2, g = \mu_1 - \mu_2$$
$$\Longrightarrow$$

$$\partial_t u = a\partial_x u - (\lambda_1 + b_0)u + \mu_1 v - f(x)u_2 + g(t)v_2,$$
$$\partial_t v = \lambda_1 u - (\mu_1 + b_0)v + f(x)u_2 - g(t)v_2(x,t),$$

$$u(x,0) = v(x,0) = 0$$

Inverse problem:

Given $x_0 \in (0, L)$, determine $f(t), g(t)$ by $u(x_0, t), v(x_0, t)$, $0 < t < T$.

Result I

$y_1, y_2 \in (0, L)$: given monitor points.

Assume

$$\det \begin{pmatrix} u_2(y_1,t) & u_2(y_2,t) \\ v_2(y_1,t) & v_2(y_2,t) \end{pmatrix} \neq 0,\ 0 \le t \le T,$$

$\Longrightarrow$

given $t_0 \in (0, T)$, $\exists\, C > 0, \theta \in (0,1)$ s.t.

$$\|f\|_{L^2(0,t_0)} + \|g\|_{L^2(0,t_0)}$$
$$\le C\left(\sum_{k=1}^{2} \|u(y_k,\cdot)\|_{L^2(0,T)} + \|v(y_k,\cdot)\|_{L^2(0,T)}\right)^{\theta}$$

under boundedness assumption on f, g.

Result II

$y_1 \in (0, L)$: given monitor point. Assume $v_2(y_1, t) \neq 0$, $0 \leq t \leq T$

given $t_0 \in (0, T)$, $\exists\, C > 0, \theta \in (0, 1)$ s.t.

$\|f\|_{L^2(0,t_0)} \leq$
$C(\|u(y_1, \cdot)\|_{L^2(0,T)} + \|v(y_1, \cdot)\|_{L^2(0,T)})^{\theta}$

under boundedness assumption on f, g.

Key to Proof

Carleman estimate:
L^2-weighted estimate with large parameter

Modification of methodology
by Bukhgeim-Klibanov (1981)

Same method for
Inverse Problem: $u(x_0, \cdot) \longrightarrow f(t)$
Here
$\partial_t^2 u = \sum_{i,j=1}^{n} \partial_i (a_{ij}(x) \partial_j u) + f(t) R(x, t)$
$u, \partial_t u$ at $t = 0$

Concluding remarks

Inverse problems for risk management with radiation contamination

- Theoretical:
  completed: various conditional stability
- Numerics: under work
- Laboratory experiment (e.g., wind tunnel test):
  not yet
- Real data: not yet

Inverse problems in Magnetic Resonance Imaging (MRI)

Shin-ichi Urayama
Human Brain Research Center, Graduate School of Medicine, Kyoto University

1. Introduction

MRI, magnetic resonance imaging, is one of medical techniques for taking cross-sectional images non-invasively. The scanner is non-radiative and can provide various kinds of bio-medical information, not only anatomical structure but functional information (metabolism, blood flow, brain activity, cell viability and so on, as shown in Fig.1). Because of these distinct advantages, MRI scanners have been spread many hospitals all over the world.

Like as another non-destructive scanners, the algorithm of MR image reconstruction is an inverse problem. Although the problem is known to be based on Fourier transfer (FT) in general, recent strong demands for scan time shortening push non-FT based image reconstruction. Here, I introduce reconstruction problems in MRI from principles to recent trend.

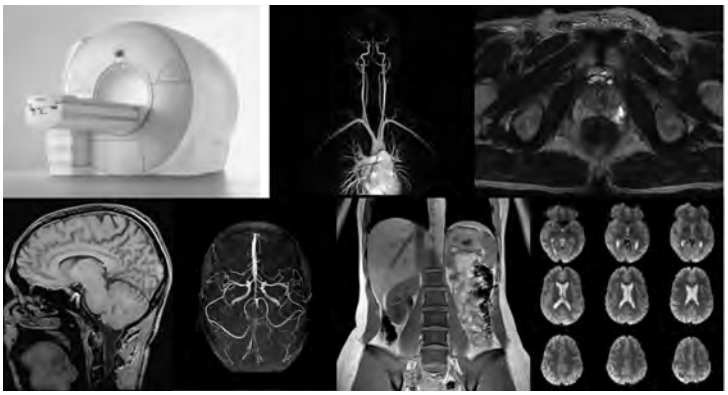

Fig.1 MRI scanner and variety of MR images.

2. Principle of MRI

Principle of MRI is based on Nuclear Magnetic Resonance (NMR) phenomenon. NMR is one of resonance phenomena in which a mass of nulei in magnetic field resonates with an electromagnetic (EM) wave, like a tuning fork does with a sound wave. Although exact understanding of this phenomenon needs quantum physics, an intuitive explanation based on classical mechanics is possible as below.

When a mass of nuclei is in a static magnetic field, it is magnetized and a magnetization vector parallel to the magnetic field is produced. This vector resonates with an EM wave like a tuning fork (Fig.2).

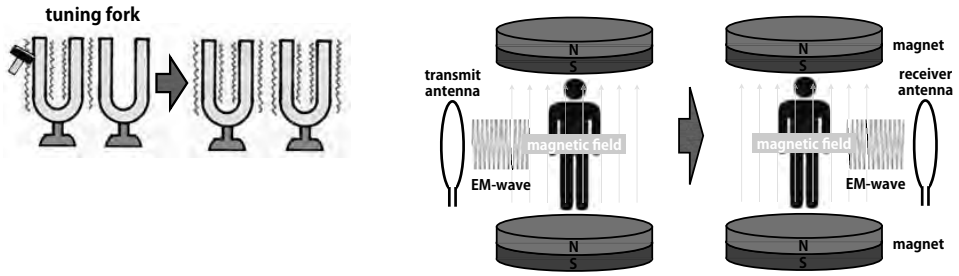

Fig.2 Like a tuning fork, MRI is based on a resonance effect (NMR effect).

A tuning fork has a resonance frequency because of its U-shape. Similarly, a magnetization vector also has because it is spinning, more precisely, it has an angular momentum. If the vector does not spin, an EM wave with any frequency works as a magnetic vibrator and the vector starts to vibrate with the same frequency. However, because of the low of conservation of angular momentum, the spinning vector is not effected by a magnetic vibrator in general and can be effected only by that whose frequency is the same as the angular frequency. This means that NMR phenomenon has a frequency selectivity property and its resonance frequency is known to be proportional to strength of the magnetic field **B**, that is, the resonance frequency ω is given by

$$\omega = \gamma |\mathbf{B}| \qquad (1)$$

where γ is so-called gyromagnetic ratio, a constant specific for each nucleus (for example, 4.26 x 10^7 Hz/T for hydrogen nucleus, i.e., proton). Therefore, a specific nuclei can be "*excited*" with the corresponding resonance frequency. And, if there is linear magnetic field gradient, a slice or slab volume perpendicular to the gradient direction can be excited, that is, "*slice-selection*".

A difference between tuning fork and magnetization vector is that a vector effected by the magnetic vibration does not vibrate but precess like a spinning top (Fig.3), because of the spinning property. Then, when the spinning vector **M** is tilted from the rotation axis (parallel to **B** and conventionally it's set to Z-axis), the vector in precession has a rotating component M_{xy} with rotating frequency of ω, and the component causes an EM wave of which frequency is also ω. This EM wave can be detected with a receiver antenna (so-called a *receiver coil*) before the vector goes back to its initial state. This is so-called *NMR phenomenon* and the detected signal is called *NMR signal*.

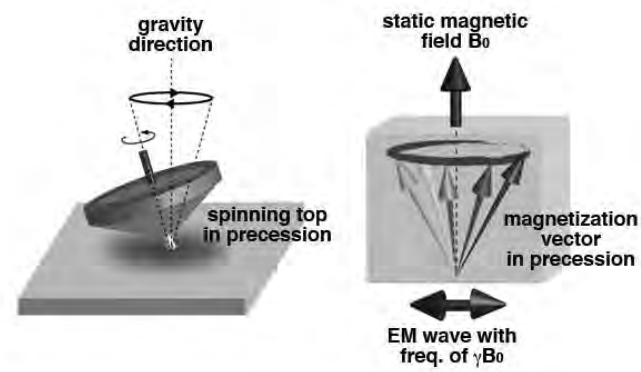

Fig.3 A magnetization vector in static magnetic field precesses like a spinning top.

Since NMR signal is coherent (the precessions are synchronized), position information of the signal source must be encoded in order to reconstruct an image (= spatial distribution of the signal). Interestingly, the precession frequency (= frequency of the EM wave) can be changed by modifying the local magnetic field and this characteristic is applied to the encoding by using so-called a *gradient coil*.

Gradient coil, a hardware differentiating MRI from NMR, is consist of X/Y/Z coils producing linear magnetic field modulation along each direction (Fig.4). When the coefficients of produced linear modulation along each direction is **G** = (*Gx, Gy, Gz*), the resultant magnetic field **B**(**r**) at position **r** is given by

$$\mathbf{B}(\mathbf{r}) = \mathbf{B}_0 + \mathbf{G} \cdot \mathbf{r} \qquad (2)$$

where $\mathbf{B}_0$ is the magnetic field strength at the origin of the MRI coordinate. Since the frequency of the NMR signal is proportional to local magnetic field as shown in eq.1, a linear gradient $\mathbf{G}$ being produced for $\triangle t$ causes relative phase modulation $\phi(\mathbf{r})$ given by

$$\phi(\mathbf{r}) = 2\pi\gamma(\mathbf{G}\cdot\mathbf{r})\triangle t \qquad (3)$$

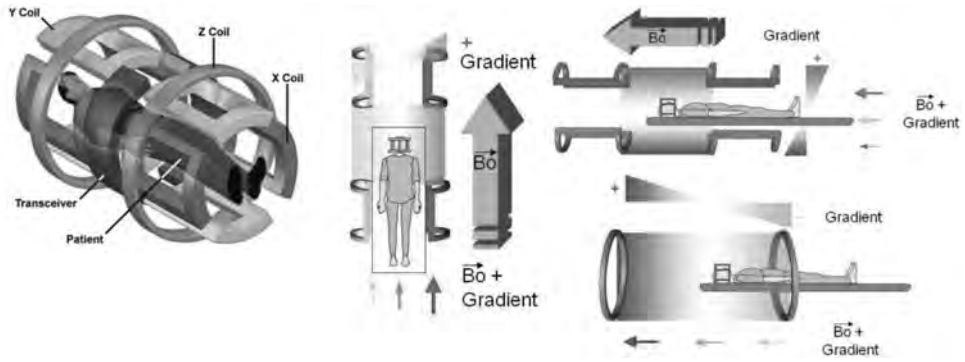

Fig.4 Gradient coil produces linear magnetic field modulations along three orthogonal directions and makes linear spatial modulation of precession frequency.

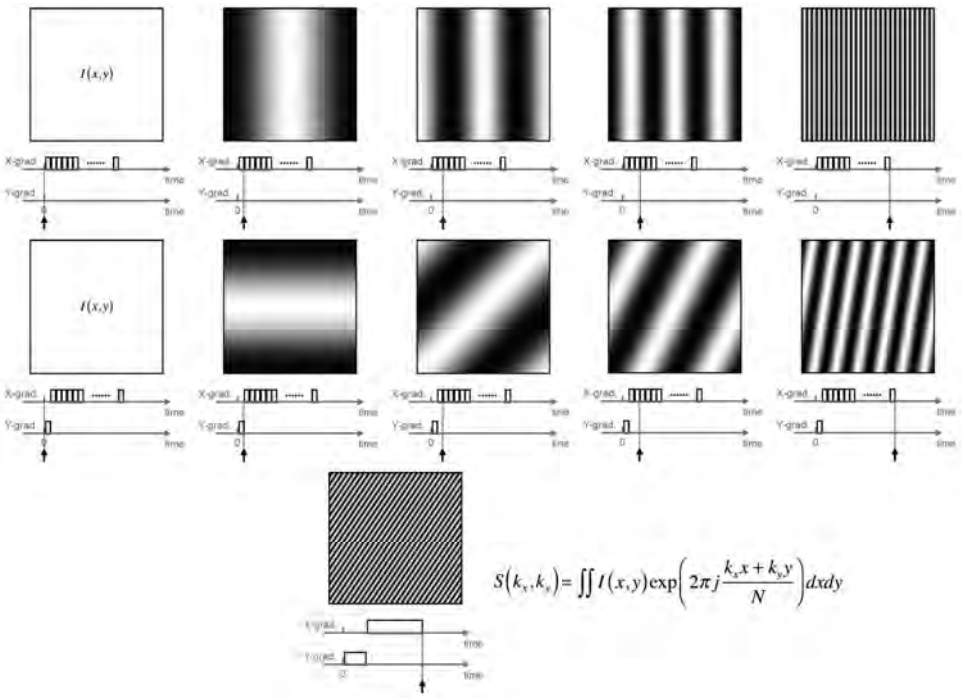

Fig.5 Spatial phase modulation and the corresponding time course of pulse gradients. Top row shows phase modulation changes without Y-gradient pulses and middle row does those with only single Y-gradient pulse. As shown in bottom row, phase modulation can be controlled with numbers of gradient pulses in two directions, k_x and k_y.

Now let's consider a rectangular solid region covering the target object centered at the origin. The three orthogonal unit vectors are $\mathbf{e}_j$ (j=1,2,3) and the corresponding length, number of voxels and gradient coefficients are l_j, n_j and g_j respectively, where they are satisfying

$$\gamma g_j l_j \Delta t = 1 \qquad (j = 1,2,3) \tag{4}$$

When three pulse gradient along the $\mathbf{e}_j$ directions are generated with the strengths of $k_j g_j$, the resultant relative phase shift is given by (Fig.5)

$$\begin{aligned} \phi(\mathbf{r},\mathbf{k}) &= 2\pi\gamma\Delta t \sum_{j=1}^{3} k_j g_j \left(\mathbf{e}_j \cdot \mathbf{r}\right) \\ &= 2\pi \sum_{j=1}^{3} \frac{k_j \left(\mathbf{e}_j \cdot \mathbf{r}\right)}{l_j} \end{aligned} \tag{5}$$

Considering that a Cartesian coordinate **r'** based on $\mathbf{e}_j$ gives **r** as

$$\mathbf{r} = \sum_{j=1}^{3} r_j' \left(l_j / n_j\right) \mathbf{e}_j \tag{6}$$

detected NMR signals are expressed by

$$S(\mathbf{k}) = \iiint M_{xy}(\mathbf{r}') \exp\left\{2\pi i \sum_{j=1}^{3} \frac{k_j r_j'}{n_j}\right\} dr_1' dr_2' dr_3' \tag{7}$$

where M_{xy}(**r'**) is the rotating component of the magnetization vector. This equation shows that NMR signal distribution M_{xy}(**r'**) and detected signal S(**k**) (this raw data volume is so-called "*k-space*") are linked with discrete Fourier transform (DFT) and so the MR image can be obtained by applying inverse DFT to the signal.

This is the principle of MR imaging and image reconstruction.

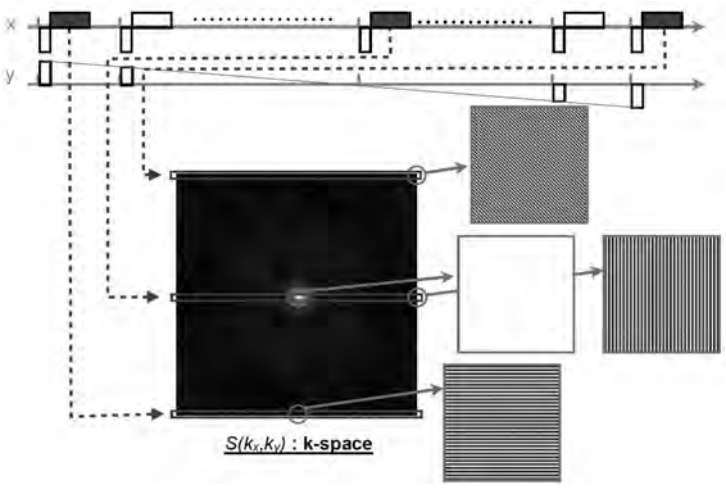

Fig.6 K-space and time courses of gradient pulses in basic sequences. Generally k-space is filled line by line with changing strength of Y-gradient pulses and in each line scanning, to refocus spin phase at the center of the line, an inverted gradient pulse is applied just before data acquisition. Phase modulation patterns corresponding to k-space positions assigned by red circles are shown at the left side of k-space.

3. Recent non-FT reconstruction

Although DFT based reconstruction is a very easy solution in MRI, scan time for filling all of k-space is too long in clinical exams. Recent improvement of calculation speed allows non-FT based reconstruction algorithms based on sparsely sampled data for shortening scan time. And now there are mainly two ways, *arbitrary trajectory method* (or *non-Cartesian method*) [1] and *parallel imaging* [2].

Considering redundancy in MR images (for example, high correlation between neighboring pixel values, signal void in background region and so on), there can be some reconstruction algorithms based on sparsely sampled data, including data at non-integer k_j point in k-space.

Since duration for measuring single data point in k-space is sufficiently shorter comparing with NMR signal decay, a handred to a few thousand of data points are measured successively after each excitation along a trajectory in k-space. Generally the trajectory is parallel to a side of the rectangular k-space, but in arbitrary trajectory method, various kind of sampling trajectories in k-space are adopted as shown Fig.7. These arbitrary trajectories are effective to reduce the number of data points in k-space without hamparing the reconstructed image.

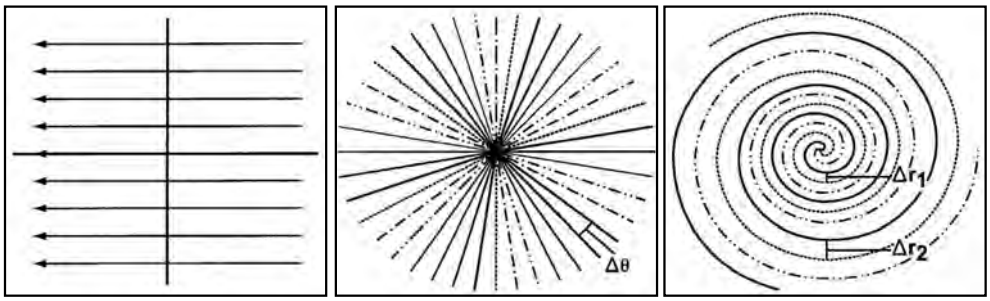

Fig.7 Various trajectories in k-space, conventional (left), radial (middle) and spiral (right).

In parallel imaging, inhomogeneous sensitivity distributions of receiver coils are utilized for additional spatial information. Generally, a large receiver coil covers large area with homogeneous sensitivity, but signal to noise ratio (SNR) is low. Therefore, to cover large area with maintaining sufficient SNR, a number of small coils (so-called *phased-array coil*) arranged to cover the target region are used (Fig.8).

In standard usage, an inhomogeneous image is reconstructed with each coil data and then all images are summed up to the final image. However, if the sensitivity map of each small coil is known, that is applicable as spatial information addition to that by the gradient based phase encoding explained in the previous section.

Although DFT can not be applied in these methods, these are still linear systems. Now let **m** be a vector of discretized $M_{xy}(\mathbf{r}')$ of which the size is $n_1n_2n_3$ and **s** be that of $S(\mathbf{k})$ of the size n_cn_k, where n_c is the number of the receiver coils and n_k is the number of the data points measured in the k-space. Then, the system is given by

$$\mathbf{s} = \mathbf{E}\mathbf{m} \tag{8}$$

where **E** is the $n_c n_k \times n_1 n_2 n_3$ matrix representing gradient and coil encoding, given by

$$E_{(q,p),\rho} = \exp\left\{2\pi i\left(\mathbf{k}_p \cdot \bar{\mathbf{r}}'_\rho\right)\right\} \cdot C_q\left(\bar{\mathbf{r}}'_\rho\right) \tag{9}$$

$$\left(1 \le q \le n_c, 1 \le p \le n_k, 1 \le \rho \le n_1 n_2 n_3\right)$$

where $\mathbf{k}_p$ is the p-th position of the measured data point in the k-space, $\bar{\mathbf{r}}'_\rho$ is the normalized ρ-th voxel position $\bar{r}'_{\rho j} = r'_{\rho j}/n_j$ and $C_q\left(\bar{\mathbf{r}}'_\rho\right)$ is the complex sensitivity of the q-th coil.

The image reconstruction is the inverse problem of Eq.8. Since often $n_c n_k$ exceeds $n_1 n_2 n_3$, this inverse problem is underdetermined so that additional constraints, like noise level optimization, are necessary. And because of the large matrix size and necessity for rapid reconstruction in clinical exams, this is solved with iterative ways based on the conjugate gradient [1] or recently compressed sensing approaches [3,4].

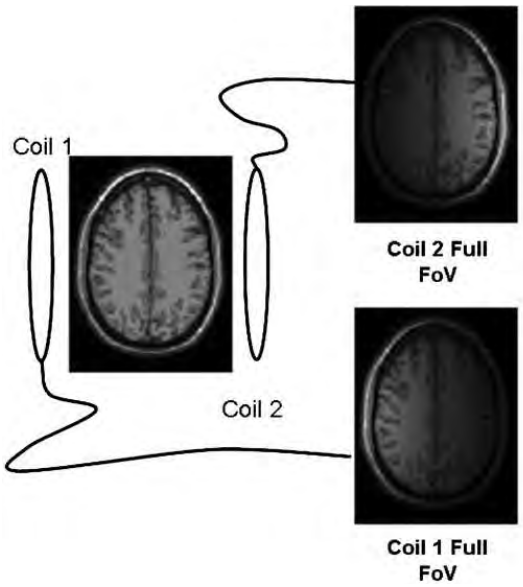

Fig.8 Two reciver coil system and inhomogeous images obtained from individual coils. (From fig. 5 in ref. 2)

4. Discussion

Image reconstruction algorithms in MRI including recent non-FT ones are described. As shown, they are basically linear systems and so many techniques have been proposed. However, the non-FT based algorithms are based on iterative ways with optimization and, that means, resultant images depend on the energy function of the optimization algorithm. Considering that clinically it is important that a contrast should be imaged if it exists and that it should not if it does not, these solutions are intuitively problematic because the best energy function is unknown and because there is no guarantee on the importance.

Another recent interesting trials are ones using non-linear gradient coils. A linear gradient is necessary for a FT-based reconstruction, but it is not for non-FT based one and the trials with non-linear gradients are expected that potentially they have some advantages [5-7].

Although almost all of reconstruction algorithms in MRI are also linear systems, it must be considerably useful if there are analytical solutions of them.

References

1. Pruessmann KP, Weiger M, Börnert P, Boesiger P., Advances in sensitivity encoding with arbitrary k-space trajectories., Magn Reson Med. 2001;46(4):638-51
2. Larmkan DJ, Nunes RG, Parallel magnetic resonance imaging, Phys. Med. Biol. 52 (2007) R15–R55
3. Cand´es EJ, Tao T., Decoding by linear programming, IEEE Trans. Info. Theory, 51 (2005), 12, 4203
4. Lustig M, Donoho D, Pauly JM, Sparse MRI: The Application of Compressed Sensing for Rapid MR Imaging, Magn Reson Med. 2007;58: 1182–1195
5. Hennig J, Welz AM, Schultz G, Korvink J, Liu Z, Speck O, Zaitsev M, Parallel imaging in non-bijective, curvilinear magnetic field gradients: a concept study, MAGMA. 2008 March; 21(1-2): 5–14.
6. Lin FH, Withal T, Schultz G, Gallichan D, Kuo WJ, Wang FN, Hennig J, Zaitsev M, Belliveau JW, Reconstruction of MRI data encoded by multiple nonbijective curvilinear magnetic fields, Magn Reson Med. 2012;68(4):1145–1156
7. Galiana G, Constable RT, Ultrafast Single Shot Imaging with Rotating Nonlinear Fields, Proc. Intl. Soc. Mag. Reson. Med. (2013), 13

A numerical method for an inverse source problem for a scalar wave equation without optimisation procedures

Takashi Ohe
Department of Applied Mathematics, Faculty of Science, Okayama University of Science
e-mail:ohe@xmath.ous.ac.jp

1 Introduction

Many important problems in engineering and sciences can be formulated as inverse problems for partial differential equations. In practical applications of inverse problems, studies for numerical methods are very important as well as studies for theoretical uniqueness and stability. Most of numerical studies for inverse problems apply optimisation procedures to solve the problem. Such approaches have some merits, for an example, we can apply well-established solver for partial differential equations and optimisation problems. However, they have also demerits. For an example, they are usually expensive because we have to solve partial differential equations many times iteratively.

Since 1990s, some researchers started to study the "reconstruction formula" for the solution of inverse problems without optimisation procedures. Such studies are developed for inverse scattering problems and inverse source problems, and give successful results. (For inverse scattering problems, see Ikehata[3, 4], Kirsch[5], and Potthast[11], and for inverse source problems, see El-Badia[1, 2], Nara[7, 8], and our papers[6, 10, 9, 12].) In this paper, we discuss an inverse source problem for a wave equation, and propose a numerical method for the problem without optimisation procedures.

2 Problem formulation

Let u be the solution of the following initial- and boundary-value problem for a three-dimensional scalar wave equation:

$$\frac{1}{c^2}\frac{\partial^2 u}{\partial t^2}(\boldsymbol{x},t) - \Delta u(\boldsymbol{x},t) = F(\boldsymbol{x},t), \quad \boldsymbol{x} = (x_1,x_2,x_3) \in \Omega,\ t \in (0,T), \tag{1}$$

$$u(\boldsymbol{x},0) = 0, \quad \boldsymbol{x} \in \Omega, \tag{2}$$

$$\frac{\partial u}{\partial t}(\boldsymbol{x},0) = 0, \quad \boldsymbol{x} \in \Omega, \tag{3}$$

$$u(\boldsymbol{x},t) = 0, \quad \boldsymbol{x} \in \Gamma,\ t \in (0,T), \tag{4}$$

where $\Omega \subset \mathbb{R}^3$ is a simply connected domain with smooth boundary Γ, $c\,(>0)$ denotes the wave propagation speed, $F(\boldsymbol{x},t)$ is an unknown wave source, and $T > 2\cdot \mathrm{diam}(\Omega)/c$. We consider the problem to estimate unknown source term $F(\boldsymbol{x},t)$ from observations of the normal derivative of the solution u on Γ given by

$$\phi(\boldsymbol{x},t) = \frac{\partial u}{\partial \nu}(\boldsymbol{x},t), \quad \boldsymbol{x} \in \Gamma,\ t \in (0,T). \tag{5}$$

In this paper, we assume that the source term $F(\boldsymbol{x},t)$ is expressed by multiple moving point sources as follows:

$$F(\boldsymbol{x},t) = \sum_{m=1}^{M} \lambda_m(t)\delta_{\boldsymbol{p}_m(t)}(\boldsymbol{x}). \tag{6}$$

Here, M is the number of wave sources, $\boldsymbol{p}_m(\cdot) = (p_{m,1}(\cdot), p_{m,2}(\cdot), p_{m,3}(\cdot)) \in C^2([0,T];\,\Omega)$ and $\lambda_m(\cdot) \in C^1(0,T)$ denote the location and magnitude of m-th wave source, and $\delta_{\boldsymbol{p}_m}$ is the three-dimensional Dirac's delta distribution at $\boldsymbol{p}_m$. We assume that $\boldsymbol{p}_m(t) \neq \boldsymbol{p}_{m'}(t)$ at every instance t

if $m \neq m'$, and $|\dot{\boldsymbol{p}}_m(t)| < c$, where $\dot{\boldsymbol{p}}_m(t)$ is the time-derivative of $\boldsymbol{p}_m(t)$. In this case, our problem becomes to estimate the number M, locations $\boldsymbol{p}_m(t)$ and magnitudes $\lambda_m(t)$ of point sources from $\phi(\boldsymbol{x}, t)$.

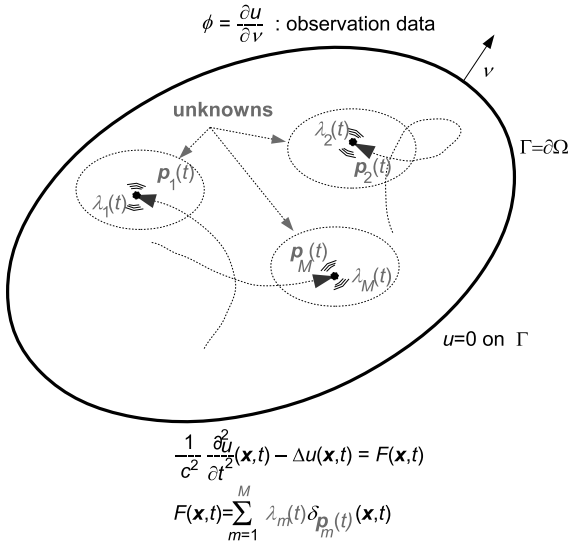

Figure 1: An inverse source problem for a scaler wave equation with moving point sources.

3 Reconstruction of wave sources

In this section, we discuss a reconstruction of unknown wave sources without optimisation procedures. Our method is based on the concept of reciprocity gap, and so we first introduce the reciprocity gap functional for scalar wave equations.

Let $\mathcal{W}$ be a class of complex-valued functions $v \in H^2((0,T); H^2(\Omega))$ that satisfy the homogeneous wave equation:

$$\frac{1}{c^2}\frac{\partial^2 v}{\partial t^2}(\boldsymbol{x}, t) - \Delta v(\boldsymbol{x}, t) = 0, \ \boldsymbol{x} \in \Omega, \ t \in (0, T).$$

The reciprocity gap functional $\mathcal{R}(\cdot)$ for scalar wave equation is the linear functional on $\mathcal{W}$ defined by

$$\begin{aligned} \mathcal{R}(v) \ \equiv \ & -\int_0^T \int_\Gamma \phi(\boldsymbol{x}, t) v(\boldsymbol{x}, t) dS(\boldsymbol{x}) dt + \frac{1}{c^2}\int_\Omega \frac{\partial u}{\partial t}(\boldsymbol{x}, T) v(\boldsymbol{x}, T) dV(\boldsymbol{x}) \\ & -\frac{1}{c^2}\int_\Omega u(\boldsymbol{x}, T)\frac{\partial v}{\partial t}(\boldsymbol{x}, T) dV(\boldsymbol{x}), \end{aligned} \tag{7}$$

where $u \in C^1((0,T); L^2(\Omega)) \cap C^0([0,T]; L^2(\Omega))$ is a weak solution of the initial- and boundary-value

problem (1)-(4) in the sense where

$$\begin{aligned}
&\frac{1}{c^2}\int_\Omega \frac{\partial u}{\partial t}(\boldsymbol{x},T)v(\boldsymbol{x},T)dV(\boldsymbol{x}) - \frac{1}{c^2}\int_\Omega u(\boldsymbol{x},T)\frac{\partial v}{\partial t}(\boldsymbol{x},T)dV(\boldsymbol{x}) - \int_0^T\int_\Gamma \frac{\partial u}{\partial \nu}(\boldsymbol{x},t)v(\boldsymbol{x},t)dS(\boldsymbol{x})dt \\
&+\int_0^T\int_\Omega u(\boldsymbol{x},t)\left(\frac{1}{c^2}\frac{\partial^2 v}{\partial t^2}(\boldsymbol{x},t) - \Delta v(\boldsymbol{x},t)\right)dV(\boldsymbol{x})dt \\
=\ &\int_0^T\int_\Omega F(\boldsymbol{x},t)v(\boldsymbol{x},t)dV(\boldsymbol{x})dt, \qquad (8)
\end{aligned}$$

for any $v \in H^2((0,T);H^2(\Omega))$, and ϕ is the observation data defined by (5). From (7) and (8), we can establish the following relation between $\mathcal{R}(v)$ and the source term $F(\boldsymbol{x},t)$:

$$\mathcal{R}(v) = \int_0^T\int_\Omega F(\boldsymbol{x},t)v(\boldsymbol{x},t)dV(\boldsymbol{x})dt. \qquad (9)$$

The equation (9) shows that the reciprocity gap functional $\mathcal{R}(v)$ gives some information on the source term $F(\boldsymbol{x},t)$, and we may reconstruct unknown source term from $\mathcal{R}(v)$ with suitable choice of functions $v \in \mathcal{W}$. In the case where the source term $F(\boldsymbol{x},t)$ is expressed by (6), we note that $\mathcal{R}(v)$ is rewritten as follows :

$$\mathcal{R}(v) = \sum_{m=1}^M \int_0^T \lambda_m(t)v(\boldsymbol{p}_m(t),t)dt.$$

Now, we consider a choice of $v \in \mathcal{W}$ for the reconstruction of moving wave sources. We use the following three sequences of functions in $\mathcal{W}$ with two positive parameters τ and ε:

$$\begin{aligned}
f_n(\boldsymbol{x},t;\ \tau,\varepsilon) &= \rho_\varepsilon\left(t + \frac{x_3}{c} - \tau\right)(x_1 + \mathrm{i}x_2)^n, \qquad n = 0,1,2,3,\cdots, \\
g_n(\boldsymbol{x},t;\ \tau,\varepsilon) &= -\frac{\partial}{\partial t}f_n(\boldsymbol{x},t;\ \tau,\varepsilon), \qquad n = 0,1,2,3,\cdots, \\
h_n(\boldsymbol{x},t;\ \tau,\varepsilon) &= x_3\left(\frac{\partial}{\partial x_1} - \mathrm{i}\frac{\partial}{\partial x_2}\right)f_n(\boldsymbol{x},t;\ \tau,\varepsilon) - (x_1 - \mathrm{i}x_2)\frac{\partial}{\partial x_3}f_n(\boldsymbol{x},t;\ \tau,\varepsilon), \\
&\qquad n = 1,2,3,\cdots,
\end{aligned}$$

where $\rho_\varepsilon \in C_0^\infty(\mathbb{R})$ denotes the mollifier function that satisfies $\operatorname{supp}\rho_\varepsilon \subset [-\varepsilon,\ \varepsilon]$ and $\int_{\mathbb{R}}\rho_\varepsilon(s)ds = 1$. We note that these functions are also introduced for the reconstruction of fixed point wave sources in our previous paper[10].

First, we show the identification of the number M of wave sources, and the reconstruction of parameters $p_{m,1}(\boldsymbol{x},t)$ and $p_{m,2}(\boldsymbol{x},t)$. Suppose that $\varepsilon \ll 1$, then we obtain the following estimate for $\mathcal{R}(f_n)$:

$$\begin{aligned}
\mathcal{R}(f_n)(\tau,\varepsilon) &= \sum_{m=1}^M \xi_m(t_m(\tau))\lambda_m(t_m(\tau))(p_{m,1}(t_m(\tau)) + \mathrm{i}p_{m,2}(t_m(\tau)))^n + O(\varepsilon) \\
&= \sum_{m=1}^M \widetilde{\lambda_m}(t_m(\tau))(z_m(t_m(\tau)))^n + O(\varepsilon), \quad n = 0,1,2,\cdots, \qquad (10)
\end{aligned}$$

where

$$\begin{aligned}
\widetilde{\lambda_m}(t) &\equiv \xi_m(t)\lambda_m(t), \quad m = 1, 2, \cdots, M, \\
z_m(t) &\equiv p_{m,1}(t) + \mathrm{i}p_{m,2}(t), \quad m = 1, 2, \cdots, M, \\
\xi_m(t) &\equiv \frac{1}{1 + \dfrac{\dot{p}_{m,3}(t)}{c}}, \quad m = 1, 2, \cdots, M,
\end{aligned}$$

and $t_m(\tau)$ is the solution of the nonlinear equation

$$t_m(\tau) + \frac{p_{m,3}(t_m(\tau))}{c} = \tau, \quad m = 1, 2, \cdots, M.$$

Since $|\dot{\boldsymbol{p}}(t)| < c$, $t_m(\tau)$ is uniquely determined for each τ.

For every τ, let $M(\tau)$ be the number of point sources such that $\lambda_m(t_m(\tau)) \neq 0$, and suppose that $\lambda_m(t_m(\tau)) \neq 0$ for $m = 1, 2, \cdots, M(\tau)$. We define $L \times L$-matrices

$$H_{L,\mu}(\tau, \varepsilon) = \begin{pmatrix} \mathcal{R}(f_\mu) & \mathcal{R}(f_{\mu+1}) & \cdots & \mathcal{R}(f_{\mu+L-1}) \\ \mathcal{R}(f_{\mu+1}) & \mathcal{R}(f_{\mu+2}) & \cdots & \mathcal{R}(f_{\mu+L}) \\ \vdots & \vdots & \ddots & \vdots \\ \mathcal{R}(f_{\mu+L-1}) & \mathcal{R}(f_{\mu+L}) & \cdots & \mathcal{R}(f_{\mu+2L-2}) \end{pmatrix}, \quad \mu = 0, 1,$$

where $\mathcal{R}(f_\mu) = \mathcal{R}(f_\mu)(\tau, \varepsilon)$. Neglecting $O(\varepsilon)$ term in (10), we can identify $M(\tau)$ as the maximum integer L such that $\det H_{L,0}(\tau, \varepsilon) \neq 0$, and reconstruct $z_m(t_m(\tau)),\ m = 1, 2, \cdots, M(\tau)$ as eigenvalues of $H_{M(\tau),0}^{-1} H_{M(\tau),1}$ [1, 7]. Suppose that $z_m(t_m(\tau)) \neq z_{m'}(t_{m'}(\tau))$ if $m \neq m'$, then we can also estimate $\widetilde{\lambda_m}(t_m(\tau)),\ m = 1, 2, \cdots, M(\tau)$ as a solution of the system of linear equations (10) for $n = 0, 1, 2, \cdots, M(\tau) - 1$.

Next, we consider the reconstruction of $p_{m,3}(t_m(\tau)),\ m = 1, 2, \cdots, M(\tau)$. For this purpose, we use two kinds of reciprocity gap functionals $\mathcal{R}(g_n)$ and $\mathcal{R}(h_n)$. In these reciprocity gap functionals, $\mathcal{R}(g_n)$ are used for the identification of some working variables in the reconstruction of $p_{m,3}(t_m(\tau))$.

Suppose that $\varepsilon \ll 1$, then we obtain the following estimate for $\mathcal{R}(g_n)$:

$$\begin{aligned}
\mathcal{R}(g_n)(\tau, \varepsilon) &= \sum_{m=1}^{M(\tau)} (\xi_m(t_m(\tau)))^2 \left(\dot{\lambda}_m(t_m(\tau)) - \xi_m(t_m(\tau))\lambda_m(t_m(\tau)) \frac{\ddot{p}_{m,3}(t_m(\tau))}{c} \right) (z_m(t_m(\tau)))^n \\
&+ \sum_{m=1}^{M(\tau)} n(\xi_m(t_m(\tau)))^2 \lambda_m(t_m(\tau)) \dot{z}_m(t_m(\tau)) (z_m(t_m(\tau)))^{n-1} \\
&+ O(\varepsilon), \quad n = 0, 1, 2, \cdots. \qquad (11)
\end{aligned}$$

Let

$$\begin{aligned}
b_m(t_m(\tau)) &\equiv (\xi_m(t_m(\tau)))^2 \left(\dot{\lambda}_m(t_m(\tau)) - \xi_m(t_m(\tau))\lambda_m(t_m(\tau)) \frac{\ddot{p}_{m,3}(t_m(\tau))}{c} \right), \\
&\qquad m = 1, 2, \cdots, M(\tau), \\
c_m(t_m(\tau)) &\equiv \lambda_m(t_m(\tau))(\xi_m(t_m(\tau)))^2 \dot{z}_m(t_m(\tau)), \quad m = 1, 2, \cdots, M(\tau),
\end{aligned}$$

and consider complex vectors

$$\boldsymbol{b}(\tau) \equiv \begin{pmatrix} b_1 \\ b_2 \\ \vdots \\ b_{M(\tau)} \end{pmatrix} \in \mathbb{C}^{M(\tau)}, \quad \boldsymbol{c}(\tau) \equiv \begin{pmatrix} c_1 \\ c_2 \\ \vdots \\ c_{M(\tau)} \end{pmatrix} \in \mathbb{C}^{M(\tau)}, \quad \boldsymbol{r}(\tau) \equiv \begin{pmatrix} \mathcal{R}(g_1) \\ \mathcal{R}(g_2) \\ \vdots \\ \mathcal{R}(g_{M(\tau)}) \end{pmatrix} \in \mathbb{C}^{2M(\tau)},$$

where $b_m \equiv b_m(t_m(\tau))$, $c_m \equiv c_m(t_m(\tau))$, and $\mathcal{R}(g_m) \equiv \mathcal{R}(g_m)(t_m(\tau))$ for $m = 1, 2, \cdots, M(\tau)$. Also we consider $2M(\tau) \times M(\tau)$-matrices

$$
\begin{aligned}
A_L(\tau) &\equiv \begin{pmatrix} 1 & 1 & \cdots & 1 \\ z_1 & z_2 & \cdots & z_{M(\tau)} \\ z_1^2 & z_2^2 & \cdots & z_{M(\tau)}^2 \\ \vdots & \vdots & \ddots & \vdots \\ z_1^{2M(\tau)-1} & z_2^{2M(\tau)-1} & \cdots & z_{M(\tau)}^{2M(\tau)-1} \end{pmatrix}, \\
A_R(\tau) &\equiv \begin{pmatrix} 0 & 0 & \cdots & 0 \\ 1 & 1 & \cdots & 1 \\ 2z_1 & 2z_2 & \cdots & 2z_{M(\tau)} \\ 3z_1^2 & 3z_2^2 & \cdots & 3z_{M(\tau)}^2 \\ \vdots & \vdots & \ddots & \vdots \\ (2M(\tau)-1)z_1^{2M(\tau)-2} & (2M(\tau)-1)z_2^{2M(\tau)-2} & \cdots & (2M(\tau)-1)z_{M(\tau)}^{2M(\tau)-2} \end{pmatrix},
\end{aligned}
$$

where $z_m \equiv z_m(t_m(\tau))$. Then, neglecting $O(\varepsilon)$ term in (11), we obtain the following linear equation for $\boldsymbol{b}(\tau)$ and $\boldsymbol{c}(\tau)$:

$$
\begin{pmatrix} A_L(\tau) & A_R(\tau) \end{pmatrix} \begin{pmatrix} \boldsymbol{b}(\tau) \\ \boldsymbol{c}(\tau) \end{pmatrix} = \boldsymbol{r}(\tau). \tag{12}
$$

Assume that $z_m(t_m(\tau)) \neq z_{m'}(t_{m'}(\tau))$ for $m \neq m'$, then $\det \begin{pmatrix} A_L(\tau) & A_R(\tau) \end{pmatrix}$ does not vanish, and we can obtain $\boldsymbol{b}(\tau)$ and $\boldsymbol{c}(\tau)$ uniquely.

Now, we reconstruct the parameter $p_{m,3}(t_m(\tau))$, $m = 1, 2, \cdots, M(\tau)$ using reciprocity gap functional $\mathcal{R}(h_n)$. Under the same assumption for the derivation of equation (10), we obtain the following estimate for $\mathcal{R}(h_n)$:

$$
\begin{aligned}
\mathcal{R}(h_n)(\tau,\varepsilon) &= 2n \sum_{m=1}^{M} p_{m,3}(t_m(\tau)) \xi_m(t_m(\tau)) \lambda_m(t_m(\tau)) (z_m(t_m(\tau)))^{n-1} \\
&+ \frac{1}{c} \sum_{m=1}^{M} (\xi_m(t_m(\tau)))^2 \left(\dot{\lambda}_m(t_m(\tau)) - \xi_m(t_m(\tau)) \lambda_m(t_m(\tau)) \frac{\ddot{p}_{m,3}(t_m(\tau))}{c} \right) \\
&\quad \times \overline{z_m(t_m(\tau))} (z_m(t_m(\tau)))^n \\
&+ \frac{1}{c} \sum_{m=1}^{M} (\xi_m(t_m(\tau)))^2 \lambda_m(t_m(\tau)) \overline{\dot{z}_m(t_m(\tau))} (z_m(t_m(\tau)))^n \\
&+ \frac{n}{c} \sum_{m=1}^{M} (\xi_m(t_m(\tau)))^2 \lambda_m(t_m(\tau)) \dot{z}_m(t_m(\tau)) \overline{z_m(t_m(\tau))} (z_m(t_m(\tau)))^{n-1} \\
&+ O(\varepsilon), \\
&= 2n \sum_{m=1}^{M} p_{m,3}(t_m(\tau)) \widetilde{\lambda_m}(t_m(\tau)) (z_m(t_m(\tau)))^{n-1} \\
&+ \frac{1}{c} \sum_{m=1}^{M} b_m(t_m(\tau)) \overline{z_m(t_m(\tau))} (z_m(t_m(\tau)))^n \\
&+ \frac{1}{c} \sum_{m=1}^{M} \overline{c_m(t_m(\tau))} (z_m(t_m(\tau)))^n + \frac{n}{c} \sum_{m=1}^{M} c_m(t_m(\tau)) \overline{z_m(t_m(\tau))} (z_m(t_m(\tau)))^{n-1} \\
&+ O(\varepsilon).
\end{aligned} \tag{13}
$$

Since we have already identified $M(\tau)$, and $z_m(t_m(\tau))$, $\widetilde{\lambda_m}(t_m(\tau))$, $b_m(t_m(\tau))$, $c_m(t_m(\tau))$ for $m = 1, 2, \cdots, M(\tau)$, only $p_{m,3}(t_m(\tau)), m = 1, 2, \cdots, M(\tau)$ are unknown in (13). Let

$$q_m(t_m(\tau)) \equiv \widetilde{\lambda_m}(t_m(\tau))p_{m,3}(t_m(\tau)),\ m = 1, 2, \cdots, M(\tau),$$

and

$$\begin{aligned} s_n(\tau) &\equiv \frac{1}{c}\sum_{m=1}^{M} b_m(t_m(\tau))\overline{z_m(t_m(\tau))}(z_m(t_m(\tau)))^n \\ &+ \frac{1}{c}\sum_{m=1}^{M} \overline{c_m(t_m(\tau))}(z_m(t_m(\tau)))^n + \frac{n}{c}\sum_{m=1}^{M} c_m(t_m(\tau))\overline{z_m(t_m(\tau))}(z_m(t_m(\tau)))^{n-1}, \end{aligned}$$

then, we can rewrite (13) as

$$\mathcal{R}(h_n)(\tau,\varepsilon) - s_n(t_m(\tau)) = 2n\sum_{m=1}^{M(\tau)} q_m(t_m(\tau))(z_m(t_m(\tau)))^{n-1} + O(\varepsilon), \qquad n = 1, 2, \cdots. \tag{14}$$

Assume that $z_m(t_m(\tau)) \neq z_{m'}(t_{m'}(\tau))$ for $m \neq m'$, and neglecting $O(\varepsilon)$ term, we can solve equation (14) for $q_m(t_m(\tau))$ uniquely. Then $p_{m,3}(t_m(\tau))$ can be reconstructed by

$$p_{m,3}(t_m(\tau)) = \frac{q_m(t_m(\tau))}{\widetilde{\lambda_m}(t_m(\tau))}, \quad m = 1, 2, \cdots, M(\tau).$$

Finally, we estimate $\dot{p}_{m,3}(t_m(\tau))$ with a suitable numerical differentiation method, and we can reconstruct $\lambda_m(t_m(\tau))$ by

$$\lambda_m(t_m(\tau)) = \frac{\widetilde{\lambda_m}(t_m(\tau))}{\xi_m(t_m(\tau))} = \widetilde{\lambda_m}(t_m(\tau))\left(1 + \frac{\dot{p}_{m,3}(t_m(\tau))}{c}\right), \quad m = 1, 2, \cdots, M(\tau).$$

4 Numerical Experiments

In this section, we show a numerical experiment for our reconstruction method. We consider the case where Ω is the unit ball $\{\boldsymbol{x} \,|\, |\boldsymbol{x}| = 1\}$, and set the wave propagation speed $c = 1$. Unknown wave source consists of two point wave sources given by

Wave source 1:

$\boldsymbol{p}_1(t) = (0.5\cos(0.2t),\ 0.2\sin(0.2t),\ 0.2\sin(0.45t))$,

$\lambda_1(t) = \dfrac{1}{2}\sin\dfrac{\pi}{9}t$,

Wave source 2 :

$\boldsymbol{p}_2(t) = (r(t)\cos\theta(t),\ r(t)\sin\theta(t)\cos(0.7\pi),\ r(t)\sin\theta(t)\sin(0.7\pi))$,

$\theta(t) = (2\pi - 2\theta_0)t/50 + \theta_0,\ (\theta_0 = \cos^{-1}0.6875)$,

$r(t) = 0.25/(1.0 - \cos(\theta(t)))$,

$$\lambda_2(t) = \begin{cases} 1.0 - \cos\left(2\pi(t-5.0)/19.5\right)) & 5.0 \le t \le 24.5, \\ 0 & \text{others.} \end{cases}$$

We show the profile of locations $\boldsymbol{p}_m(t_m(\tau))$ and magnitudes $\widetilde{\lambda_m}(t_m(\tau))$ as blue lines in Figures 2 and 3. To give the observation data ϕ, we solve the initial- and boundary-value problem (1)-(4) numerically using the boundary integral equation method, and compute $\phi = \frac{\partial u}{\partial \nu}$ and 386 points on Γ. We numerically add 0.1% noise to the observations ϕ to simulate a practical observation situation. In the computation of reciprocity gap functionals $\mathcal{R}(f_n)$, $\mathcal{R}(g_n)$ and $\mathcal{R}(g_n)$, we apply the trapezoidal rule with respect to the longitude axis, and the Gauss-Legangdre formula with respect to the latitude axis.

We show the estimation results of locations $\boldsymbol{p}_m(t_m(\tau))$ and magnitudes $\widetilde{\lambda_m}(t_m(\tau))$ of wave sources 1 and 2 as red lines in Figures 2 and 3, respectively. For the wave source 1, both of the location and magnitude are estimated well in the whole interval $[0, 40]$. For the wave source 2, the estimation result becomes bad when the source starts up ($\tau \sim 6$) and vanishes ($\tau \sim 24$), however, the result is very good in the interval $7 \leq \tau \leq 20$. From these results, we consider that our method gives good estimates for locations and magnitudes of unknown wave sources.

5 Conclusions

In this paper, we discuss a numerical method for an inverse source problem for three-dimensional scalar wave equations. We assume that the source term is expressed by multiple point wave sources, and they move around in the known domain. For the problem, we propose a method based on the concept of reciprocity gap without optimisation procedures. We examine our method by a numerical experiment with two wave sources, and show that our method gives a good estimation of the sources under noisy observation conditions. We have some further works for our method, for examples, application to limited aperture cases, and to practical problems.

Acknowledgement This work was partially supported by Grant-in-Aid for Scientific Research(C)of JSPS KAKENHI Grant Number 23540173.

References

[1] A. El Badia and T. Ha-Duong, An inverse source problem in potential analysis, Inverse Problems, **16**, (2000), No. 3, 651–663.

[2] A. El Badia and T. Ha-Duong, Determination of point wave sources by boundary measurements, Inverse Problems, **17**, (2001), No. 4, 1127–1139.

[3] M. Ikehata, Extraction formula in inverse problems, Bulletin of JSIAM, **16**, (2006), No. 1, 53–62.(in Japanese)

[4] M. Ikehata, Analytical methods for extracting discontinuity in inverse problems: The probe method after 10 years, Sugaku Expositions, **26**, (2013), No. 1.

[5] A. Kirsch and N. Grinberg, The Factorization Method for Inverse Problems (Oxford Lecture Series in Mathematics and Its Applications 36), Oxford University Press, 2008.

[6] E. Nakaguchi, H. Inui and K. Ohnaka, An algebraic reconstruction of a moving point source for a scalar wave equation, Inverse Problems, **28**, (2012), No. 6, 065018, 21 pp.

[7] T. Nara and S. Ando, An inverse potential analysis via projection onto the Riemann sphere, Bulletin of JSIAM, **13**, (2003), No. 3, 45–57. (in Japanese)

[8] T. Nara, Algebraic reconstruction of the general-order poles of a meromorphic function, Inverse Problems, **28**, (2012), no. 2, 025008, 19 pp.

[9] T. Ohe and K. Ohnaka, Determination of locations of point-like masses in an inverse source problem of the Poisson equation, J. Comput. Appl. Math., **54**, (1994), No. 2, 251–261.

[10] T.Ohe, H. Inui and K. Ohnaka, Real-time reconstruction of time-varying point sources in a three-dimensional scalar wave equation, Inverse Problems, **27**, (2011), No. 11, 115011, 19 pp.

[11] R. Potthast, Point Sources and Multipoles in Inverse Scattering Theory (Chapman & Hall/CRC Research Notes in Mathematics 427), Chapman & Hall/CRC, 2001.

[12] K. Yamatani, T. Ohe and K. Ohnaka, A direct identification method for current dipoles from electromagnetic fields, J. Comput. Appl. Math., **201**, (2007), No. 1, 164–174.

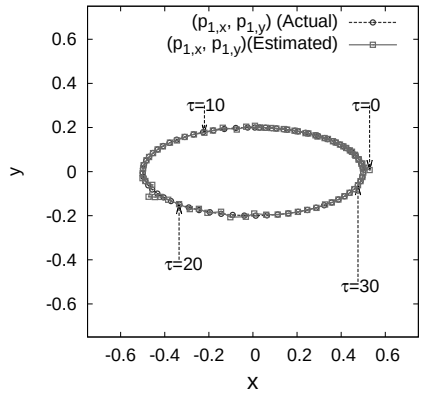

xy-plane $((p_{1,1}(t_1(\tau)), p_{1,2}(t_1(\tau))))$

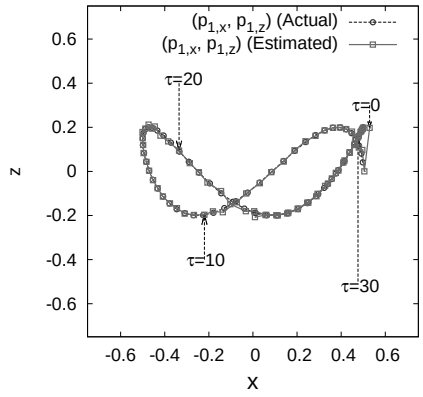

xz-plane $((p_{1,1}(t_1(\tau)), p_{1,3}(t_1(\tau))))$

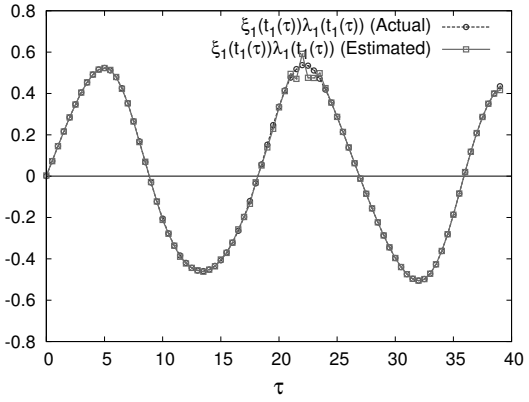

the magnitude $(\widetilde{\lambda_1}(t_1(\tau)))$

Figure 2: Estimation results for wave source 1

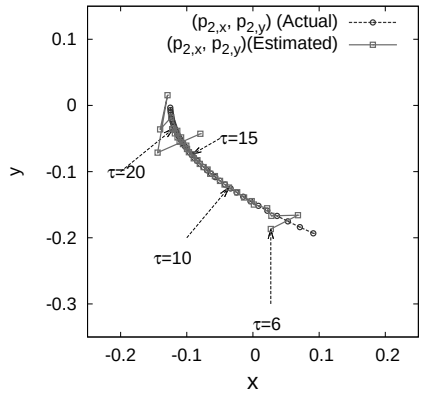

xy-plane $((p_{2,1}(t_2(\tau)), p_{2,2}(t_2(\tau))))$

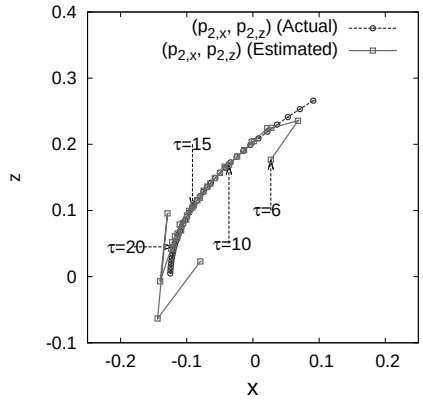

xz-plane $((p_{2,1}(t_2(\tau)), p_{2,3}(t_2(\tau))))$

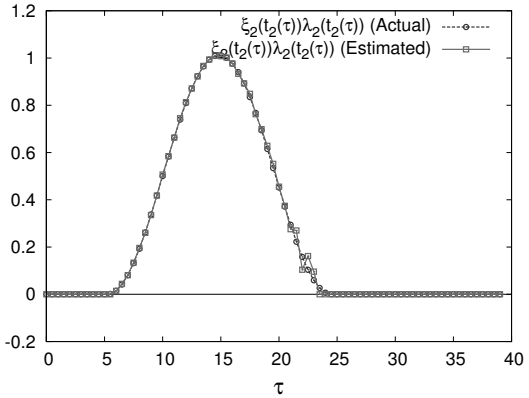

the magnitude $(\widetilde{\lambda_2}(t_2(\tau)))$

Figure 3: Estimation results for wave source 2

An inverse problem to detect an inclusion in a homogeneous medium by the Dirichlet to Dirichlet data for the heat equation

Takashi TAKIGUCHI* and Ryusei YAMASHITA

Abstract

We discuss an inverse problem to detect an inclusion in a homogeneous medium. For this problem, application of the X-ray tomography being well studied, several problems are pointed out, such as harmful influence of the X-ray on the human body, the expensive cost of the industrial computerized tomography and so on. In this paper, we discuss another approach to this problem where we try to apply the heat conduction to detect an inclusion in a homogeneous medium.

Keywords: inverse problem, the heat equation

1 Introduction

In this paper, we discuss an inverse problem to detect an inclusion in a homogeneous medium. An approach to this problem, the application of the X-ray is being studied, where the reconstruction is performed to reconstruct the object, by its section by section. As examples of application of the X-ray tomography, the following problems of non-destructive testing are under investigation.

(a) Non-destructive testing for mixed materials of the two kinds

(b) Non-destructive testing for the fuel tank of the rockets

(c) Non-destructive testing for die casting of the aluminium

The problem (a) arose from the development of the three dimensional CAD system which enables us to describe the inner structure of the pillars and the walls in the buildings. In this problem, it is necessary to investigate the internal structure of the pillars consisted of the steel and the aluminium, which is not clear from their production process. It seems that it is not difficult to understand the motivation to study problems (b) and (c), which are typical problems in non-destructive testing.

*Supported in part by JSPS Grant-in-Aid for Scientific Research (C) 22540214. Department of Mathematics, National Defense Academy of Japan, 1-10-20, Hashirimizu, Yokosuka, Kanagawa, 239-8686, JAPAN tel: +81-46-841-3810 (ext. 3249) fax: +81-46-844-5902 (shared) email: takashi@nda.ac.jp

For the time being, the same algorithm as the computerized tomography (CT) is applied to all of the problems, (a), (b) and (c). Since the objects in these problems are much simpler than the interior structure of the human body, it is expected to reduce the X-ray data for the reconstruction of the object. This problem is closely related to the geometric tomography and there are many studies on it both in the viewpoint of theory and in the viewpoint of application. For example, confer [1, 8, 9] for the results in the viewpoint of theory and [2, 11, 12, 13] for the studies in the viewpoint of practical application. Unfortunately, the results mentioned above are not still satisfactory for practical application in view of the following points.

- In the case where we project parallel beams of the X-ray from two directions, we can classify the shape of the inclusions into the two classes, one is the uniquely determined ones by these data and the other is non-uniquely determined one ([8, 9, 11]). For the unique class, reconstruction formulas ([8, 11]) are given and we gave further studies, treatment of the errors, construction of a reconstruction algorithm and its implementation by computers and so on, satisfactory for practical application ([2, 11]). It is, however, proved that there are very few sets reconstructed by this method ([12]) and it is not known how to find the exact two directions for the reconstruction for the uniquely reconstructed sets, even if they exist. In addition to them, since they apply cone beams of the X-ray in most industrial CT devices, we have to develop the counterpart of the above theory for the cone beams.

- For general inclusions, the exact data of the beams of the X-ray for the reconstruction are not known. Needless to say their reconstruction methods, treatment of the errors, construction of an approximate reconstruction algorithm, its implementation by computers and so on.

There are other problems of the use of the X-ray tomography.

(d) The cost of the testing is very expensive if we apply the X-ray tomography.

(e) We cannot ignore harmful influence of the X-ray on the human body.

In order to solve the problems (d) and (e), we try another approach. We study to detect an inclusion in a homogeneous medium applying the heat. It was M.Ikehata and M.Kawashita [3, 4, 5, 6] who developed the study began to study to detect an inclusion in a homogeneous medium applying the heat. They studied the following problem.

Problem 1.1. *Let Ω be a bounded domain of $\mathbb{R}^n$, $n = 2, 3$, with smooth boundary. Let D be an open subset of Ω with smooth boundary and satisfy that $\overline{D} \subset \Omega$ and $\Omega \setminus D$ is connected. We denote the unit outward normal vectors to $\partial\Omega$ and ∂D by the same symbol ν. Let $T > 0$ be an arbitrary. Given $f = f(x,t)$, $(x,t) \in \partial\Omega \times (0,T)$, let $u = u(x,t)$ be the solution of the initial boundary value problem for the heat equation*

$$\begin{cases} \partial_t u - \Delta u = 0 \quad \text{in } (\Omega \setminus D) \times (0,T), \\ \partial_\nu u = 0 \quad \text{on } \partial D \times (0,T), \\ \partial_\nu u = f \quad \text{on } \partial\Omega \times (0,T), \\ u(x,0) = 0 \quad \text{in } \Omega \setminus D. \end{cases} \tag{1}$$

In this case, is it possible to reconstruct D by the boundary data $u|_{\partial\Omega}$ if we suitably control the heat flux f?

This is an inverse problem to apply "Neumann to Dirichlet" boundary data. They proved that the convex hull, as well as some other information, of the inclusion D is reconstructed with the choice of a suitable adjoint solution of the heat equation.

Their theory being very excellent and beautiful as mathematical one, it seems that there are several points to be modified in view of practical application.

- In practical application, it is not easy give the heat flux as the boundary data. In addition to it, its observation is not easy, either.
- Though Ikehata-Kawashita controlled the input of the heat $f(x,t)$ on the whole boundary of Ω, in view of the practical application, it is easier to give a point source $\delta(x)f(t)$ on the boundary.

In view of these remarks, we study the following problem.

Problem 1.2. *Let Ω be a bounded domain of $\mathbb{R}^n$ $n = 2, 3$ with smooth boundary. Let D be an open subset of Ω with smooth boundary and satisfy that $\overline{D} \subset \Omega$ and $\Omega \setminus D$ is connected. We denote the unit outward normal vectors to $\partial\Omega$ and ∂D by the same symbol ν. Let $T > 0$ be an arbitrary. Given $f = f(t)$, $t \in \times(0,T)$ and $x_0 \in \partial\Omega$, let $u = u(x,t)$ be the solution of the initial boundary value problem for the heat equation*

$$\begin{cases} \partial_t u - \Delta u = \delta(x_0)f(t) \quad \text{in } (\Omega \setminus D) \times (0,T), \\ \partial_\nu u = 0 \quad \text{on } \partial D \times (0,T), \\ \partial_\nu u = 0 \quad \text{on } \partial\Omega \times (0,T), \\ u(x,0) = 0 \quad \text{in } \Omega \setminus D. \end{cases} \tag{2}$$

In this case, is it possible to reconstruct D by the boundary data $u|_{\partial\Omega}$ if we suitably control the heat source $f(t)$ for all $x_0 \in \partial\Omega$?

It is our main purpose in this paper to study Problem 1.2. For this purpose, we apply the idea of hyperfunctions to treat the Delta functions on the boundary $\partial\Omega$. Even if the reconstruction formulas for the inclusions are obtained, the known results on Problems 1.1 and 1.2 are far from being applied for practice. At the end of this paper, we mention open problems to be solved in order that the studies of these problems should be applied for practice.

We shall develop our theory in the following sections. In the second section, we review the known results on Problem 1.1. We shall discuss our main problem, Problem 1.2, in the third and fourth sections, where we shall prove our main theorems (Theorems 3.2 and 4.1). In the third section, we introduce the essential idea for our theory by studying the one spatial dimensional case, the result of which is one of the main theorems in this paper (Theorems 3.2). In the fourth section, we generalize the result proved in the third section. This generalization is the other main theorem (Theorems 4.1) in this paper. In the final section, we summarise the conclusion of this paper and mention open problems to be solved for further development.

2 Known results

In this section, we review the known results on the inverse problem of the heat equation to reconstruct an inclusion in a homogeneous medium. The first study on this problem is by M. Ikehata [4], where this inverse problem for the one spatial dimensional heat equation is discussed applying Neumann-to-Dirichlet data on the boundary. This idea was generalized by M. Ikehata and M. Kawashita [5, 6], which we shall review.

Theorem 2.1 (M. Ikehata and M. Kawashita [5]). *Let $T > 0$ be an arbitrary. Given $\omega \in S^{n-1}$, $n = 2, 3$, let f be the function of $(x,t) \in \partial\Omega \times (0,T)$ having a parameter $\tau > 0$ defined by the equation $f(x,t;\tau) = \partial_\nu v(x)\varphi(t)$, where $v(x) = e^{\sqrt{\tau}x\cdot\omega}$ and $\varphi \in L^2(0,T)$ satisfying the following condition: there exists $\mu \in \mathbb{R}$ such that*

$$\liminf_{\tau\to\infty} \tau^\mu \left| \int_0^t e^{\tau t}\varphi(t)dt \right| > 0. \tag{3}$$

Let $u_f(x,t)$ be the weak solution of (1) with $f(x,t;\tau)$. Then there holds

$$\lim_{\tau\to\infty} \frac{1}{2\sqrt{\tau}} \log \left| \int_{\partial\Omega}\int_0^T e^{\tau t} \left(v(x)f(x,t;\tau) - u_f(x,t)\partial_\nu v(x)\right) dtdS \right| = h_D(\omega). \tag{4}$$

Theorem 2.2 (M. Ikehata and M. Kawashita [6]). *Let $n = 3$, $y \in \mathbb{R}$, $f(x,t;\tau) = \partial_\nu v(x)\varphi(t)$, where $v(x;\tau) = \frac{e^{-\tau|x-p|}}{|x-p|}$, for $x \in \Omega$ and $p \in \mathbb{R}^3 \setminus \Omega$. Assume that $u_f(x,t)$ be the weak solution of (1) with $f(x,t;\tau,p)$. Then assuming (3), one has the formula*

$$\lim_{\tau\to\infty} \frac{1}{2\sqrt{\tau}} \log \left| \int_{\partial\Omega}\int_0^T e^{\tau t} \left(v(x;\tau)f(x,t;\tau,p) - u_f(x,t)\partial_\nu v(x;\tau)\right) dtdS \right| = -d_D(p), \tag{5}$$

where $d_D(p) = \inf_{x\in D} |x-p|$.

Theorem 2.3 (M. Ikehata and M. Kawashita [6]). *Let $n = 3$, $t \in \mathbb{R}$, $f(x,t;\tau) = \partial_\nu v(x)\varphi(t)$, where*

$$v(x) = \begin{cases} \frac{e^{\sqrt{\tau}|x-y|} - e^{-\sqrt{\tau}|x-y|}}{|x-y|}, & \text{if } x \neq y, \\ 2\sqrt{\tau}, & \text{if } x = y. \end{cases} \tag{6}$$

Assume that $u_f(x,t)$ be the weak solution of (1) with $f(x,t;\tau,y)$. Then assuming (3), one has the formula

$$\lim_{\tau\to\infty} \frac{1}{2\sqrt{\tau}} \log \left| \int_{\partial\Omega}\int_0^T e^{\tau t} \left(v(x)f(x,t;\tau,y) - u_f(x,t)\partial_\nu v(x)\right) dtdS \right| = R_D(y), \tag{7}$$

where $R_D(y) = \sup_{x\in D} |x-y|$.

As we can see in Theorems 2.1, 2.2 and 2.3, their theory is very excellent and beautiful as mathematical ones, however, we cannot directly apply their theory for practice. Let us summarise the points to be improved for practice.

Remark 2.1.

- In practical application, it is not easy give the heat flux as the boundary data. In addition to it, its observation is not easy, either. What we can do is to give heat sources on the boundary and observe the temperature on the boundary.
- Though Ikehata-Kawashita controlled the input of the heat $f(x,t)$ on the whole boundary of Ω, in view of the practical application, it is much easier give a point source of the form $\delta(x-x_0)f(t)$ at a point x_0 on the boundary.
- In Theorems 2.1, 2.2 and 2.3, it is essential to give test objects such high temperature on the boundary that they would be melted down. This point is fatal for practical application.

Having these remarks in mind, we shall study modification of the theory by Ikehata-Kawashita in view of practical application in the following sections.

3 Main theorem I. —One spatial dimensional case—

In this section, we try to modify Theorems 2.1, 2.2 and 2.3 for one spatial dimensional case. Let $\Omega = (0, X)$, $D = (a, b)$ and $0 < a < b < X$. We study the one spatial dimensional linear heat equation with the inhomogeneous term as the heat source at the origin $x = 0$.

$$\begin{cases} \partial_t u - \partial_x^2 u = \delta(x) f(t) & \text{in } (0, a) \times (0, T), \\ \partial_x u = 0 & \text{on } \{0\} \times (0, T), \\ \partial_x u = 0 & \text{on } \{a\} \times (0, T), \\ u(x, 0) = 0 & \text{in } (0, a) \times (0, T). \end{cases} \tag{8}$$

In the initial and the boundary value problem (8), an inclusion $D = (a, b)$ is included in a homogeneous medium $\Omega = (0, X)$. We pose an inverse problem to reconstruct the inclusion by observing the boundary data at $x = 0, X$ with controlling the input heat source at the boundary $x = 0, X$. This case, it is impossible to reconstruct some information about the point $x = b$ from the boundary value at $x = 0$ and vise versa, that is, it is also impossible to reconstruct some information about the point $x = a$ from the boundary value at $x = X$. Therefore, we pose the following inverse problem.

Problem 3.1. *Let $u(x, t)$ be the solution of the initial boundary value problem for the heat equation* (8)*. In this case, is it possible to recover a by the boundary data $u(0, t) =: g(t)$ if we suitably control the heat source f?*

In this problem, we try to reconstruct the information of the inclusion, namely, its position $x = a$, by observing the boundary data at $x = 0$ with controlling the input heat source $f(t)$ at the boundary point $x = 0$.

It is our main purpose in this section to give a positive answer to Problem 3.1. For this purpose, we treat linear ordinary differential equations with Dirac delta function and its derivatives in the inhomogeneous term, which let us prepare before discussing the main problem in this section.

Let us study the following linear ordinary differential equation with Dirac delta function and its derivatives in the inhomogeneous term.

$$y^{(n)} + a_{n-1} y^{(n-1)} + \cdots + a_1 y' + a_0 y = \sum_{k=0}^{n-1} \alpha_k \delta^{(k)}(x), \tag{9}$$

where $y = y(x)$ is a function of $x \in \mathbb{R}$ and $a_k,\ \alpha_k,\ k = 0, 1, \cdots, n-1$ are constants. We study the initial value problem of the equation (9), that is,

Problem 3.2. *Solve the initial value problem of* (9) *with*

$$y^{(k)}(0) = 0, \tag{10}$$

where $k = 0, 1, \cdots, n-1$.

Let us prepare several lemmas in order to solve Problem 3.2. Before proving them, let us review the definition of the Laplace transform, which plays an important role in the solution of Problem 3.2.

Definition 3.1. For a function $\varphi(x)$ defined in $[0, \infty)$, its Laplace transform $\mathcal{L}\varphi$ is defined by

$$\mathcal{L}\varphi(p) := \int_0^\infty e^{-px}\varphi(x)dx, \tag{11}$$

for $p \in \mathbb{C}$ for which the integral (11) is convergent.

Lemma 3.1.

$$\mathcal{L}\delta(p) \equiv 1, \tag{12}$$

where $\delta(x)$ is the Dirac's delta function (cf. [7, 10] for whose definition).

Proof. For the proof of this lemma, we apply the idea of hyperfunctions. We first remark that $\mathrm{supp}\delta = \{0\}$ (cf. [7]). We regard the Delta function $\delta(x)$ as a hyperfunction defined on $\mathbb{R}$, whose defining holomorphic function is $F(z) = -\frac{1}{2\pi iz}$ (cf. [7] for more detail), which we denote by

$$\delta(x) = [F(z)] = \left[-\frac{1}{2\pi iz}\right] = F(x+i0) - F(x-i0) = -\frac{1}{2\pi}\left(\frac{1}{x+i0} - \frac{1}{x-i0}\right). \tag{13}$$

Assume that $f(x) = [F(z)]$ is a hyperfunction defined on $\mathbb{R}$ whose support is compact and whose defining holomorphic function is $F(z)$. Note that $f(x)$ can be regarded as a real analytic functional. Let φ be a real analytic function then it can be extended as a holomorphic function defined in a neighborhood $V \subset \mathbb{C}$ of $\mathrm{supp}f$. Then we can define the duality $< f, \varphi >$ by

$$< f, \varphi > := -\int_\gamma F(z)\varphi(z)dz \tag{14}$$

where the integral route γ can be taken arbitrarily so that it can be the boundary of the domain in V containing $\mathrm{supp}f$ (cf. Figure 1).

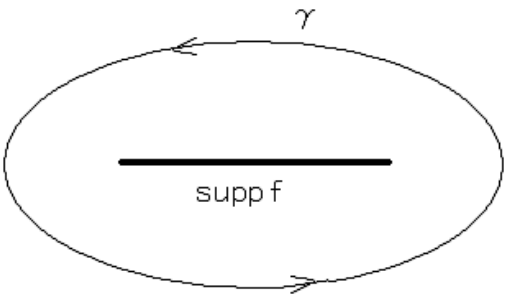

Figure 1: An example of the integral route γ.

For more detail about hyperfunctions, confer [7]. We can define the Laplace transform $\mathcal{L}\delta(p)$ of the Delta function $\delta(x)$ by taking $\delta(x)$ as a real functional and e^{-px} as a real analytic function with p as a parameter. We have, for $p \in \mathbb{C}$, that

$$\begin{aligned}\mathcal{L}\delta(p) &= \int_0^\infty e^{-px}\delta(x)dx =< \delta(x), e^{-px} > \\ &:= -\int_\gamma e^{-pz}\left(-\frac{1}{2\pi iz}\right)dz = \frac{1}{2\pi i}\int_\gamma \frac{e^{-pz}}{z}dz\end{aligned} \tag{15}$$

where the integral route γ is an arbitrary closed Jordan curve in $\mathbb{C}$ such that it can be the boundary of the domain in $\mathbb{C}$ containing the origin. Cauchy's integral formula yields that the right hand side of (15) is equal to $e^{-p0} = 1$ for any $p \in \mathbb{C}$, which proves the lemma. □

When we study the initial value problem of ordinary differential equations containing the Delta function and its derivatives, it may be necessary to treat the value of the Heaviside function at the origin. It having no meaning in usual, we can define its value in the following sense.

Lemma 3.2. *When we apply $\mathcal{L}\delta(p) \equiv 1$ as in (12), $\vartheta(0)$ must be treated as 0, where*

$$\vartheta(x) := \begin{cases} 1 & (x > 0), \\ 0 & (x < 0) \end{cases} \tag{16}$$

is the Heaviside function.

Proof. In order to prove this theorem, we apply the idea of tempered distributions, for more in detail of which, confer [10]. Take a function φ in the space $\mathcal{S}(\mathbb{R})$ of the rapidly decreasing smooth functions, for the definition of which confer [10]. It being well known that $\vartheta'(x) = \delta(x)$, we have

$$\begin{aligned}1 = \mathcal{L}\delta(p) &= \int_0^\infty e^{-px}\delta(x)dx = \int_0^\infty e^{-px}\vartheta'(x)dx \\ &= [e^{-px}\vartheta(x)]_0^\infty + \int_0^\infty \vartheta(x)px^{-px}dx \\ &= -\vartheta(0) + \int_0^\infty px^{-px}dx = -\vartheta(0) + 1.\end{aligned} \tag{17}$$

Therefore the lemma is proved. □

Making use of Lemmas 3.1 and 3.2, we shall solve the initial value problem to (9). The solution of the initial value problem to (9) for $k = 0$ is obtained by the following theorem.

Theorem 3.1. *Consider the following initial value problem to the following ordinary differential equation.*

$$\begin{cases} y^{(n)} + a_{n-1}y^{(n-1)} + \cdots + a_1y' + a_0y = \delta(x), \\ y(0) = y'(0) = \cdots = y^{n-1}(0) = 0 \end{cases} \tag{18}$$

where $a_k,\ k = 0, 1, \cdots, n-1$ *are constants. The solution of* (18) *is given by*

$$y(x) = Y(x\vartheta(x)) \tag{19}$$

for $x > 0$*, where* $Y(x)$ *is the solution of the following initial value problem*

$$\begin{cases} y^{(n)} + a_{n-1}y^{(n-1)} + \cdots + a_1 y' + a_0 y = 0, \\ y^{(j)}(0) = \delta_{j(n-1)}, \quad j = 0, 1, \cdots, n-1, \end{cases} \tag{20}$$

where

$$\delta_{jk} := \begin{cases} 1 & (j = k), \\ 0 & (j \neq k) \end{cases} \tag{21}$$

is the Kronecker's delta function.

Proof. Remarking Lemma 3.2 and the facts

$$\begin{aligned} &x\delta(x) = 0, \\ &\vartheta^2(x) = \vartheta(x), \\ &Y^{(j)}(x\vartheta(x))\delta(x) = Y^{(j)}(0)\delta(x),\ j = 0, 1, 2, \cdots, n, \end{aligned} \tag{22}$$

holding in the space of tempered distributions, there holds that

$$\begin{aligned} y'(x) &= Y'(x\vartheta)(\vartheta(x) + x\delta(x)) = Y'(x\vartheta)\vartheta(x), \\ y''(x) &= Y''(x\vartheta)\vartheta^2(x) + Y'(x\vartheta)\delta(x) = Y''(x\vartheta)\vartheta(x), \\ &\vdots \\ y^{(n-1)}(x) &= Y^{(n-1)}(x\vartheta)\vartheta(x), \\ y^{(n)}(x) &= Y^{(n)}(x\vartheta)\vartheta(x) + Y^{(n-1)}(x\vartheta)\delta(x) = Y^{(n)}(x\vartheta)\vartheta(x) + \delta(x). \end{aligned} \tag{23}$$

The function y in (23) turns out to be the solution of (18), since

$$Y^{(j)}(x\vartheta(x))\vartheta(x) = Y^{(j)}(x\vartheta(x)) = Y^{(j)}(x), \tag{24}$$

for $j = 0, 1, 2, \cdots, n$ and $x > 0$. □

For $x < 0$ the solution of (18) is obtained by

$$y(x) := Y(-x\vartheta(-x)), \tag{25}$$

where $Y(x)$ is the solution of (20).

The motivation to prove Theorem 3.1 is the application of the Laplace transform. If we try to solve the initial value problem (18) by the Laplace transform with applying Lemma 3.1 then we obtain the solution of (20). The essence to prove Theorem 3.1 is how to modify the solution of (20) in order to obtain the solution of (18) in view of the proofs of Lemmas 3.1 and 3.2. We can construct the elementary solutions to partial differential equations with constant coefficients by applying the Fourier transform, which shall be discussed in our forthcoming paper [14].

Let us give an answer to Problem 3.1 applying Theorem 3.1. The following theorem is one of the main theorems in this paper, to prove which is our main purpose in this section.

Theorem 3.2. *For $p \leq 0$, let*

$$\varphi_\lambda(x,t) = \varphi(x,t) = e^{-\lambda^2 t} e^{\lambda(p-x)}, \tag{26}$$

where λ is a constant and

$$I(\varphi_\lambda) := \int_0^T g(t)(\varphi(0,t) + \partial_x \varphi(0,t))dt + e^{\lambda p} \int_0^T f(t) e^{-\lambda^2 t} dt. \tag{27}$$

A solution of Problem 3.1 is given in the following way.

$$\lim_{\lambda \to \infty} \frac{1}{\lambda} |I(\varphi_\lambda)| = p - a. \tag{28}$$

By (28), we claim that we can reconstruct the information of the inclusion, namely, its location $x = a$, by controlling the heat source $f(t)$ at the boundary point $x = 0$ and by observing the temperature $g(t)$ at the boundary point $x = 0$. In the rest of this section, we give a proof of this theorem. We first give a simple representation of the indicator function defined in (27).

Lemma 3.3.

$$I(\varphi_\lambda) = (1-\lambda) e^{\lambda(p-a)} \int_0^T u(a,t) e^{\lambda^2 t} dt. \tag{29}$$

Proof. Let $u(x,t)$ be the solution of the initial and the boundary value problem for the heat equation (8) and $\varphi(x,t)$ be the function defined in (26).

By integration by parts, we have

$$\begin{aligned} \int_0^T \int_0^a u_t(x,t)\varphi(x,t)dxdt &= \int_0^T u(a,t)\varphi(a,t)dt - \int_0^T g(t)\varphi(0,t)dt \\ &\quad - \int_0^T \int_0^a u(x,t)\varphi_t(x,t)dxdt, \end{aligned} \tag{30}$$

since $u(0,t) = g(t)$ and

$$\begin{aligned} &\int_0^T \int_0^a u_{xx}(x,t)\varphi(x,t)dxdt \\ &\quad = \int_0^T u_x(a,t)\varphi(a,t)dt - \int_0^T u_x(0,t)\varphi(0,t)dt \\ &\qquad - \int_0^T u(a,t)\varphi_x(a,t)dt + \int_0^T u(0,t)\varphi_x(0,t)dt + \int_0^T \int_0^a u(x,t)\varphi_{xx}(x,t)dxdt \\ &\quad = -\int_0^T u(a,t)\varphi_x(a,t)dt + \int_0^T g(t)\varphi_x(0,t)dt + \int_0^T \int_0^a u(x,t)\varphi_{xx}(x,t)dxdt, \end{aligned} \tag{31}$$

since $u_x(0,t) = u_x(a,t) = 0$ by (8) and $u(0,t) = g(t)$. On the other hand, it is easy to obtain

$$\int_0^T \int_0^a \delta(x) f(t)\varphi(x,t)dxdt = e^{\lambda p} \int_0^T f(t) e^{-\lambda^2 t} dt. \tag{32}$$

It is clear by the definition (26) that the function φ is a solution of the adjoint heat equation;

$$\varphi_t + \varphi_{xx} = 0. \tag{33}$$

By virtue of (8), (30), (31), (32) and (33), we obtain that

$$\begin{aligned}
&\int_0^T \int_0^a (u_t(x,t) - u_{xx}(x,t))\varphi(x,t)dxdt \\
&\qquad = \int_0^T u(a,t)\varphi(a,t)dt - \int_0^T g(t)\varphi(0,t)dt \\
&\qquad\quad + \int_0^T u(a,t)\varphi_x(a,t)dt - \int_0^T g(t)\varphi_x(0,t)dt \\
&\qquad = e^{\lambda p}\int_0^T f(t)e^{-\lambda^2 t}dt,
\end{aligned} \tag{34}$$

which, together with (27), it is proved that

$$\begin{aligned}
I(\varphi_\lambda) &= \int_0^T g(t)(\varphi(0,t) + \partial_x\varphi(0,t))dt + e^{\lambda p}\int_0^T f(t)e^{-\lambda^2 t}dt \\
&= \int_0^T u(a,t)(\varphi(a,t)\varphi_x(a,t))dt \\
&= (1-\lambda)e^{\lambda(p-a)}\int_0^T u(a,t)e^{\lambda^2 t}dt,
\end{aligned} \tag{35}$$

which proves the lemma. □

We divide the integral $\int_0^T u(x,t)e^{-\lambda^2 t}dt$ in the right hand side of (29) into two parts;

$$\int_0^T u(x,t)e^{-\lambda^2 t}dt =: \widetilde{w}(x,\lambda) = w(x,\lambda) + \varepsilon(x,\lambda), \tag{36}$$

where $w(x,\lambda)$ is the solution of the following initial value problem

$$\begin{cases}
(\partial_x^2 - \lambda^2)w = -\delta(x)\int_0^T f(t)e^{-\lambda^2 t}dt, \\
w_x(0,\lambda) = 0, \\
w(0,\lambda) = \int_0^T \theta(t)e^{-\lambda^2 t}dt,
\end{cases} \tag{37}$$

and $\varepsilon(x,\lambda)$ is the solution of the following initial value problem

$$\begin{cases}
(\partial_x^2 - \lambda^2)\varepsilon = ue^{-\lambda^2 T}, \\
\varepsilon_x(0,\lambda) = 0, \\
\varepsilon(0,\lambda) = 0.
\end{cases} \tag{38}$$

The initial value problem (38) is a simple one for the second order ordinary equation and we can solve (37) by virtue of Theorem 3.1.

Lemma 3.4. *The solutions to the initial value problems* (37) *and* (38) *are obtained as follows.*

$$w(x;\lambda) = -S\cosh(\lambda x) + \frac{K}{\lambda}\sinh(\lambda x\vartheta(x)), \tag{39}$$

$$\varepsilon(x;\lambda) = ue^{-\lambda^2 T}\int_0^x u(x-y,T)\frac{1}{\lambda}\sinh(\lambda y)dy, \tag{40}$$

where

$$K := \int_0^T f(t)e^{-\lambda^2 t} = K, \quad S := \int_0^T \theta(t)e^{-\lambda^2 t}. \tag{41}$$

With the above preparation, we can prove the main theorem in this section.

Proposition 3.1. *A solution to Problem 3.1 is given in the following way.*

$$\lim_{\lambda\to\infty} \frac{1}{\lambda} \log |I(\varphi_\lambda)| = p - a. \tag{42}$$

Proof. By (29) and (36),

$$I(\varphi_\lambda) = (1-\lambda)e^{\lambda(p-a)}\widetilde{w}(x,\lambda) = (1-\lambda)e^{\lambda(p-a)}(w(x,\lambda) + \varepsilon(x,\lambda)) \tag{43}$$

holds. It is easily proved that

$$\lim_{\lambda\to\infty} \frac{1}{\lambda} \log |\widetilde{w}(x,\lambda)| = 0 \tag{44}$$

since the function $\widetilde{w}(x,\lambda)$ is concretely represented by Lemma 3.4. Therefore, the representation (43) of the indicator function $I(\varphi_\lambda)$ and the estimate (44) of the function $\widetilde{w}(x,\lambda)$ prove the theorem. □

Proposition 3.1 completes the proof of Theorem 3.2. Let us comment several remarks on Theorem 3.2.

Remark 3.1.

- By Theorem 3.2, we can reconstruct the inclusion $x = a$ by the observation of the temperature at the boundary point $x = 0$ with controlling the heat source $f(t)$ on the boundary point $x = 0$. As mentioned above, it is very important, in view of practical application, that the source term $f(t)$ to be controlled is the heat source, not the heat flux.
- We claim that the idea to prove Theorem 3.2 is essential for the study of the higher spatial dimensional case, where we reconstruct some information on the inclusion by the observation of the temperature on the boundary with controlling the heat source $f(t)$ on a boundary point.

4 Main theorem II. —General case—

In this section, we study Problem 1.2, which yields a generalization of Theorem 3.2. Concretely, we study the following problem.

Problem 4.1. *Assume the same assumptions as Problem 1.2. Reconstruct the inclusion D by the observation of the boundary data*

$$g(x_1, t) := u|_{\partial\Omega}(x_1, t), \tag{45}$$

for $x_1 \in \partial\Omega$, with suitably controlling the heat source $f(t)$ for $x_0 \in \partial\Omega$.

In the case $x_0 = x_1$, we have an answer to this problem as follows.

Theorem 4.1. *Assume the same assumptions as Problem 1.2 and For $x_0 \in \partial\Omega$ and a constant λ, let*

$$\varphi_\lambda(x, t) = \varphi(x, t) = e^{-\lambda^2 t} e^{-\lambda\omega\cdot x}, \tag{46}$$

where $\omega \in S^{n-1}$, and let

$$I(\varphi_\lambda) := \int_0^T \int_{\partial\Omega} (g(x, t)(\varphi(x, t) + \partial_\nu\varphi(x, t)))dS_x dt \tag{47}$$

For $n = 2, 3$, a solution of Problem 4.1 is given by

$$\lim_{\tau\to\infty} \frac{1}{\lambda} |I(\varphi_\lambda)| = -d_\omega(x_0, D), \tag{48}$$

where

$$d_\omega(x_0, D) := \inf\{t \in \mathbb{R} \mid x_0 + t\omega \in D\}. \tag{49}$$

The proof of this theorem is given by modifying the proof of Theorem 3.2. The essential idea of both theorems are the same. In the proof of Theorem 4.1, we can treat the heat conduction like one spatial dimensional one in the direction $\omega \in S^{n-1}$ if we consider the high temperature state, which is the essence to generalize the idea of the proof of Theorem 3.2.

We proved Theorem 4.1 as the first step to study the inverse problem of the heat conduction in view of practical application. We remark that Theorem 4.1 is not still enough for practical application. There are many better generalizations, some of which we shall mention, as well as the merits of our main theorems, in the following remark.

Remark 4.1.

(a) In Theorems 3.2 and 4.1, we control the heat source, not the heat flux, at one point of the boundary, which generalizes Theorems 2.1, 2.2 and 2.3 in two senses. One is that the heat source is much more easily controlled in practical application that the heat flux. The other is that controlling the heat at one point is more desirable for practice, since if we would try to control the heat on the whole boundary in practice we have to prepare a special device in accordance with the shape of the test object.

(b) In Theorems 2.1, 2.2 and 2.3, M. Ikehata and M. Kawashita extracted information on the inclusion with theoretical one measurement, which is one of the excellent and superior points of their study. It is possible to prove similar result by modifying Theorem 4.1 with the observation of the boundary value $g(x,t)$ defined in (45) for all $x \in \partial\Omega$. For this purpose, it is an interesting problem to find a more suitable solution φ to the adjoint heat equation in the construction of the indicator function. In the paper [6], M. Ikehata and M. Kawashita studied the relation between the solutions to the adjoint heat equation and the information of the inclusion D to be obtained in the study of Problem 1.1, which is very suggestive for the study of our problem (Problem 1.2).

(c) In all Theorems 2.1, 2.2, 2.3, 3.2 and 4.1, the limit $\lambda \to \infty$ is required, which means that the heat source or the heat flux f to be controlled must be in such high temperature that the test object would be melt down. This is the fatal fault to be modified in these theorems, in view of the practical application.

5 Conclusion and open problems

As the final section of this paper, we conclude the conclusion of this paper and mention some open problems left to be solved for further development. Let us first summarise what we have discussed in this paper.

Conclusion 5.1 (Conclusion of this paper)**.**

(i) *We have given generalizations* (Theorems 3.2 and 4.1) *of the theory by M. Ikehata and M. Kawashita* (Theorems 2.1, 2.2 and 2.3)*, which was the main purpose in this paper. Confer Remark 4.1 (a) for more detail.*

(ii) *It is possible to generalize Theorem 4.1. As an example of these generalizations, confer Remark 4.1 (b).*

(iii) *As a by-product of the proof of Theorem 3.2. We have given a solution* (Theorem 3.1) *to the initial value problem of linear ordinary differential equation with Dirac delta function and its derivatives in the inhomogeneous term, which itself is interesting and may be applied to the construction of the elementary solutions to linear partial differential equations.*

As we have mentioned at the end of the last section, Theorems 3.2 and 4.1 are not enough for practical application. In addition to it, there are many open problems for further development. At the end of this paper, we shall mention these open problems.

Problem 5.1. (i) *Let us first remark the most important open problem. In both Theorems 3.2 and th.ndim, the heat source f to be controlled on the boundary is required to be very high. It must tend to infinity to obtain the information of the inclusion, which is impossible in practice in two ways. One reason is very simple; we cannot give infinitely high heat source or heat flux. The other reason is that the object will be melt down at high temperature* (cf. Remark 4.1 (c))*. Therefore, we have to develop a method which enables us to detect the inclusion without tending the temperature to infinity. For this purpose, we propose two ways to generalize our main theorems.*

- *One approach to this problem is to develop another method to extract some information of the inclusion in the low temperature state.*
- *The other way is to give suitable error estimates for the limiting processes (28) and (48) in order that Theorems 3.2 and th.ndim can be applied for practice in the reasonable temperature state.*

We claim that both approaches are interesting and are to be studied.

(ii) *Even if the above problem is solved, there still are a number of problems left to be solve for practice; the treatment of the errors, construction of a approximation algorithm for the inclusions, its implementation by computers and so on.*

(iii) *There are many generalization of Theorem 4.1, the study of which is interesting and important. One of them is remarked in Remark 4.1 (b).*

(iv) *Theorem 3.1 is obtained as a by-product of the proof of Theorem 3.2. More generally, it is an interesting problem to study the initial value problem of linear ordinary differential equation with Dirac delta function and its derivatives in the inhomogeneous term* (Problem 3.2)*, as well as its application to the theory of partial differential equations.*

References

[1] Gardner R.J. : *X-rays of polygons,* Discrete Comput. Geom., **7** (1992), pp. 281-293.

[2] Huang L. and Takiguchi T. : *The reconstruction of uniquely determined plane sets from two projections,* J. Inv. Ill-Posed Problems, **6** (1998), pp. 217-242.

[3] Ikehata M. : *Reconstruction of the support function for inclusion from boundary measurements,* J. Inv. Ill-Posed Problems, **8** (2000), pp. 367-378.

[4] —— : *Extracting discontinuity in a heat conductive body. One-space dimensional case,* Appl. Anal., **86** (2007), pp. 963-1005.

[5] Ikehata M. and Kawashita M. : *The enclosure method for the heat equation,* Inverse Problems, **25** (2009), 075005.

[6] —— : *On the reconstruction of inclusions in a heat conductive body from dynamical boundary data over a finite time interval,* Inverse Problems, **26** (2010), 095004.

[7] A. Kaneko : *Introduction to hyperfunctions* (translated by Y. Yamamoto), Kluwer Academic Publishers, Dordrecht, Boston, London, 1988.

[8] Kuba A. and Volčič A. : *Characterization of measurable plane sets which are reconstructable from their two projections,* Inverse Problems, **4** (1988), pp. 513-527.

[9] Lorentz G.G. : *A problem of plane measure,* Amer. J. Math., **71** (1949), pp. 417-426.

[10] L. Schwartz : *Théorie des distributions* (*Nouvelle édition*), Hermann, Paris, 1966.

[11] Takiguchi T. : *Reconstruction of measurable plane sets from their orthogonal projections,* Contemporary Mathematics, **348** (2004), pp. 199-208.

[12] —— : *Reconstruction of the measurable sets in the two dimensional plane by two projections,* Journal of Physics, Conference Series, **73** (2007), 012022.

[13] —— : *Non-uniqueness of the reconstruction for connected and simply connected sets in the plane by their fixed finite projections,* Acta Mathematica Scientia, **32B** (2012), pp. 1637-1646.

[14] Takiguchi T. and Yamashita R. : *Solutions to linear ordinary differential equations with the derivatives of the delta function in the inhomogenous term and elmentary solutions to partial differential equations,* in preparation.

MI レクチャーノートシリーズ刊行にあたり

本レクチャーノートシリーズは、文部科学省 21 世紀 COE プログラム「機能数理学の構築と展開」(H.15-19 年度) において作成した COE Lecture Notes の続刊であり、文部科学省大学院教育改革支援プログラム「産業界が求める数学博士と新修士養成」(H19-21 年度) および、同グローバル COE プログラム「マス・フォア・インダストリ教育研究拠点」(H.20-24 年度) において行われた講義の講義録として出版されてきた。平成 23 年 4 月のマス・フォア・インダストリ研究所 (IMI) 設立と平成 25 年 4 月の IMI の文部科学省共同利用・共同研究拠点として「産業数学の先進的・基礎的共同研究拠点」の認定を受け、今後、レクチャーノートは、マス・フォア・インダストリに関わる国内外の研究者による講義の講義録、会議録等として出版し、マス・フォア・インダストリの本格的な展開に資するものとする。

平成 25 年 9 月
マス・フォア・インダストリ研究所
所長　若山正人

Inverse problems for practice, the present and the future

発　行　2014年 1 月30日
編　集　滝口孝志, 藤原宏志
発　行　九州大学マス・フォア・インダストリ研究所
九州大学大学院数理学府
〒819-0395 福岡市西区元岡744
九州大学数理・IMI 事務室
TEL 092-802-4402　FAX 092-802-4405
URL http://www.imi.kyushu-u.ac.jp/

印　刷　城島印刷株式会社
〒810-0012 福岡市中央区白金 2 丁目 9 番 6 号
TEL 092-531-7102　FAX 092-524-4411

シリーズ既刊

Issue	Author／Editor	Title	Published
COE Lecture Note	Mitsuhiro T. NAKAO Kazuhiro YOKOYAMA	Computer Assisted Proofs - Numeric and Symbolic Approaches - 199pages	August 22, 2006
COE Lecture Note	M.J.Shai HARAN	Arithmetical Investigations - Representation theory, Orthogonal polynomials and Quantum interpolations- 174pages	August 22, 2006
COE Lecture Note Vol.3	Michal BENES Masato KIMURA Tatsuyuki NAKAKI	Proceedings of Czech-Japanese Seminar in Applied Mathematics 2005 155pages	October 13, 2006
COE Lecture Note Vol.4	宮田　健治	辺要素有限要素法による磁界解析 - 機能数理学特別講義 21pages	May 15, 2007
COE Lecture Note Vol.5	Francois APERY	Univariate Elimination Subresultants - Bezout formula, Laurent series and vanishing conditions - 89pages	September 25, 2007
COE Lecture Note Vol.6	Michal BENES Masato KIMURA Tatsuyuki NAKAKI	Proceedings of Czech-Japanese Seminar in Applied Mathematics 2006 209pages	October 12, 2007
COE Lecture Note Vol.7	若山　正人 中尾　充宏	九州大学産業技術数理研究センター キックオフミーティング 138pages	October 15, 2007
COE Lecture Note Vol.8	Alberto PARMEGGIANI	Introduction to the Spectral Theory of Non-Commutative Harmonic Oscillators 233pages	January 31, 2008
COE Lecture Note Vol.9	Michael I.TRIBELSKY	Introduction to Mathematical modeling 23pages	February 15, 2008
COE Lecture Note Vol.10	Jacques FARAUT	Infinite Dimensional Spherical Analysis 74pages	March 14, 2008
COE Lecture Note Vol.11	Gerrit van DIJK	Gelfand Pairs And Beyond 60pages	August 25, 2008
COE Lecture Note Vol.12	Faculty of Mathematics, Kyushu University	Consortium “MATH for INDUSTRY” First Forum 87pages	September 16, 2008
COE Lecture Note Vol.13	九州大学大学院 数理学研究院	プロシーディング「損保数理に現れる確率モデル」 ― 日新火災・九州大学 共同研究 2008 年 11 月 研究会 ― 82pages	February 6, 2009

シリーズ既刊

Issue	Author／Editor	Title	Published
COE Lecture Note Vol.14	Michal Beneš, Tohru Tsujikawa Shigetoshi Yazaki	Proceedings of Czech-Japanese Seminar in Applied Mathematics 2008 77pages	February 12, 2009
COE Lecture Note Vol.15	Faculty of Mathematics, Kyushu University	International Workshop on Verified Computations and Related Topics 129pages	February 23, 2009
COE Lecture Note Vol.16	Alexander Samokhin	Volume Integral Equation Method in Problems of Mathematical Physics 50pages	February 24, 2009
COE Lecture Note Vol.17	矢嶋　　徹 及川　正行 梶原　健司 辻　　英一 福本　康秀	非線形波動の数理と物理 66pages	February 27, 2009
COE Lecture Note Vol.18	Tim Hoffmann	Discrete Differential Geometry of Curves and Surfaces 75pages	April 21, 2009
COE Lecture Note Vol.19	Ichiro Suzuki	The Pattern Formation Problem for Autonomous Mobile Robots —Special Lecture in Functional Mathematics— 23pages	April 30, 2009
COE Lecture Note Vol.20	Yasuhide Fukumoto Yasunori Maekawa	Math-for-Industry Tutorial: Spectral theories of non-Hermitian operators and their application 184pages	June 19, 2009
COE Lecture Note Vol.21	Faculty of Mathematics, Kyushu University	Forum “Math-for-Industry” Casimir Force, Casimir Operators and the Riemann Hypothesis 95pages	November 9, 2009
COE Lecture Note Vol.22	Masakazu Suzuki Hoon Hong Hirokazu Anai Chee Yap Yousuke Sato Hiroshi Yoshida	The Joint Conference of ASCM 2009 and MACIS 2009: Asian Symposium on Computer Mathematics Mathematical Aspects of Computer and Information Sciences 436pages	December 14, 2009
COE Lecture Note Vol.23	荒川　恒男 金子　昌信	多重ゼータ値入門 111pages	February 15, 2010
COE Lecture Note Vol.24	Fulton B.Gonzalez	Notes on Integral Geometry and Harmonic Analysis 125pages	March 12, 2010
COE Lecture Note Vol.25	Wayne Rossman	Discrete Constant Mean Curvature Surfaces via Conserved Quantities 130pages	May 31, 2010
COE Lecture Note Vol.26	Mihai Ciucu	Perfect Matchings and Applications 66pages	July 2, 2010

シリーズ既刊

Issue	Author／Editor	Title	Published
COE Lecture Note Vol.27	九州大学大学院 数理学研究院	Forum “Math-for-Industry” and Study Group Workshop Information security, visualization, and inverse problems, on the basis of optimization techniques 100pages	October 21, 2010
COE Lecture Note Vol.28	ANDREAS LANGER	MODULAR FORMS, ELLIPTIC AND MODULAR CURVES LECTURES AT KYUSHU UNIVERSITY 2010 62pages	November 26, 2010
COE Lecture Note Vol.29	木田　雅成 原田　昌晃 横山　俊一	Magma で広がる数学の世界 157pages	December 27, 2010
COE Lecture Note Vol.30	原　　隆 松井　　卓 廣島　文生	Mathematical Quantum Field Theory and Renormalization Theory 201pages	January 31, 2011
COE Lecture Note Vol.31	若山　正人 福本　康秀 高木　　剛 山本　昌宏	Study Group Workshop 2010 Lecture & Report 128pages	February 8, 2011
COE Lecture Note Vol.32	Institute of Mathematics for Industry, Kyushu University	Forum “Math-for-Industry” 2011 “TSUNAMI-Mathematical Modelling” Using Mathematics for Natural Disaster Prediction, Recovery and Provision for the Future 90pages	September 30, 2011
COE Lecture Note Vol.33	若山　正人 福本　康秀 高木　　剛 山本　昌宏	Study Group Workshop 2011 Lecture & Report 140pages	October 27, 2011
COE Lecture Note Vol.34	Adrian Muntean Vladimír Chalupecký	Homogenization Method and Multiscale Modeling 72pages	October 28, 2011
COE Lecture Note Vol.35	横山　俊一 夫　　紀恵 林　　卓也	計算機代数システムの進展 210pages	November 30, 2011
COE Lecture Note Vol.36	Michal Beneš Masato Kimura Shigetoshi Yazaki	Proceedings of Czech-Japanese Seminar in Applied Mathematics 2010 107pages	January 27, 2012
COE Lecture Note Vol.37	若山　正人 高木　　剛 Kirill Morozov 平岡　裕章 木村　正人 白井　朋之 西井　龍映 栄　伸一郎 穴井　宏和 福本　康秀	平成 23 年度 数学・数理科学と諸科学・産業との連携研究ワークショップ　拡がっていく数学　～期待される “見えない力” ～ 154pages	February 20, 2012

シリーズ既刊

Issue	Author／Editor	Title	Published
COE Lecture Note Vol.38	Fumio Hiroshima Itaru Sasaki Herbert Spohn Akito Suzuki	Enhanced Binding in Quantum Field Theory 204pages	March 12, 2012
COE Lecture Note Vol.39	Institute of Mathematics for Industry, Kyushu University	Multiscale Mathematics: Hierarchy of collective phenomena and interrelations between hierarchical structures 180pages	March 13, 2012
COE Lecture Note Vol.40	井ノ口順一 太田　泰広 筧　　三郎 梶原　健司 松浦　　望	離散可積分系・離散微分幾何チュートリアル 2012 152pages	March 15, 2012
COE Lecture Note Vol.41	Institute of Mathematics for Industry, Kyushu University	Forum “Math-for-Industry” 2012 “Information Recovery and Discovery” 91pages	October 22, 2012
COE Lecture Note Vol.42	佐伯　　修 若山　正人 山本　昌宏	Study Group Workshop 2012 Abstract, Lecture & Report 178pages	November 19, 2012
COE Lecture Note Vol.43	Institute of Mathematics for Industry, Kyushu University	Combinatorics and Numerical Analysis Joint Workshop 103pages	December 27, 2012
COE Lecture Note Vol.44	萩原　　学	モダン符号理論からポストモダン符号理論への展望 107pages	January 30, 2013
COE Lecture Note Vol.45	金山　　寛	Joint Research Workshop of Institute of Mathematics for Industry (IMI), Kyushu University “Propagation of Ultra-large-scale Computation by the Domain-decomposition-method for Industrial Problems (PUCDIP 2012)” 121pages	February 19, 2013
COE Lecture Note Vol.46	西井　龍映 栄　伸一郎 岡田　勘三 落合　啓之 小磯　深幸 斎藤　新悟 白井　朋之	科学・技術の研究課題への数学アプローチ ―数学モデリングの基礎と展開― 325pages	February 28, 2013
COE Lecture Note Vol.47	SOO TECK LEE	BRANCHING RULES AND BRANCHING ALGEBRAS FOR THE COMPLEX CLASSICAL GROUPS 40pages	March 8, 2013
COE Lecture Note Vol.48	溝口　佳寛 脇　　隼人 平坂　　貢 谷口　哲至 島袋　　修	博多ワークショップ「組み合わせとその応用」 124pages	March 28, 2013

シリーズ既刊

Issue	Author／Editor	Title	Published
COE Lecture Note Vol.49	照井　章 小原　功任 濱田　龍義 横山　俊一 穴井　宏和 横田　博史	マス・フォア・インダストリ研究所　共同利用研究集会 II 数式処理研究と産学連携の新たな発展　137pages	August 9, 2013
MI Lecture Note Vol.50	Ken Anjyo Hiroyuki Ochiai Yoshinori Dobashi Yoshihiro Mizoguchi Shizuo Kaji	Symposium MEIS2013: Mathematical Progress in Expressive Image Synthesis　154pages	October 21, 2013
MI Lecture Note Vol.51	Institute of Mathematics for Industry, Kyushu University	Forum “Math-for-Industry” 2013 “The Impact of Applications on Mathematics”　97pages	October 30, 2013
MI Lecture Note Vol.52	佐伯　修 岡田　勘三 髙木　剛 若山　正人 山本　昌宏	Study Group Workshop 2013 Abstract, Lecture & Report 142pages	November 15, 2013
MI Lecture Note Vol.53	四方　義啓 櫻井　幸一 安田　貴徳 Xavier Dahan	平成25年度　九州大学マス・フォア・インダストリ研究所 共同利用研究集会　安全・安心社会基盤構築のための代数構造 ～サイバー社会の信頼性確保のための数理学～　158pages	December 26, 2013

九州大学マス・フォア・インダストリ研究所
九州大学大学院 数理学府

〒819-0395 福岡市西区元岡744　TEL 092-802-4402　FAX 092-802-4405
URL http://www.imi.kyushu-u.ac.jp/